THE UNIVERSITY OF MANITOBA

Experimental Hydrocephalus and Cerebrospinal Fluid Shunting in Rabbits

by

Marc Ronald DEL BIGIO

A thesis

submitted to the Faculty of Graduate Studies

in partial fulfillment of the requirements

for the degree of Doctor of Philosophy

Department of Anatomy

Faculty of Medicine

Winnipeg, Manitoba

ISBN 0-315-37278-8

EXPERIMENTAL HYDROCEPHALUS AND CEREBROSPINAL FLUID SHUNTING IN RABBITS

BY

MARC RONALD DEL BIGIO

A thesis submitted to the Faculty of Graduate Studies of the University of Manitoba in partial fulfillment of the requirements of the degree of

DOCTOR OF PHILOSOPHY

TABLE OF CONTENTS

"Would you tell me, please, which way I ought to go from here?"

"That depends a good deal on where you want to get to," said the Cat.

"I don't much care where --" said Alice.

"Then it doesn't matter which way you go," said the Cat.

"-- so long as I get somewhere," Alice added as an explanation.

"Oh, you're sure to do that," said the Cat, "if you only walk long enough."

Conversation between Alice and the Cheshire Cat,
Alice's Adventures in Wonderland
by Lewis Carroll, 1865.

ACKNOWLEDGEMENTS

I am grateful to Dr. Ed Bruni, my supervisor, for four years of teaching and guidance.

Dr. T.V.N. Persaud, Professor and Head, deserves thanks for giving me the opportunity to work in the Department of Anatomy.

Drs. Bill Anderson, Erico Cardoso and Anders Sima acted on my advisory committee and provided valuable input into the project.

Mr. Paul Perumal and Mr. Rainer Persaud provided expert technical assistance over the years and Mr. Roy Simpson assisted with the photography.

Without personal financial assistance from the University of Manitoba Graduate Student Fellowship Fund, the Health Sciences Centre Research Foundation, and the Medical Research Council of Canada, I would not have had such an enjoyable time while completing this work.

Dr. Dwight Parkinson, Professor of Neurosurgery, opened my mind to scientific research, showed me the fascination of neuroscience, and provided me with the initiative to do this work.

Lastly, and most importantly, I thank my parents and Janice for their constant support and encouragement.

ABSTRACT

Experimental hydrocephalus was induced in adult rabbits by injection of silicone oil into the cisterna magna. Obstruction of cerebrospinal fluid (CSF) flow following oil injection significantly increased the intracranial pressure for 36 hours. Ventriculomegaly, particularly of the frontal horns of the lateral ventricles, developed within 3 days and persisted for the 8 week duration of the experiment. Changes in specific gravity indicated that water was lost from gray and white matter, except at the ventricular surface. Ventricular dilatation caused stretching and thinning of the ependymal lining of the septal area, corpus callosum, and caudate nucleus to different degrees. During the first 2 weeks post-injection, significant increases in mitotic activity among ependymal cells and subependymal astrocytes also showed regional differences. There was also a decreased number of patent capillaries in the periventricular neuropil as a result of hydrocephalus.

Reduction of ventricular size by CSF shunting reversed the ependymal and vascular changes in the caudate nucleus and corpus callosum if hydrocephalus was of 1 week duration. Similar reversal of the pathology was not observed if shunting was delayed until 8 weeks. The shunt itself caused erosion of the ependymal lining of the ventricle and stimulated mitotic activity among ependymal and astroglial cells that contributed to obstruction of the shunt by tissue ingrowth.

LIST OF TABLES PAGE

LIST OF FIGURES PAGE

LIST OF ABBREVIATIONS

ANOVA	analysis of variance
CC	corpus callosum
CC-D	corpus callosum deep to the ventricle
CC-P	corpus callosum periventricular region
CN	caudate nucleus
CN-D	caudate nucleus deep to ventricle
CN-P	caudate nucleus periventricular region
CSF	cerebrospinal fluid
ICP	intracranial pressure
LM	light microscopy
LSA	lateral septal area
LSA-P	lateral septal area periventricular region
SE,SEM	standard error of mean (statistical values)
TEM	transmission electron microscopy

1. INTRODUCTION AND OBJECTIVES

The word hydrocephalus is derived from the Greek "hydor" meaning "water" and "kephale" meaning "head". It refers to a condition characterized by abnormal accumulation of fluid within the cranial vault and consequent head enlargement. Internal hydrocephalus refers specifically to dilatation of the cerebral ventricles of the brain. In modern usage, the term hydrocephalus is applied to disorders characterized by excess cerebrospinal fluid (CSF) accumulation and ventriculomegaly with or without head enlargement (Torack, 1982). Hydrocephalus is categorized as communicating if the cerebral aqueduct is patent or non-communicating if CSF does not flow through the aqueduct. Causes of hydrocephalus include excess CSF production or, more commonly, obstruction of CSF flow through the ventricles, subarachnoid space, or arachnoid villi. A variety of pathologic conditions may obstruct CSF flow (Russell, 1949), but the result is the same; dilatation of the ventricles. Untreated, ventricular dilatation may cause irreversible damage to the cerebrum surrounding the ventricles or death. Currently, the treatment of longstanding hydrocephalus in humans consists of surgical diversion of the CSF to other body compartments, most often the peritoneal cavity (Hoffman and Smith, 1986). Valved silicone rubber tube systems known as shunts are used to redirect the CSF.

Hydrocephalus occurs in 0.5-3/1000 live births (Fernell

et al., 1986; Hay, 1971; Haynes et al., 1974; Kurtzke, 1980; Myrionthopoulos, 1979) and subsequently develops in an equal number of infants and children secondary to tumors, meningitis, hemorrhage, and trauma (Bay et al., 1979; Hoffman et al., 1982; Peacock and Currer, 1984). Hydrocephalus also occurs in adults following head trauma, intracranial surgery, intracranial hemorrhage, and central nervous system infections. Katzman (1977) estimated that 5-6% of demented elderly people may suffer from a treatable form of chronic communicating hydrocephalus. None of these estimates are based upon unequivocal data, however, and the precise overall incidence of hydrocephalus is unknown. An indicator of the prevalence of clinically relevant hydrocephalus is the number of patients treated for hydrocephalus. In Canada, approximately 1/12,000 persons per year develop hydrocephalus that requires shunting. This number is evenly divided between adults and children (Hoffman and Smith, 1986).

Because hydrocephalus is a relatively common disorder that affects both children and adults, its pathology and pathophysiology have been the subject of active research since the beginning of the 20th century. However, despite numerous clinical and experimental studies, the effect of hydrocephalus on the brain remains incompletely understood. Moreover, the treatment of hydrocephalus by shunting is fraught with troublesome and often life-threatening complications.

The following study, using silicone oil induced hydrocephalus in rabbits, was designed to:

1. Characterize the pathological changes in the periventricular tissue resulting from hydrocephalus.

2. Correlate these changes with the degree of ventricular dilatation and the intracranial pressure.

3. Determine the potential for reversing pathological changes by shunting CSF from the cerebral ventricles.

4. Characterize the pathological changes in periventricular tissue resulting from the presence of a shunt catheter.

2. REVIEW OF THE LITERATURE

2.1 Ventricular system and cerebrospinal fluid

The ventricular system of the brain and central canal of the spinal cord develop from the cavity of the embryonic neural tube. In the adult brain, the lateral ventricles within each of the telencephalic hemispheres communicate with the midline third ventricle of the diencephalon via the interventricular foramina. Caudally, the third ventricle is confluent with the narrow cerebral aqueduct of the mesencephalon which opens into the rhombencephalic fourth ventricle. A narrow central canal runs the length of the spinal cord beginning at the caudal end of the fourth ventricle. In human adults, the central canal is not normally patent (Millen and Woollam, 1962).

The ventricular system is lined by a predominantly single layer of epithelium known as the ependyma. Choroidal epithelial cells, a derivative of the ependyma, are responsible for the production and secretion of approximately 80% of CSF. The remainder of CSF is derived from the extracellular fluid of the brain parenchyma as well as the ependyma itself (McComb, 1983). The volume of CSF contained within the ventricles and subarachnoid space is replaced approximately three times per day. Flow of CSF proceeds along a pressure gradient from the lateral to the third to the fourth ventricle. CSF enters the subarachnoid space surrounding the central nervous system via the foramina of the fourth ventricle. In higher mammals, CSF

leaves the subarachnoid space through one-way "valves" called arachnoid villi and enters venous sinuses. Lymphatic channels adjacent to the sites of cranial or spinal nerve exit from the central nervous system are also important for CSF absorption. CSF absorption is dependent upon the hydrostatic pressure gradient between the CSF and venous or interstitial fluid compartments (McComb, 1983). The normal CSF pressure is maintained at 2-15 mm Hg, sufficient to support the brain tissues and maintain patency of the ventricular system (Moskalenko et al., 1980).

2.2 Ependymal lining and subependymal region of the ventricles

Within the ventricular system ependymal cell shape varies regionally (Mitro and Palkovits, 1981). Over gray matter ependymal cells are cuboidal or columnar whereas over white matter they are squamous. Similarities in the fine structure of ependyma exist between numerous species including humans (Fleischhauer, 1972). The function of the ependymal epithelium is not well established (Bruni et al., 1985). Although proliferation of ependyma occurs during pre- and early post-natal periods of development, only low levels of residual mitotic activity persist into adulthood and the response of ependyma to injury is limited.

Immediately beneath the ependymal lining is the subependymal region which consists primarily of astrocytes and a layer of astroglial fibers. In addition, this region

contains microglial cells and a population of undifferentiated cells that are believed to be remnants of the embryonic germinal matrix (Privat and Leblond, 1972). The astrocytes and the undifferentiated cells are mitotically active in the adults of several species (Kaplan, 1983; Sturrock, 1985). Capillaries, arterioles, and small venules lie within the subependymal layer along the ventricular walls. The subependymal region is best developed over the caudate nucleus and subcallosal fasciculus, a structure that lies in the dorsolateral walls of the frontal horns of the lateral ventricles. In contrast, the subependymal region is represented as a thin layer over the white matter and septal regions of the lateral ventricles and is almost nonexistent along the third ventricle, cerebral aqueduct, and fourth ventricle (Fleischhauer, 1972).

2.3 Pathophysiology of hydrocephalus

The purpose of this thesis is not to address CSF physiology and its relationship to hydrocephalus, a topic that is the subject of debate at present. Only some of the less contested aspects of hydrocephalus pathophysiology will be discussed. Hydrocephalus occurs when the production of CSF exceeds absorption. Excessive CSF production by choroid plexus tumors may cause hydrocephalus but reduced absorption due to obstruction of flow is a more common cause. Russell (1949) reported that fibrotic scarring of the subarachnoid spaces, gliotic stenosis of the aqueduct, and brain tumors

were the most common causes of obstruction of CSF flow. When adequate CSF flow is not possible, the effective pressure of the CSF acting upon the walls of the ventricles rises. Increases in radial stress within the brain parenchyma results and the ventricles dilate (Hakim et al., 1976). According to Hakim's hypothesis, the stresses acting on the brain dictate that those regions of the ventricles with the greatest diameter, i.e. the frontal horns, will dilate earliest and to the greatest degree. However, in neonatal humans the occipital horns are relatively larger and tend to dilate to the greatest degree (Oberbauer, 1985; Shackelford, 1986).

Unabated, the rising pressure and enlarging CSF compartment within the cranial vault may eventually result in death due to herniation of the brainstem through the foramen magnum. During the development of hydrocephalus, however, rapid compensation for the increased volume of CSF is believed to occur by expulsion of venous blood and brain extracellular fluid from the cranial compartment or, in neonates, by enlargement of the skull (Hakim et al., 1976). Because the capacity for CSF production remains near normal levels, alternate, primarily lymphatic, pathways for absorption become important over a variable period (McComb, 1983; Welch, 1975). These compensatory mechanisms allow the intracranial pressure (ICP) to return to normal but the ventricles remain dilated. The new physical configuration of the hydrocephalic brain is said to have different

biomechanical properties that prevent the ventricles from decreasing in size (Hakim et al., 1976; Shapiro et al., 1985). Others, however, maintain that a gradient of pressure between the ventricle and subarachnoid space persists and keeps the brain compressed (Conner et al., 1984; Geschwind, 1968). The mechanism of continued ventricular dilatation remains uncertain at present.

2.4 Experimental models of hydrocephalus

The earliest recorded model of experimental hydrocephalus was developed by Dandy and Blackfan in 1913. They produced dilatation of the lateral and third ventricles of a dog by obstructing the aqueduct with a piece of cotton. Shortly thereafter, Thomas (1914) found that inflammatory obstruction of the subarachnoid spaces surrounding the brainstem could also cause hydrocephalus. Since then, in addition to the identification of inherited hydrocephalus in several animal strains, numerous methods have been used to induce hydrocephalus experimentally. Subarachnoid space obstruction, intracerebral venous obstruction, inoculation with viruses, and exposure to teratogenic agents have all been found to induce hydrocephalus in animals (Hochwald, 1985). A more complete review of animal models of experimental hydrocephalus has recently been provided by Hochwald (1985).

Currently, two highly reproducible models are used by most investigators for studies of experimental hydrocephalus. Injection of kaolin (aluminum silicate) into

the cisterna magna causes an inflammatory reaction of the meninges that obliterates the subarachnoid spaces surrounding the brain stem and obstructs the flow of CSF (Schurr et al., 1953). Intracisternal injection of viscous silicone oil, on the other hand, is believed to produce a purely mechanical obstruction to outflow of CSF from the fourth ventricle (James and Strecker, 1973; James et al., 1974; Wisniewski et al., 1969).

2.5 Intracranial pressure changes in hydrocephalus

Because complete obstruction of the CSF flow causes continuously high ICP and death (Obenchain and Stern, 1973), the obstruction to CSF flow in chronically hydrocephalic animals must be incomplete. Many experimental studies support the concept that only a transient elevation of ICP is necessary to produce ventricular dilatation. Animals with communicating hydrocephalus created by cisternal injections of silicone oil (Miyagami et al., 1976), silicone rubber (James et al., 1973b), and kaolin (Edvinsson and West, 1971b; Gonzalez-Darder et al., 1984; Hochwald et al., 1972; Lindauer and Griffith, 1938; Miwa et al., 1982) have undergone manometric recording of CSF pressure at various times post-induction. In all models, the levels of ICP are initially elevated but return to normal within 4 days to 4 weeks following induction of hydrocephalus (Conner et al., 1984; Edvinsson and West, 1971a). Differences in the temporal pattern of ICP changes may be attributed to

differences between species, the methods of induction of hydrocephalus, and especially the methods of ICP measurement. Despite normalization of ICP, however, ventriculomegaly has been found to persist in all models.

Whereas intermittent manometric measurements of ICP may yield normal values of ICP, continuous monitoring using pressure transducers, as first described by Lundberg (1960), reveals abnormal ICP patterns in humans with hydrocephalus. Pressure variations with abnormal periodic elevations has been observed in young (DiRocco et al., 1975; Hammock et al., 1976; Shulman and Marmarou, 1971) and adult (Chawla et al., 1974; Gucer et al., 1980; Symon and Dorsch, 1975) human subjects with chronic communicating hydrocephalus. Similar ICP variations have been observed during short term monitoring in experimental models of hydrocephalus (Obenchain et al., 1973; Sibayan et al., 1970; Strecker et al., 1986). The pressure variability in hydrocephalic humans has been attributed to decreased compliance within the CSF compartment (Gucer et al., 1980) which in turn may be a result of increased resistance to CSF outflow (Borgensen, 1984).

2.6 Cerebral pathology caused by hydrocephalus

Cerebral pathology resulting from ventricular dilatation has been studied frequently in animals. Because much of the data has been collected in a poorly controlled manner from a variety of models there are many conflicting results. Available information regarding changes in the

human brain, although not extensive, is comparable to the data obtained from experimental animals. In a study comparing nine different animal models, Hirayama (1980) concluded that age and mode of induction of hydrocephalus were important factors in determining the pathology. Hydrocephalus caused by genetic mutations, viral infections, and teratogens may be associated with pathological changes in addition to those caused by the ventricular dilatation. For this reason, only the pathology of human hydrocephalus and experimental hydrocephalus induced by physical obstruction of the CSF pathways will be considered in this review.

2.6.1 Effect of hydrocephalus on the ependyma

Hydrocephalus has been shown to affect the ependymal lining of the cerebral ventricles. A detailed review of this subject has recently been published by the author and collaborators (Bruni et al., 1985). The following is an updated version of that review.

Early reports described the ventricular lining of human hydrocephalic brains as "sandy" with thickened neighboring membranes (Dickinson, 1870) or "boggy" and easily separated from the subependyma (Burr and McCarthy, 1900). More recently, ependyma ranging from normal (Bannister and Mundy, 1979) to totally destroyed (DiRocco et al., 1977; Rowlatt, 1978; Russell, 1949) has been also described in association with varying degrees of hydrocephalus. Highly attenuated

ependymal cells have been demonstrated in infants with hydrocephalus (Del Bigio et al., 1985; Weller and Shulman, 1972).

In young and adult animals with hydrocephalus, initial damage consists of flattening, stretching, and disruption of the ependyma (Akai et al., 1987; De, 1950; James et al., 1975, 1977, 1980; Ogata et al., 1972; Page, 1975; Page et al., 1979a; Rubin et al., 1976; Weller et al., 1969b, 1971) beginning as early as 1-12 hours after CSF obstruction (Clark and Milhorat, 1970; Diggs et al., 1986). Stretching of the ependyma is evidenced by separation of clusters of cilia on the surface and exposure of the microvilli (Miyagami et al., 1976; Torvik and Stenwig, 1977). Supraependymal macrophages also appear on the ependymal surface (DiRocco et al., 1979; Go et al., 1976; Gonzalez-Darder et al., 1984; James et al., 1980; Page, 1975; Torvik et al., 1981). Focal denudation of ependyma occurs in severely affected regions (Flor et al., 1979; Ogata et al., 1972; Price et al., 1976) and, in extreme cases, there may be widespread ependymal cell loss (De, 1950).

The ependyma overlying white matter along the roof and dorsolateral angle of the lateral ventricle is most severely affected (Page, 1975). In contrast, ependymal alterations are minimal over gray matter (Flor et al., 1979; Gopinath et al., 1979; Hochwald et al., 1969; James et al., 1980; Ogata et al., 1972; Page 1975; Torvik and Stenwig, 1977). Page et al. (1979a) suggested that the tortuous intercellular clefts observed between squamous ependymal cells overlying white

matter in the lateral ventricle provide a mechanism by which the ependymal lining can enlarge in hydrocephalus. The interdigitating lateral processes of adjoining cells could be stretched to increase the ependymal surface area (Page and Leure-duPree, 1983; Torvik et al., 1976). Because the ependyma over periventricular gray matter does not possess the overlapping lateral processes, such a sliding mechanism cannot occur in that region. Ependyma can likely stretch only at a finite rate, however, therefore animals with more gradually expanding ventricles are more likely to retain an intact ependymal lining (Collins, 1979).

The possibility that newly formed ependymal cells are added to the lining to maintain its integrity has been suggested. Clark and Milhorat (1970) found, in acutely hydrocephalic monkeys, evidence that new ependymal cells are produced from subependymal germinal cells. Page (1975) postulated that new cells devoid of cilia but rich in microvilli might be added to the ventricular surface by insinuating themselves between the pre-existing cells. An increase in the number of hypertrophic ependymal cells has been reported in chronically hydrocephalic primates (Flor et al., 1979; James et al., 1980). However, the so-called supra-ependymal precursors described in those studies appear to be macrophages. Other authors have stated without evidence that ependymal regeneration occurs in hydrocephalic experimental animals (Gonzalez-Darder et al., 1984) and humans (Rowlatt, 1978). Russell (1949) asserted that

ependymal cells have little or no regenerative capacity and that mitotic ependymal cells had not been identified in hydrocephalic brains. Based on quantitative studies of neonatal rats with hydrocephalus, Weller et al. (1978) concluded that the ependyma is a stable population that does not proliferate to a significant degree in hydrocephalus. Collins (1979) supported their conclusion and Page and Leure-duPree (1983) have since reported that no new ependymal cells are added to the ventricular surface in hydrocephalus.

Hydrocephalus induced changes in the choroidal epithelium, which is derived from the same cell lineage as ependyma, are less well documented than ependymal changes. Atrophy of the choroid plexus has been observed in chronically hydrocephalic humans (DiRocco et al., 1977; Russell, 1949). Experimental hydrocephalus of 1 month duration caused choroidal cell flattening, vacuolation, and distortion of microvilli (Dohrmann, 1971; Go et al., 1976; Hochwald et al., 1969). Intracellular inclusions and enlargement of the extracellular spaces have also been described (Liszczak et al., 1984; Miyagami et al., 1976). Dohrmann (1970) reviewed the literature concerning vitamin deficiency hydrocephalus and found a similar spectrum of choroid plexus pathology in those studies. The choroid plexus, however, has also been reported to be normal in hydrocephalic animals (Collins, 1979; De, 1950; Hochwald et al., 1969).

2.6.2 Effect of hydrocephalus on the subependymal region of the ventricles

Proliferation of astrocytes, reactive astrocytosis, and increased numbers of subependymal astroglial fibers are common findings in chronic hydrocephalus (Clark and Milhorat, 1970; DiRocco et al., 1977, 1979; Glick et al., 1984; Gonzalez-Darder et al., 1984; Hirayama, 1980; James et al., 1980; Miyagami et al., 1976; Ogata et al., 1972; Rowlatt, 1978; Rubin et al., 1976b; Weller et al., 1969, 1978). Following the loss of ependyma, a thickened gliotic subependymal layer is exposed to the CSF of hydrocephalic humans (Russell, 1949). Rubin et al. (1976b) concluded from nucleic acid analysis of hydrocephalic cat brains that gliosis was due to hypertrophy of pre-existing cells and not to increased cell division. Astrocytes, however, have considerable proliferative potential (Kaplan, 1983; Korr, 1980) and Weller et al. (1978) found increased numbers of cells in the subependymal region of the lateral ventricles of hydrocephalic neonatal rats. The absence of subependymal astrogliosis has only rarely been reported in experimental animals (De, 1950; Nyberg-Hansen et al., 1975).

2.6.3 Effect of hydrocephalus on white matter of the cerebrum

In severely hydrocephalic brains, thinning of the corpus callosum and central white matter is a consistent finding in both humans (Gadsdon et al., 1978; Penfield,

1929; Russell, 1949) and experimental animals (De, 1950; DiRocco et al., 1979; Edwards et al., 1984; Nakayama et al., 1983; Nyberg-Hansen et al., 1975). As in the subependymal region, astrogliosis has been reported to occur within the white matter itself following ventricular dilatation (Edwards et al., 1984; Weller and Williams, 1975).

Demyelination of intact axons, especially around the frontal horns of the lateral ventricles, has been reported in histological studies (Akai et al., 1987; Clark and Milhorat, 1970; DiRocco et al., 1977; Gadsdon et al., 1978; Price et al., 1976; Rubin et al., 1976c; Yakovlev, 1947) and in biochemical studies (Rubin et al., 1976b). Evidence that periventricular axonal degeneration precedes demyelination has also been reported (De, 1950; DiRocco et al., 1979; Glick et al., 1984; James et al., 1977; Milhorat et al., 1970; Miyagami et al., 1976; Rubin et al., 1975, 1976a; Weller et al., 1969, 1971; Weller and Mitchell, 1969; Weller and Williams, 1975; Weller and Wisniewski, 1969). Although periventricular axonal damage may begin in the acute stages of hydrocephalus (Weller et al., 1971), loss of axons is most evident in the chronic stages (DiRocco et al., 1979; Miyagami et al., 1976). Degenerative changes have been found in descending axons within the spinal cord of humans (Yakovlev, 1947) and experimental animals (James et al., 1977) with prolonged hydrocephalus.

Edema in the periventricular white matter (Section 2.6.6) has been suggested to be the cause of myelin damage (Feigin, 1983; Weller and Wisniewski, 1969) but the

consensus is that the two changes have a common cause rather than a cause-effect relationship. Nevertheless, pathological changes in the periventricular region may be difficult to interpret and many of the changes reported in axons and myelin may be artifacts of poor fixation due to the edema. Indeed, Rowlatt (1978) concluded that "at present, the evidence for actual destruction of white matter ... is not strong." Several studies have found no degradative changes in periventricular axons of hydrocephalic brains (Fishman and Greer, 1963; Friede, 1962; Nyberg-Hansen et al., 1975; Rowlatt, 1978; Torvik and Stenwig, 1977). The appearance of abnormally large amounts of myelin basic protein, a major constituent of myelin, in the CSF of hydrocephalic humans (Sutton et al., 1983) suggests, however, that damage to periventricular myelin can occur when ventricular dilatation is sufficiently severe.

2.6.4 Effect of hydrocephalus on neurons and neurotransmitters

Severe hydrocephalus causes thinning of the cortex (Edwards et al., 1984; Orton, 1908; Penfield, 1929; Yakovlev, 1947) and stretching or fenestration of the neuropil of the septal area (Clark and Milhorat, 1970; De, 1950; DiRocco et al., 1979; Russell, 1949; Weller et al., 1971). Atrophy of the basal ganglia has also been reported (De, 1950; DiRocco et al., 1977).

Neuronal pathology has been observed in cerebral cortex

distant from the dilated ventricles. Yakovlev (1947) reported a decreased number and reduction in size of large pyramidal neurons in the paracentral lobules of two chronically hydrocephalic humans. In a Golgi impregnation study, McAllister et al. (1985) found a loss of dendritic spines and increased numbers of dendritic varicosities on pyramidal neurons of the parieto-occipital cortex of neonatal rats, 10-12 days after induction of hydrocephalus. Chromatolysis, swelling, vacuolation, membrane disruption, and pyknotic degeneration have been observed in small numbers of neurons located in periventricular regions adjacent to the dilated ventricles (De, 1950; Gopinath et al., 1979; Penfield, 1929; Weller et al., 1969, 1971; Weller and Wisniewski, 1969). Many authors, however, have reported that neurons in the cortex and basal ganglia were normal in spite of hydrocephalus (Edwards et al., 1984; Glick et al., 1984; Nakayama et al., 1983; Orton, 1908; Rowlatt, 1978; Rubin et al., 1975, 1976a, 1976c; Russell, 1949; Weller et al., 1971; Weller and Williams, 1975). In those studies, subtle neuronal changes may have gone undetected following examination by standard light microscopic techniques alone.

Altered concentrations of neurotransmitters in the brain and CSF may reflect damage to neurons caused by hydrocephalus. Monoamine transmitters and their metabolites have been studied most frequently. Although abnormalities have not been found by all investigators (Yates and Minns, 1981), hydrocephalus associated with elevated CSF pressure in adults (Massarotti and Roccella, 1975) and children

(Andersson and Roos, 1965; Kawano et al., 1980; Rogers and Dubowitz, 1970) has caused elevated levels of homovanillic acid and 5-hydroxyindoleacetic acid in CSF. The changes in these metabolites of dopamine and serotonin respectively are suggestive of deranged metabolism. Rats and dogs with hydrocephalus of 2 weeks duration have also been shown to have increased CSF levels of 5-hydroxyindoleacetic acid (Andersson, 1968), possibly as a result of decreased removal from the CSF (Andersson and Roos, 1968).

In general, the effect of hydrocephalus on neurotransmitter concentrations in the brain is highly variable and difficult to interpret. Forebrains of chronically hydrocephalic rabbits have been reported to contain both elevated (Higashi et al., 1986) and reduced (Edvinsson et al., 1972; Miwa et al., 1982; Owman et al., 1971) quantities of dopamine and its metabolites. Forebrain content of serotonin is reported to be decreased in acutely hydrocephalic rabbits (Owman et al., 1971) and its metabolite increased in chronically hydrocephalic rats (Higashi et al., 1986). Studies have shown that forebrain noradrenaline is decreased acutely (Owman et al., 1971) and chronically (Ehara et al., 1982) during the course of hydrocephalus while other studies have found that noradrenaline (Higashi et al., 1986) and its metabolite methoxyhydroxyphenylglycol (Miwa et al., 1982) are increased chronically. Hydrocephalus also alters the concentrations of monoamine transmitters in other brain regions, however,

these data are inconsistent also.

2.6.5 Effect of hydrocephalus on the cerebrovasculature

Studies conducted on hydrocephalic humans have revealed decreased cerebral blood flow, especially in the frontal lobes, prior to shunting (Brooks et al., 1986; Kushner et al., 1984; Lying-Tunell et al., 1981; Meyer at al., 1985; Tamaki et al., 1984; Vorstrup et al., 1987). Decreased cerebral blood flow has been found to be more dependent upon ventriculomegaly than on elevated ICP (Hill and Volpe, 1982). Microsphere studies showed that adult hydrocephalic cats had decreased blood flow in the caudate nucleus but not in the cortex, periventricular white matter, or choroid plexus (Nakamura and Hochwald, 1973). Recent studies, however, showed reduced blood flow in cortex, thalamus, white matter, and midbrain of acutely and chronically hydrocephalic cats (Higashi et al., 1986; Rosenberg et al., 1983). Higashi et al. (1986) also demonstrated impaired metabolism, presumably due to decreased cerebral blood flow, in similar brain regions of rabbits and rats during the 2 weeks following induction of hydrocephalus. Although young rats developed no decrease in glucose utilization, an indicator of metabolic activity and blood flow, in any brain region as a result of hydrocephalus (Richards et al., 1985), adult rats have been shown to have decreased glucose utilization in the cortex and thalamus (Wako, 1983).

Penfield (1929) suggested that distortion of brain

tissue might compromise the vasculature of hydrocephalic brains. Altered architecture of arteries and arterioles in the mesencephalon, diencephalon, and periventricular regions of hydrocephalic dogs was attributed to physical distortion of the brain (Plets and van den Bergh, 1973). Paradoxically those dogs (Plets, 1979) and other animals with experimentally induced hydrocephalus developed subependymal hypervascularization (Hirayama, 1980; Sahar et al., 1971). The brains of hydrocephalic humans and rats were also found by Hassler (1964) to have more numerous arteries and veins running along the walls of the dilated ventricles although the pial and cortical vessels and capillaries in the white matter appeared normal.

In contrast, Gadsdon et al. (1978) found fewer capillaries in the corpus callosum of hydrocephalic human brains than in normals. Hydrocephalic rats also have a reduced number and narrower caliber of capillaries in the white matter and basal ganglia (Oka et al., 1985). Reduced numbers of patent capillaries have been demonstrated in the white matter and cortex of hydrocephalic mice (Wozniak et al., 1975), in the white matter of kaolin-induced hydrocephalic rats (Okuyama, 1987) and dogs (Sato et al., 1984), and in the caudate, septal area, corpus callosum, and fornix of India ink induced hydrocephalic rats (De, 1950). De (1950) attributed periventricular ependymal, axonal, and neuronal destruction to ischemia that resulted because elevated CSF pressure collapsed the periventricular vessels.

Akai et al. (1987) also concluded that sclerotic periventricular blood vessels in human hydrocephalic brains might cause local brain ischemia. If sufficiently widespread, capillary loss in hydrocephalic brains could explain the observations of decreased cerebral blood flow (Moskalenko et al., 1980).

The endothelial cells of periventricular capillaries in hydrocephalic brains were reported in one study to have a normal ultrastructure (Ogata et al., 1972) whereas edematous cytoplasm was reported in another study (Gopinath et al., 1979). Recently, the endothelial cells of capillaries in the periventricular white matter of hydrocephalic rats have been shown to develop separations at the tight junctions (Nakagawa et al., 1984, 1985; Okuyama et al., 1987). The authors speculated that this may represent an alternate pathway for CSF absorption that permits passage of small molecules into the blood. Although this hypothesis conflicts with the observation that transfer of tracer molecules from the extracellular fluid into periventricular capillaries is impaired by raised ICP (Rosenberg et al., 1983), Bundgaard (1986) has concluded that paracellular movement of substances across the blood brain barrier may be the major route for molecular transfer under normal and pathological conditions.

2.6.6 Effect of hydrocephalus on cerebral water content and extracellular spaces

Histological examination of hydrocephalic brains

consistently reveals enlargement of extracellular spaces in the white matter adjacent to the ventricular wall (DiRocco et al., 1977, 1979; Go et al., 1976; Gopinath et al., 1979; Hirayama, 1980; James et al., 1977, 1980; Miyagami et al., 1976; Nyberg-Hansen et al., 1975; Ogata et al., 1972; Page et al., 1979a; Price et al., 1976; Rubin et al., 1976c; Torvik and Stenwig, 1977; Weller et al., 1969, 1971; Weller and Mitchell, 1969; Weller and Wisniewski, 1969). Measurement of tissue water content by tissue drying or specific gravity analysis have also shown water content to be above control levels in the periventricular regions of hydrocephalic rabbits (Higashi et al., 1986), cats (Hochwald et al, 1975), and dogs (Fishman and Greer, 1963; Inaba et al., 1984). Although the extent of extracellular edema has been documented ultrastructurally to a depth of 200 um from the ventricular surface (Del Bigio et al., 1985; Ogata et al., 1972; Weller et al, 1971), computed tomographic scans performed on hydrocephalic humans and animals suggest that "periventricular edema" extends several millimeters from the ventricle (Asada et al., 1978; Hiratsuka et al., 1982; Hopkins et al., 1977; Murata et al., 1981). Takei et al. (1987) showed that rapid ventricular enlargement and elevated ICP raise the water content of white matter up to 3 mm from the surface of the frontal horn in cats.

Enlarged extracellular spaces near the surface of the ventricle (Levin et al, 1971; Shaywitz, 1972) are said to act as diffusional pathways for displaced CSF (Page, 1985;

Strecker et al., 1974; Wislocki and Putnam, 1921). Continuity between the CSF and extracellular fluid spaces has been demonstrated in hydrocephalic animals (James et al., 1980; Ogata et al., 1972; Page et al., 1979a; Weller et al., 1971). Several studies have indicated that tracer substances in the CSF cross the ependymal lining during the acute stages of hydrocephalus (Lux et al., 1970; Milhorat et al., 1970; Miyagami et al., 1976; Rosenberg et al., 1983; Sahar et al., 1969). As a result of the separation or destruction of ependyma that occurs in hydrocephalus, movement of CSF into the periventricular tissue may establish an alternate pathway for flow of CSF which results in decreased ICP (Milhorat et al., 1970; Ogata et al., 1972). Stretched and flattened but otherwise intact ependyma, however, is not inconsistent with transmural flow of CSF (Nyberg-Hansen et al., 1975).

In the caudate nucleus of hydrocephalic animals, the extracellular space has been reported to be of normal dimensions (Page et al., 1979a; Torvik and Stenwig, 1977). In the cortex of congenitally hydrocephalic mice, however, extracellular spaces are compressed during the acute stages of hydrocephalus and enlarged during later stages (McLone et al., 1973). In biopsied cortex of hydrocephalic humans, extracellular spaces have also been reported to be enlarged (Foncin et al., 1976). Physical methods of measurement have revealed decreased water in the cortex of hydrocephalic cats (Kuchiwaki et al., 1979) but not of hydrocephalic rabbits (Higashi et al., 1986). These varied findings do not clearly

indicate whether there is more or less water in the gray matter of hydrocephalic brains. Computed tomographic scans, however, suggest that there is decreased water in the cortex of hydrocephalic human brains (Penn and Bacus, 1984).

2.7 Treatment of hydrocephalus by CSF shunting

2.7.1 Efficacy of shunting

Various techniques of CSF shunting have been used since the beginning of the 20th century (Pudenz, 1981; Wallman, 1982) and shunting has been shown to improve the clinical course of hydrocephalic patients (Foltz and Shurtleff, 1963). Shunting is presently the most widely used form of treatment for hydrocephalus (Hoffman and Smith, 1986). Despite the clinical improvement enjoyed by many patients, the symptoms of as many as fifty percent of shunted adult hydrocephalic patients are not improved by reduction of ventricular size (Hughes et al., 1978).

Comparatively few studies have examined the ability of shunting to reverse or prevent the pathological changes caused by hydrocephalus. There is no doubt that shunting can reduce the size of the ventricles of hydrocephalic humans (Emery, 1965) and animals of all ages (Epstein et al., 1974; Granholm, 1966; Michejda et al., 1984). Clinical improvement following shunting, however, is not necessarily due to reduction in ventricular size (Shenkin et al., 1975). Although Emery (1964, 1965) found the brains of shunted hydrocephalic children to be within the normal range for

weights, those brains exhibited residual atrophic changes.

Gadsdon et al. (1978, 1979) compared the morphology of human hydrocephalic brains with that of shunted hydrocephalic brains and normal brains. They concluded that hydrocephalus controlled by shunting is associated with normal myelination, vascularization, and cellularity of the corpus callosum. In contrast, uncontrolled hydrocephalus was associated with abnormalities of these three tissue components. The ventricles of shunted hydrocephalic cats returned to normal size within 48 hours but the ependymal damage and white matter edema due to hydrocephalus were still present. By 1 week, the ependyma was normal in places but astrogliosis and myelin damage persisted (Rubin et al., 1975, 1976a; Rubin and Hochwald, 1983). Damaged ependyma, subependymal gliosis, and damaged white matter also persisted in shunted hydrocephalic fetal lambs following shunting (Glick et al., 1984). The flattened, vacuolated cells of the choroid plexus in hydrocephalic dogs, however, appear to return to normal following shunting (Dohrmann, 1971) and drainage of CSF from congenitally hydrocephalic mice allows the vascular architecture to regain a normal appearance (Wozniak et al., 1975). Finally, shunting has been demonstrated to reduce the flow of CSF into the periventricular tissues of hydrocephalic animals (Ito, 1976).

Investigators have concluded that the pathological changes resulting from hydrocephalus might be reversible

if shunting is performed early in the course of the disorder (Epstein et al., 1974; Gopinath et al., 1979; McAllister et al., 1985; Michejda et al., 1984; Weller and Williams, 1975). Weller et al. (1975, 1978), however, stated that gliosis and axonal damage, once established, are probably not reversible.

2.7.2 Complications of shunting

Although effective in the treatment of hydrocephalus, shunting procedures are associated with complications that necessitate frequent revisions (Alexander, 1981; Sayers, 1976). Currently, the infection rate for shunt operations is approximately 4% and the mortality rate negligable (Shurtleff et al., 1985). Patients require an average of 2 revisions of their shunt apparatus (Hoffman et al., 1982). Obstruction of the proximal catheter located within the cerebral ventricle has been reported to be the most common complication (Occhipinti et al., 1980; Sekhar et al., 1982). Ventricular catheters obtained at the time of revision have been found to be occluded by ependyma, glia, brain tissue, and choroid plexus (Bigner et al., 1985; Collins et al., 1978; Go et al., 1981; Hakim, 1969; Reinhardt and Nau, 1980; Sekhar et al., 1982; Zumstein and Landolt, 1974). Giuffre (1976) suggested that choroid plexus and ependyma may respond to the presence of the shunt catheter by growing around and into the catheter.

3. MATERIALS AND METHODS

3.1 Animal care and anesthesia

One hundred and one 4-5 month old male New Zealand White rabbits (2.5-3.0 kg) were used in this investigation. All were cared for in accordance with the guidelines of the Canadian Council on Animal Care. The rabbits were individually caged in rooms maintained at 20°C and illuminated for 12 hours per day. Pellet food and tap water were available ad libitum.

During all operative procedures the rabbits were premedicated with atropine (0.2 mg/kg, intramuscular) and anesthetized with intramuscular injections of ketamine (35 mg/kg) - xylazine (5 mg/kg). Anesthesia was supplemented with acepromazine (1 mg/kg, intramuscular) during the more lengthy ICP transducer implantation. While under anesthesia, rabbits were allowed to breathe spontaneously and body temperature was maintained with a warming blanket. All surgical procedures were performed under aseptic conditions with the head and neck shaved. With the neck flexed, the head was secured in a zygomatic clamp (David Kopf Inst.; Tujunga, CA). Following surgery, the rabbits were allowed to recover from the anesthesia before being returned to their cages. No prophylactic systemic antibiotics were administered.

3.2 Induction of hydrocephalus

Forty-one rabbits were used in this part of the study.

Through a vertical skin incision, the dorsal cervical muscles were divided in the midline to expose the atlanto-occipital membrane. A #20 gauge polyethylene catheter was inserted through the membrane into the cisterna magna and, following removal of 1.0-1.5 ml of CSF, silicone oil (dimethyl polysiloxane, Sigma Chemical Co.; St. Louis, MO) of 5000 centistoke viscosity was injected (0.5ml/kg) over a 5-10 minute period. To prevent reflux of the oil, a gelatin sponge was placed over the punctured membrane and the overlying muscles and skin were sutured. Sham-operated control rabbits received an intracisternal injection of an equivalent volume of sterile saline solution (0.9%) but were otherwise treated identically.

Rabbits were sacrificed (Section 3.7) at intervals of 3 days (n=3) and 1 (n=4), 2 (n=2), 4 (n=4), 6 (n=3), and 8 (n=3) weeks following injection of silicone oil. Sham-operated controls (n=4) were sacrificed at 1 week post-injection along with intact, unoperated control rabbits (n=2). Sixteen randomly selected rabbits that had been injected with silicone oil underwent a subsequent CSF shunting procedure (Section 3.6) at 1 (n=5), 4 (n=2), or 8 weeks (n=9) after silicone oil injection.

3.3 Intracranial pressure monitoring

Fourteen rabbits were used in this part of the study. Through a midline scalp incision, a craniectomy (6 x 10 mm) was made over the coronal suture, 1 mm from the sagittal

suture. Following calibration using a mercury manometer, the sensor tip of a 12 cm long intracranial pressure transducer (Model ICT/b, Medical Measurements Inc., Gaeltec; Hackensack, NJ) was inserted through the opening into the epidural space over the frontal lobe (Figure 1) and the skull defect was sealed with bone wax. The transducer connecting plug was secured to a 1 x 10 cm stainless steel support anchored to the skull with screws and dental acrylic. After the scalp was sutured, betadine ointment was applied to the exit sites of the support and transducer catheter.

Extradural ICP was recorded from the time of transducer insertion until recovery from anesthesia and again 6 hours later using an amplifier (Gould Inc.; Cleveland, OH) and strip chart recorder. ICP recordings of 20-40 minute duration were obtained daily thereafter in the conscious, unrestrained rabbits. Prior to each recording the transducer was recalibrated. Activities of the rabbits during the recording sessions were correlated with ICP changes. Without further intervention, six rabbits underwent daily pressure recordings. When the amplitude of the ICP pulse wave began to deteriorate, recordings were discontinued.

The eight remaining rabbits were re-anesthetized 1-21 days after ICT/b implantation and hydrocephalus was induced by intracisternal injection of silicone oil (Section 3.2). ICP was monitored during this procedure, during the recovery period, and daily thereafter as described above. At the end of the experimental period, all rabbits were sacrificed

Figure 1. Diagram of the dorsal aspect of the rabbit skull showing placement of the ICT/b intracranial pressure transducer. The 2 mm diameter transducer cable (cross hatching) extends from the connecting plug (ICT/b) through a craniectomy to the sensor inserted under the skull. The transducer is secured to a stainless steel support which is anchored to the skull by screws and dental acrylic cement (stippling). In parasagittal section (lower diagram) the flat sensor tip of the transducer is shown in the epidural space with its connecting cable (cross hatched) traversing the skull opening. SAS, subarachnoid space.

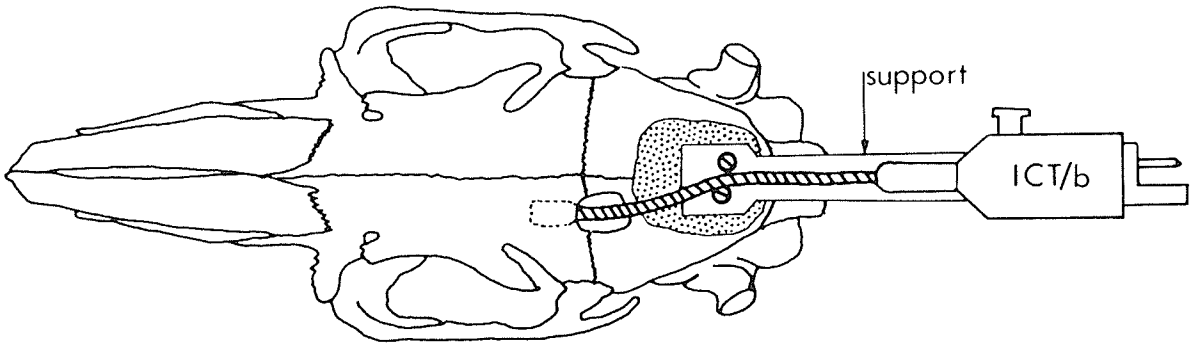
support
ICT/b

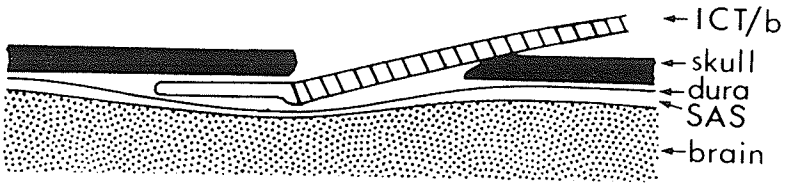
ICT/b
skull
dura
SAS
brain

(Section 3.7) to permit confirmation of hydrocephalus.

3.4 Determination of specific gravity of the cerebrum

Twenty rabbits were used in this part of the study. Rabbits were sacrificed by decapitation at one week (n=5) following saline injection or 3 days (n=4), 1 (n=5),and 4 weeks (n=6) following induction of hydrocephalus (Section 3.2). The unfixed brains were removed intact from the skull and, over dry ice in a humid atmosphere, sectioned coronally at the level of the anterior commissure. Size of the frontal horns was assessed visually on these sections to confirm ventriculomegaly.

Tissue samples of cerebrum rostral to the anterior commissure were then excised bilaterally using a 4.5 mm diameter cylindrical punch. The tissue which extended from the pial to the ventricular surface was then sectioned serially at 0.5 mm intervals (Figure 2) to produce discs of tissue weighing 40-50 mg. Tissue samples were placed immediately into kerosene and allowed to thaw for 2-3 minutes at room temperature. Specific gravity of the tissue was then determined by recording the depth to which samples sank within 1 minute after being gently placed into a kerosene - bromobenzene gradient column.

Comparable bilateral samples of cerebral tissue caudal to the level of the anterior commissure were also serially sectioned at 0.5 mm intervals, placed in aluminum foil envelopes, and desiccated at 100^{o}C for 3 days. Specific

Figure 2. Diagram of a coronal section through the rabbit cerebrum at the level of the anterior commissure showing the location of tissue samples taken for specific gravity determinations. From each cylindrical tissue sample (4.5 mm diameter), extending from the pial to ventricular surface, up to eight serial slices (0.5 mm thick) were taken . C1 and C2 represent slices of gray matter near the pial surface, V1 and V2 represent slices of white matter near the ventricular surface and M represents the intervening slices of gray matter. CC, corpus callosum; NC, caudate nucleus; SA, septal area; V, frontal horn of lateral ventricle.

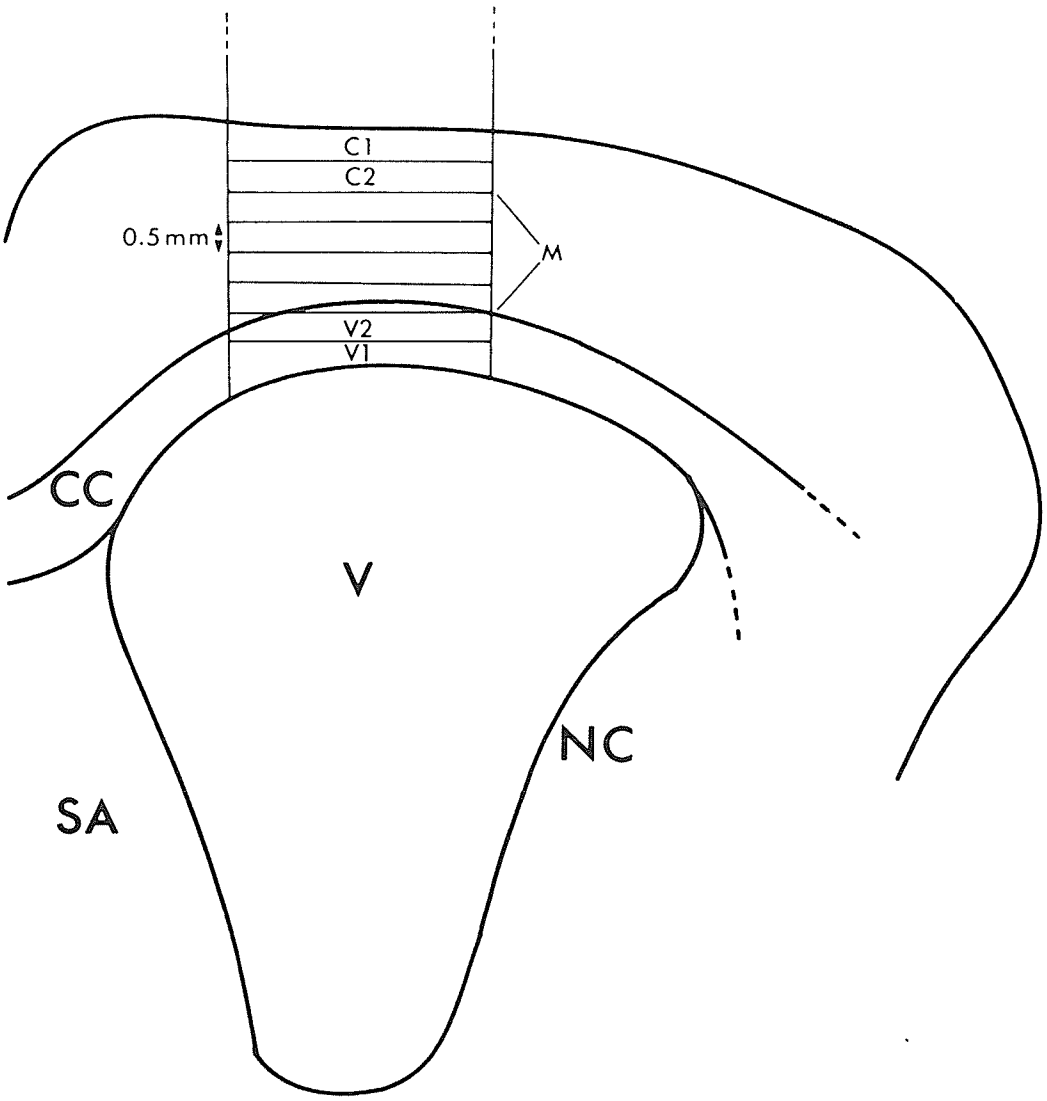
C1
C2
0.5 mm
M
V2
V1
CC
V
NC
SA

gravity of these dehydrated cerebral tissue samples weighing 5-10 mg each was determined as described above.

Prior to each experiment, 500 ml kerosene - bromobenzene specific gravity gradient columns were prepared according to the method described by Marmarou et al. (1978) and allowed to stabilize at room temperature for two hours before use. For hydrated tissue determinations, kerosene - bromobenzene mixtures with initial specific gravity values of 1.02 and 1.07 g/cm^3 were used to prepare the final gradient columns. Calibration of these columns was achieved using aqueous potassium sulfate solutions with specific gravity values of 1.025, 1.03, 1.035, 1.04, 1.045, 1.05, 1.055, and 1.06 g/cm^3 (Wolf et al., 1983). For desiccated tissue determinations, the initial kerosene - bromobenzene mixtures had specific gravities of 1.02 and 1.32 g/cm^3. Calibration was achieved using aqueous sucrose solutions with specific gravities of 1.1, 1.15, 1.2, 1.25, and 1.3 g/cm^3 (Wolf et al., 1983). Correlation coefficient analysis showed all specific gravity gradient columns to be highly linear.

3.5 Shunt implantation into the ventricle of non-hydrocephalic rabbits

Twenty-six rabbits were used in this part of the study. Through a midline scalp incision, bilateral 5 mm diameter craniectomies were made 1 mm from the sagittal suture, immediately rostral to the coronal suture. Through cerebral incisions, the frontal horns of the lateral

ventricles were opened. A sterile 5 mm long piece of barium-impregnated silicone rubber shunt tubing (2 mm outside diameter) with six 0.4 mm side holes was then inserted into each frontal horn. The wound was then irrigated with a 0.9% saline solution and the scalp sutured. Sham-operated control rabbits were identically treated except that no shunt tubing was implanted into the opened ventricles.

Rabbits were sacrificed (Section 3.7) at post-implantation intervals of 3 days (n=3) and 1 (n=3), 2 (n=3), 3 (n=2), 4 (n=3), 6 (n=3), 8 (n=3), and 16 weeks (n=2). Sham-operated rabbits (n=2) were sacrificed 1 week post-operatively along with intact rabbits (n=2). The response of the periventricular tissue to non-functioning shunts was studied in these rabbits and compared to that in shunted hydrocephalic rabbits.

3.6 Shunt insertion into the ventricle of hydrocephalic rabbits

Hydrocephalic rabbits were re-anesthetized 1 (n=5), 4 (n=2), and 8 (n=9) weeks following injection of silicone oil. Through a midline scalp incision, a 4 mm diameter unilateral craniectomy was made in the skull over the coronal suture, 1 mm from the sagittal suture. A sterile barium impregnated silicone rubber shunt catheter was inserted into the frontal horn of the lateral ventricle. After CSF flow was established, the distal end of the shunt was tunneled under the skin of the neck and into a pocket

created in the subcutaneous tissue over the scapulae. Two of the 8 week hydrocephalic rabbits were shunted into the peritoneal cavity. The shunts were secured to the skull with acrylic cement and the scalp was sutured.

One week following the CSF shunt procedure, 1 week (n=5) and 8 week (n=5) hydrocephalic rabbits were sacrificed (Section 3.7). The 4 week (n=2) and remaining 8 week hydrocephalic rabbits (n=4) were sacrificed 4 weeks after shunting. Patency of the CSF shunt was tested following sacrifice.

3.7 Sacrifice of animals and fixation of tissue

At the time of sacrifice, animals were anesthetized with pentobarbital (50 mg/kg) injected intravenously. They were then perfused by the transcardiac route with 2.5% glutaraldehyde - 2% paraformaldehyde in 0.12 M phosphate buffer with 0.02 mM calcium chloride. The 37°C fixative was delivered from a column height of 110 cm. The brains were removed from the skull intact and stored overnight in a fresh mixture of the same fixative at 4°C. Subsequent preparation of tissue for microscopy is described in Section 3.9.

Randomly selected hydrocephalic rabbits, non-hydrocephalic shunt implanted rabbits, and appropriate controls received a subcutaneous injection of colchicine (2mg/kg) 6 hours prior to sacrifice to arrest dividing mitotic cells in metaphase (Leblond and Walker, 1956).

3.8 Determination of ventricular size

The fixed brains of shunted and non-shunted hydrocephalic rabbits along with their controls were sectioned coronally at the level of the anterior commissure, the mid-tuberal hypothalamus, and the mammillary bodies and the cut surfaces were photographed. Areas and perimeters of the lateral and third ventricles and cerebrum were measured on x10 magnification photographs of the three coronal levels by computerized planimetry (Stereometric Image Processing Programs Rev. 3.2, Scientific Microprograms, 1980; Apple II+ computer and Apple Graphics Tablet, Apple Computer Corp., CA). At each coronal level a ratio of the area of the ventricle to the area of the cerebrum was calculated as an index of the degree of ventricular dilatation. A ratio of the perimeter of the ventricle to the perimeter of the cerebrum was also calculated to quantify the degree of periventricular tissue stretching associated with ventricular dilatation.

3.9 Preparation of tissue for microscopy

Following fixation and photography of the brain slices, tissue samples were excised from the following regions: the walls of the frontal horn of the lateral ventricle, the walls of the posterior horn of the lateral ventricle, the walls of the third ventricle, and the floor of the fourth ventricle. Where shunt catheters had been inserted into either non-hydrocephalic or hydrocephalic rabbits, the

tissue blocks were processed with the shunt tubing in situ. All tissue samples were post-fixed in buffered 2% aqueous osmium tetroxide for 2 hours.

For light microscopy (LM) and transmission electron microscopy (TEM), specimens were stained en bloc with a saturated aqueous solution of uranyl acetate, dehydrated in graded alcohols, and embedded in Epon 812. Semithin Epon sections (0.5 um thick) stained with methylene blue / azure II were used for LM examination. Ultrathin sections stained on grids with lead citrate were examined with a Philips 201 TEM. For scanning electron microscopy, tissues were dehydrated in graded ethanol solutions and critical point dried from carbon dioxide. The specimens were mounted with conductive silver paint onto studs, sputter coated with gold:palladium (60:40), and examined with a JEOL JSM 35C scanning electron microscope.

3.10 Morphometric analysis of the pathologic changes

3.10.1 Effect of ventricular dilatation on the periventricular tissue

Pathological changes in the periventricular tissue surrounding the frontal horn of the lateral ventricle were quantified and compared with sham-operated control rabbits (n=4) and 3 day and 1, 2, 4, and 8 week hydrocephalic rabbits (all n=2). Hydrocephalic rabbits of 1 and 8 week duration (both n=3) that had been shunted for 1 week were also compared. Bilateral tissue samples from non-shunted

rabbits were studied whereas tissues from shunted hydrocephalic rabbits were studied only contralateral to the hemisphere shunted.

The tissue blocks consisted of periventricular structures surrounding the frontal horn of the lateral ventricle rostral to the level of the anterior commissure. They were cut serially in the coronal plane at 25 um intervals. The caudate nucleus (CN), corpus callosum (CC), and lateral septal area (LSA) were studied in 12-15 consecutive serial sections using an ocular graticule and x40 objective magnification. Along a 200 um length of ventricular surface over the CN, CC, and LSA (Figure 3A), ependymal cells with a complete nucleus profile were counted. Astrocytes to a depth of 30 um from the ventricular surface were also counted. These values were used as indices of ventricular surface stretching and cell proliferation.

Ependymal cells over the dorsal CN (100 cells per section), the CC at the roof of the ventricle (100 cells per section), and the dorsal LSA (50 cells per section) were examined using x100 oil immersion objective magnification (Figure 3A). Cells arrested in metaphase during the 6 hour exposure to colchicine were identified and the proportion of mitotic ependymal cells was calculated. In the same regions of the wall of the ventricle, the proportion of mitotic figures among astrocytes within 30 um of the ventricular lumen was determined.

Blood vessels and neurons in the periventricular region were also examined to determine the effect of ventricular

Figure 3. Diagrams showing the frontal horn (V) of the rabbit lateral ventricle and surrounding structures in coronal section at the level of the anterior commissure.

A) Stippling indicates the locations over the corpus callosum (CC), caudate nucleus (CN), and lateral septal area (LSA) where ependymal cells and astrocytes were examined to determine the number of cells per unit length of ventricular lining and the proportion of cells in metaphase.

B) Stippling indicates the locations where blood vessels were counted in the immediate periventricular region (p) and 0.43 mm deep to the ventricular surface (d). fs, fasciculus subcallosus.

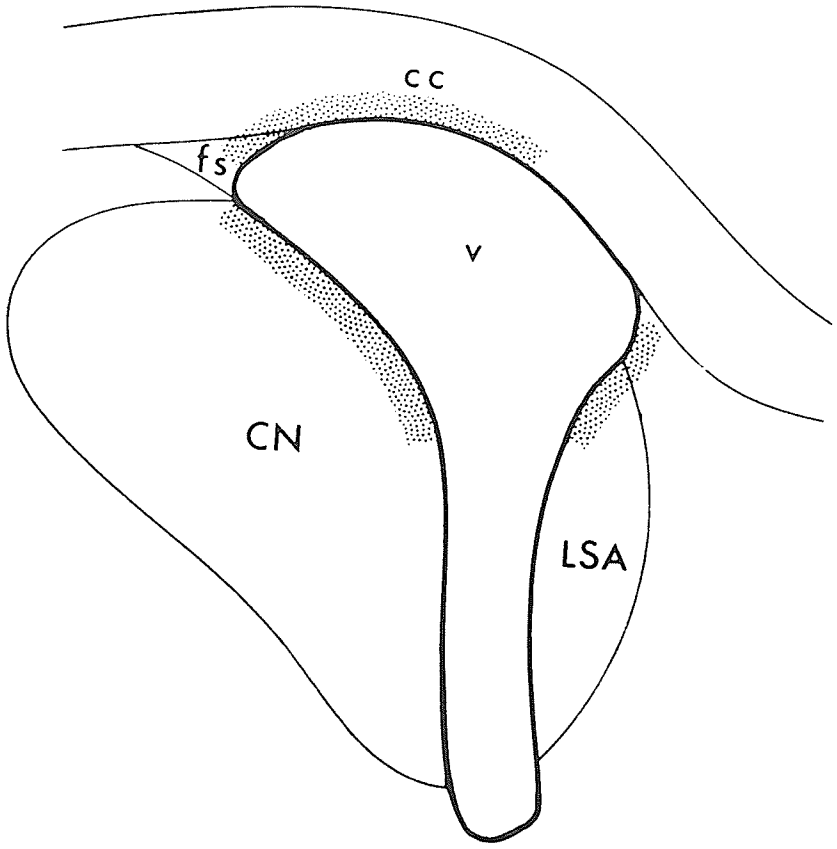

A

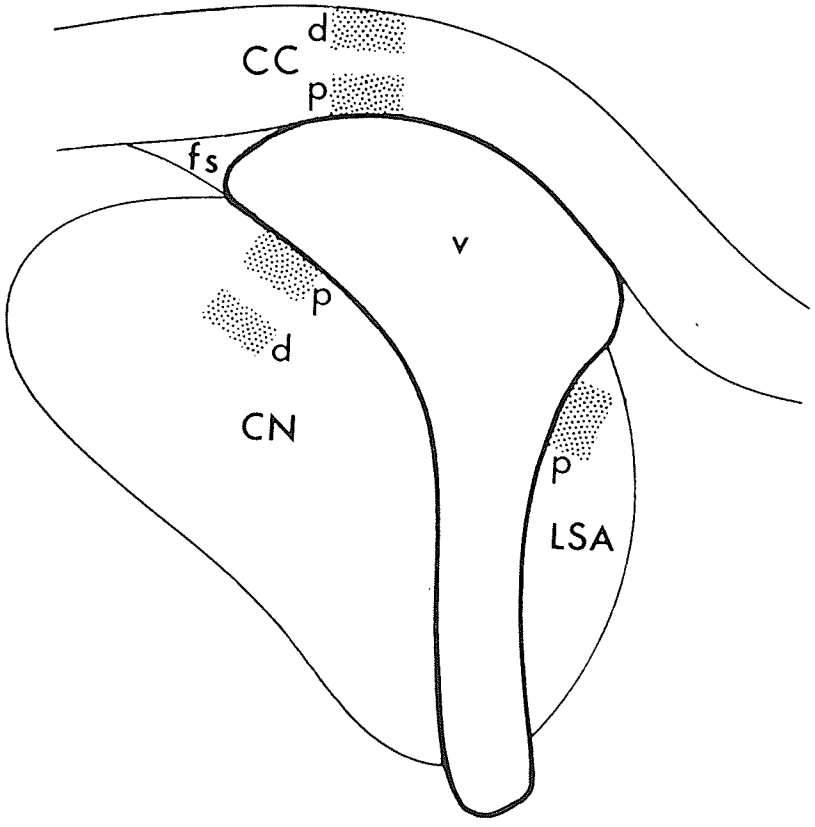

B

dilatation on them. Five consecutive sections at 100 um intervals were examined under x40 magnification oil immersion objective. The areas examined were immediately adjacent the ventricle in the caudate nucleus (CN-P), corpus callosum (CC-P), and lateral septal area (LSA-P) and 0.43 mm from the ventricular surface in the caudate nucleus (CN-D) and corpus callosum (CC-D) (Figure 3B). The lumens of blood vessels and single nucleoli of neurons within a rectangular area (0.43 x 0.28 mm) were traced onto paper using the ocular graticule and camera lucida. The number of blood vessels $\leq$10 um, 10-25 um, and $\geq$25 um and the number of nucleoli were counted in each of the five regions.

3.10.2 Effect of silicone oil on the lining of the ventricle

To exclude a mitogenic or pathogenic effect of silicone oil, the ependymal cells lining the fourth ventricle and in direct contact with the silicone oil were examined. The fourth ventricle floor of rabbits that had 1 week previously received intracisternal injections of silicone oil (n=2) or saline (n=2) were used. Tissue samples were sectioned in the coronal plane at 25 um intervals proceding caudally from the middle cerebellar peduncle. The number of ependymal cells arrested in metaphase was counted and an index of mitotic activity among ependymal cells lying between the sulci limitans was calculated.

3.10.3 Effect of shunt tubing on the periventricular tissue

To assess the effect of shunt catheters on the ventricular surface, bilateral tissue samples from intact non-hydrocephalic rabbits (n=2), sham-operated rabbits (n=2), and 3 day (n=1), 1 week (n=2), 2 week (n=2), and 4 week (n=2) shunt-implanted rabbits were examined. Specimen blocks from the frontal lobe containing the implanted tubing were sectioned serially at 25 um intervals along a plane perpendicular to the long axis of the shunt tubing. The number of mitotic ependymal cells, astroglial cells, and macrophages in the region adjacent to the implanted tubing were counted in 10 consecutive sections.

3.11 Statistical analysis of the data

ICP in control and hydrocephalic rabbits was compared using the one-tailed (Student's) t test.

Specific gravity data, numbers of ependymal cells and astrocytes per unit length of ventricular lining, and number of blood vessels and neurons per unit area were analyzed statistically in control, hydrocephalic, and shunted hydrocephalic rabbits using one-way analysis of variance (ANOVA) and post-hoc two-tailed t-tests (Steel and Torrie, 1960)

The area and perimeter ratios of the ventricle and cerebrum were compared in control and hydrocephalic rabbits using one-way ANOVA and post-hoc one-tailed t-tests (Steel

and Torrie, 1960).

Mitotic activity was compared in control and hydrocephalic rabbits (Sections 3.10.1 and 3.10.2), and control and shunt implanted rabbits (Section 3.10.3) using the one-tailed z-test (Mendenhall, 1979).

All values are expressed as mean $\pm$ standard error of the mean (SEM).

RESULTS

4.1 Effect of hydrocephalus and shunting on the size of the ventricles

Immediately following silicone oil injection, the rabbits were less active in their cages but otherwise exhibited no abnormal neurologic signs. One rabbit that underwent ICP monitoring (Section 4.2) died 10 minutes following injection of silicone oil and was found to have severe ventriculomegaly with extensive periventricular gliosis suggestive of a pre-existing chronic hydrocephalus. Necropsy of all other rabbits revealed silicone oil present in the fourth ventricle and subarachnoid space surrounding the brainstem. Silicone oil compressed the vermal region of the cerebellum in five rabbits.

The lateral ventricles of the rabbit consist of frontal and temporal horns contained within their respective lobes of the cerebral hemispheres and a large narrow body that connects the two horns and extends posteriorly for a short distance into the occipital lobe. The ratio of the area of the lateral and third ventricles to the area of the cerebrum did not differ between intact and sham-operated control rabbits. Sixteen of nineteen (84%) silicone oil injected rabbits at all survival periods exhibited symmetrical dilatation of the lateral ventricles that only moderately compressed the cerebrum. Elevation of the corpus callosum relative to the anterior commissure was also noted (Figure 4). Dilatation was most consistent and maximal in

Figure 4. Coronal sections through the rabbit brain at the levels of the anterior commissure and mammillary bodies showing the frontal and occipital portions of the lateral ventricles (outlinedby broken lines). In normal rabbits (left), the ventricles are slit-like. In hydrocephalic rabbits, 2 weeks after silicone oil injection into the cisterna magna, the ventricles are greatly enlarged (right) and the corpus callosum (arrow) is displaced dorsally.

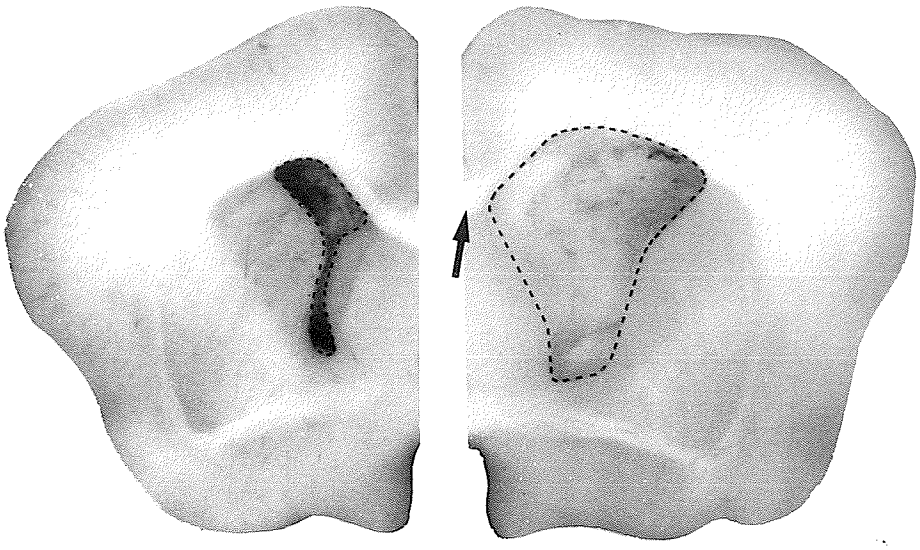

frontal

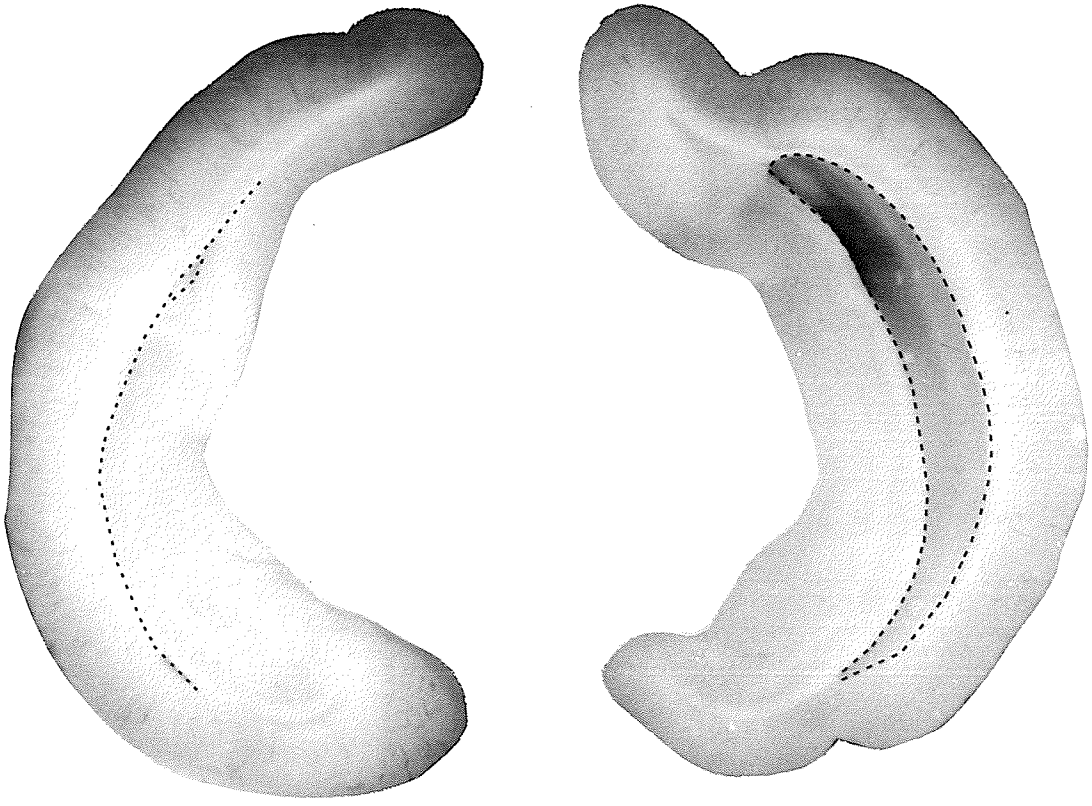

occipital

the frontal horns (Figures 4 and 5). The ratio of ventricle to cerebral area in the frontal lobes increased significantly ($P<0.01$) above control values within 3 days of silicone oil injection. There were, however, no significant differences among hydrocephalic groups at any post-injection interval thereafter suggesting that maximum dilatation had been achieved within 3 days. The body and temporal horns of the lateral ventricles at the mid-tuberal level were also larger than controls, but significantly enlarged ($P<0.025$) only at 3 days post-injection. Occipital poles of the lateral ventricles were only inconsistently enlarged from 3 days to 4 weeks post-injection. At post-injection periods of 2 weeks and longer, the third ventricle was enlarged but not significantly. Similarly, the cerebral aqueduct was enlarged in some rabbits after two weeks, but this was not quantified. The fourth ventricle, which was always filled with silicone oil, did not increase in size.

The ratio of the perimeter of the frontal horn to the perimeter of the cerebrum at the level of the anterior commissure increased significantly ($P<0.005$) from 0.307 ± 0.033 in sham-operated control rabbits to 0.373 ± 0.029 in 3 day hydrocephalic rabbits. This ratio did not change significantly at any of the subsequent post-injection intervals. Changes in perimeter of the frontal horn correlated well ($r=.943$, $P<0.001$) with changes in the area of the ventricle.

Shunting of CSF from both 1 and 8 week hydrocephalic

Figure 5. Graphs showing the ratio of the area of the ventricle to the area of the cerebrum at the level of the anterior commissure (frontal), the mid-tuberal region (body + temporal, third) and mammillary bodies (occipital) plotted as a function of time after silicone oil injection. Solid and interrupted lines represent values in pre- and post-shunted hydrocephalic rabbits respectively. The frontal horns of the lateral ventricles were significantly ($P<0.025$) enlarged within 3 days of injection and remained enlarged for the duration of the experimental period. The body and temporal horns of the lateral ventricles were also larger in hydrocephalus, but significantly so ($P<0.025$) only at 3 days post-injection. The occipital poles of the lateral ventricles were larger from 3 days to 4 weeks post-injection but not significantly so. At post-injection periods of 2 weeks and longer the third ventricle was enlarged but not significantly. Following shunting of both 1 and 8 week hydrocephalic rabbits, the size of the ventricles returned to control values within one week. *, $P<0.025$ (as determined by ANOVA and post hoc one-tailed t-test).

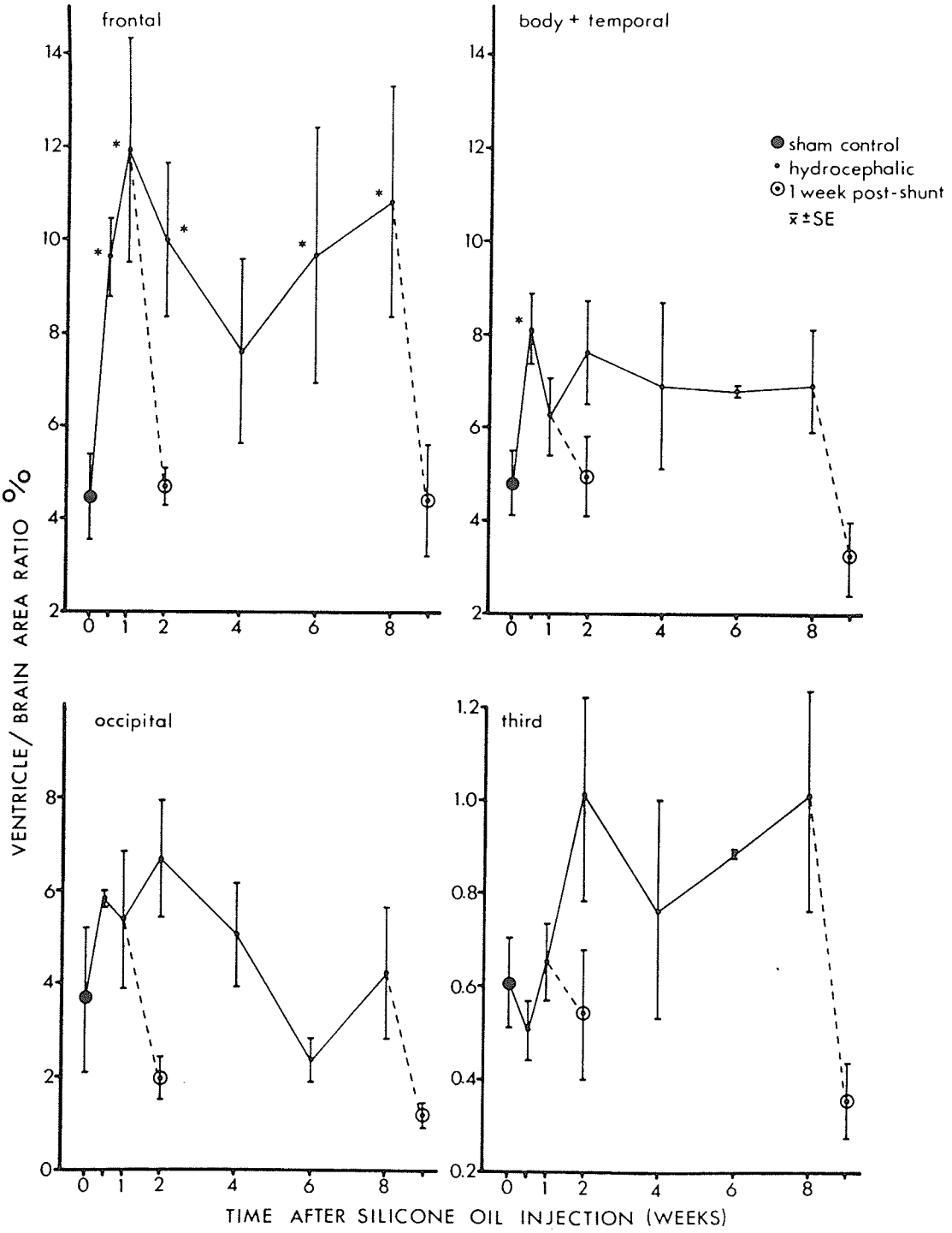
frontal
body + temporal
occipital
third
sham control
hydrocephalic
1 week post-shunt
x̄ ± SE
VENTRICLE / BRAIN AREA RATIO %
TIME AFTER SILICONE OIL INJECTION (WEEKS)

rabbits caused all enlarged regions of the ventricular system to return to control values within 1 week (Figure 5). The ratio of ventricle to brain perimeter also returned to control values within 1 week of shunting.

4.2 ICP in control and hydrocephalic rabbits

The presence of the ICT/b intracranial pressure transducer in the epidural space did not affect the neurologic function of the rabbits. One animal, however, died within 3 hours of implantation following brain herniation that resulted from acute frontal lobe compression by an improperly placed transducer. In the thirteen rabbits, ICP was monitored for a maximum of 21 days under control conditions. In seven rabbits subsequently injected with silicone oil, ICP was monitored for a maximum of 21 days. The total duration of ICP monitoring was up to 1 week in six rabbits, 1-4 weeks in seven rabbits, and 6 weeks in one rabbit. At sacrifice, five of twelve rabbits had pus under the scalp but no rabbit had evidence of leptomeningeal or cerebral infection. Six of the seven silicone oil injected rabbits exhibited moderate ventriculomegaly comparable to that measured in hydrocephalic rabbits that did not undergo ICP monitoring (Section 4.1).

Baseline ICP recorded in control and hydrocephalic rabbits is shown in Figure 6. In conscious control rabbits, ICP remained unchanged at 4.4 ± 0.8 mm Hg from the time of transducer implantation until 21 days post-implantation. When CSF was drained just prior to silicone oil injection,

Figure 6. Graph showing intracranial pressure (ICP) in control (circle) and hydrocephalic (diamonds) rabbits at several post-injection intervals. The control value represents the mean pressure (n=13) up to 21 days after implantation of the transducer. At the time of silicone oil injection, ICP increased rapidly from control values of 4.4 ± 0.8 mm Hg to 33.6 ± 7 mm Hg. Within 6 hours, the ICP dropped to 7.7 ± 1.7 mm Hg but remained significantly ($P<0.05$) elevated until Day 1 post-injection. From Day 2 till Day 21 post-injection, ICP was not significantly different from control values. *, $P<0.05$ as determined by the one-tailed Student's t-test.

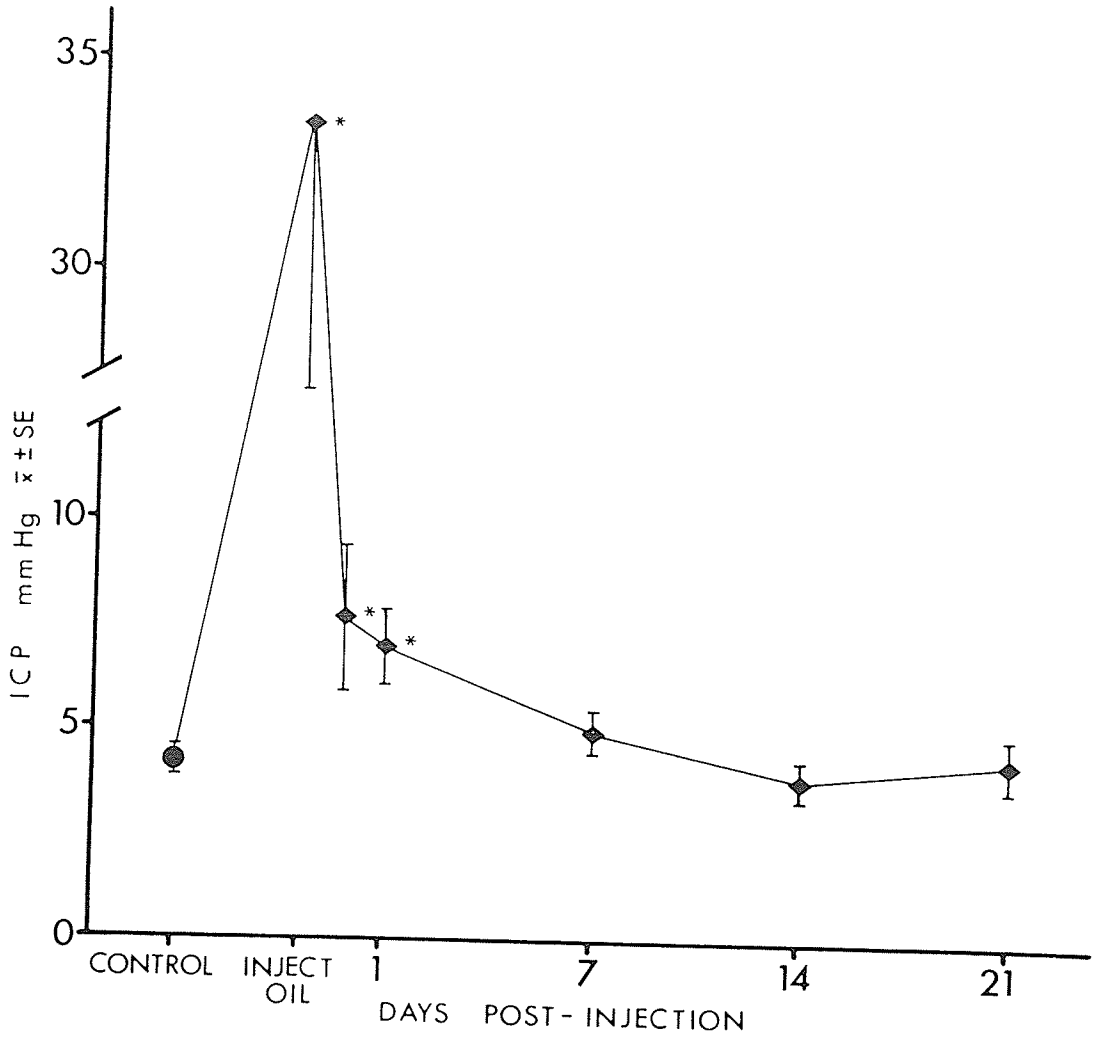
35
30
10
5
0
ICP mm Hg x̄ ± SE
*
*
*
CONTROL
INJECT OIL
1
7
14
21
DAYS POST-INJECTION

the ICP approached 0 mm Hg and during the injection of oil ICP rose transiently to 33.6±7 mm Hg (maximum 79 mm Hg). In conscious hydrocephalic rabbits, ICP was 7.7±1.7 mm Hg, 6 hours following silicone oil injection, and 7.0±0.9 mm Hg on day 1. ICP was significantly ($P<0.05$) elevated above control values for only 36 hours. From day 2-21 post-injection the baseline ICP of hydrocephalic rabbits fell to 4.5±0.7 mm Hg and did not differ significantly from that of controls.

Consistent with the known effect of ketamine on ICP (Sari et al., 1972), in both control and hydrocephalic rabbits ICP was significantly higher ($P<0.05$) while anesthetized than while conscious. In addition, body position significantly affected ICP. During anesthesia, ICP was lower ($P<0.05$) when the heads were elevated than when the rabbits were recumbent.

Although the baseline ICP in hydrocephalic rabbits returned to control levels 2 days after induction of hydrocephalus, significant differences persisted in the pattern of the ICP tracings. Control ICP tracings were essentially flat with infrequent variations due to changes in head position and sudden movements only. ICP tracings from hydrocephalic rabbits, however, were highly variable (Figure 7). Spontaneous elevations of ICP were observed in resting rabbits throughout the period of hydrocephalus. In control rabbits, 5.8±1.0 brief (≤5 seconds) pressure peaks per minute with an amplitude of 2.3±0.3 mm Hg were recorded. In hydrocephalic rabbits at 2-21 days post-injection,

Figure 7. ICP recordings from a conscious rabbit before (normal) and 1 day and 2 weeks after silicone oil injection. In the unrestrained but motionless rabbit, normal ICP was 4-5 mm Hg and relatively stable. In the same rabbit, 1 day after induction of hydrocephalus, baseline ICP was elevated to 11-15 mm Hg and displayed frequent pressure peaks of 18-22 mm Hg. In the same rabbit, 2 weeks after induction of hydrocephalus, baseline ICP decreased to 7-10 mm Hg but the pressure remained highly variable with peaks up to 17 mm Hg. 1 vertical division = 1 mm Hg pressure; 1 horizontal division = 1 minute.

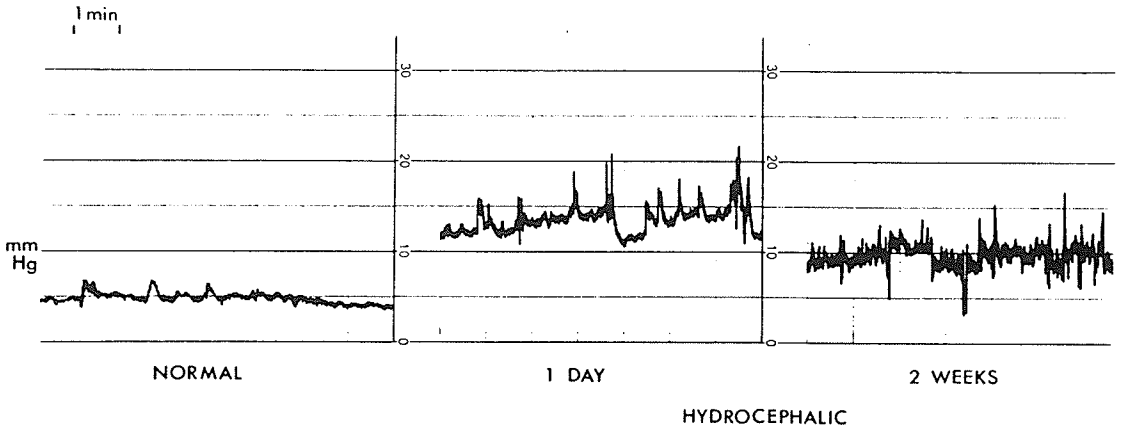
1 min
mm Hg
30
20
10
0
NORMAL
1 DAY
2 WEEKS
HYDROCEPHALIC

8.6±2.2 peaks per minute with an amplitude of 2.9±0.6 mm Hg were recorded. Prolonged pressure elevations, up to 1 minute in duration, were also recorded in hydrocephalic rabbits but not in controls. Activities such as grooming and walking were observed to evoke large ICP increases in hydrocephalic rabbits and even eye-blinking momentarily elevated the ICP 2-3 mm Hg.

4.3 Cerebral water content

At the time of sacrifice, twelve of the fifteen (80%) silicone oil injected rabbits used in this part of the experiment had hydrocephalus. The degree of ventriculomegaly was comparable to that observed in rabbits whose ventricular size was quantified (Section 4.1). Rabbits that did not exhibit ventriculomegaly were excluded from further study. As a result, specific gravity of cerebral tissue was determined in three 3 day, five 1 week, and four 4 week hydrocephalic rabbits and five control rabbits.

Five to eight 0.5 mm slices were obtained from each of the bilateral cerebral samples (Figure 2). Comparable sections taken from fixed brains were characterized histologically. Sections designated V1 and V2, adjacent to the ventricle, consisted entirely of white matter of the corpus callosum. Section C1 included laminae I and II of the cerebral cortex and section C2 included laminae II and III. Sample M consisted of 1-4 sections that contained laminae IV to VI of the cortex and only small amounts of subjacent white matter. Data from cortical gray matter designated M

were pooled for analysis because of variations in the number of sections obtained from different animals.

In control rabbits, specific gravity determinations made on the fresh cerebral tissue revealed that the density of the cerebrum increased from the pial surface (C1) toward the deep cortex (M) and then decreased toward the ventricular surface (V1) (Figure 8). Samples taken at the pial surface (C1) were significantly ($P<0.05$) less dense than the other four samples. With this exception, there were no statistically significant differences between the specific gravity of samples taken from C2, M, V2, and V1.

In rabbits killed 3 days following injection of silicone oil, the specific gravity of samples taken at C2 were significantly ($P<0.01$) higher than control values. Samples V2 and V1 were lower than controls, but not significantly so. The 1 and 4 week specific gravity values were comparable and, in both, samples C1, C2, M, and V2 were increased significantly ($P<0.02$) above control values. The specific gravity of tissue samples immediately adjacent to the ventricular surface (V1), however, did not differ from control values.

The desiccated tissue samples, because of their small and variable size, exhibited greater variation of specific gravity than their fresh counterparts. In both control and hydrocephalic rabbits, the specific gravity of desiccated gray matter (C1,C2,M) was significantly ($P<0.001$) higher than that of white matter (V1, V2) (Figure 9). This is

Figure 8. Graph showing the specific gravity (g/cm^3) of fresh cerebral tissue samples taken from control and hydrocephalic rabbit brains. C1, C2, M, V2, and V1 represent successive sections through a sample of cerebrum extending from the pial (C1) to the ventricular (V1) surface (see Figure 2). In controls, the specific gravity was lowest in the superficial cortical gray matter (C1) and highest in the deep gray matter (M) indicating a density gradient through the cerebrum. At 3 days following induction of hydrocephalus, specific gravity was increased in samples at C2. The specific gravity of samples taken 1 and 4 weeks post-induction were not different from one another but were higher than controls at all locations except V1. *, $P<0.02$; **, $P<0.01$ as determined by ANOVA and post hoc two-tailed t-tests.

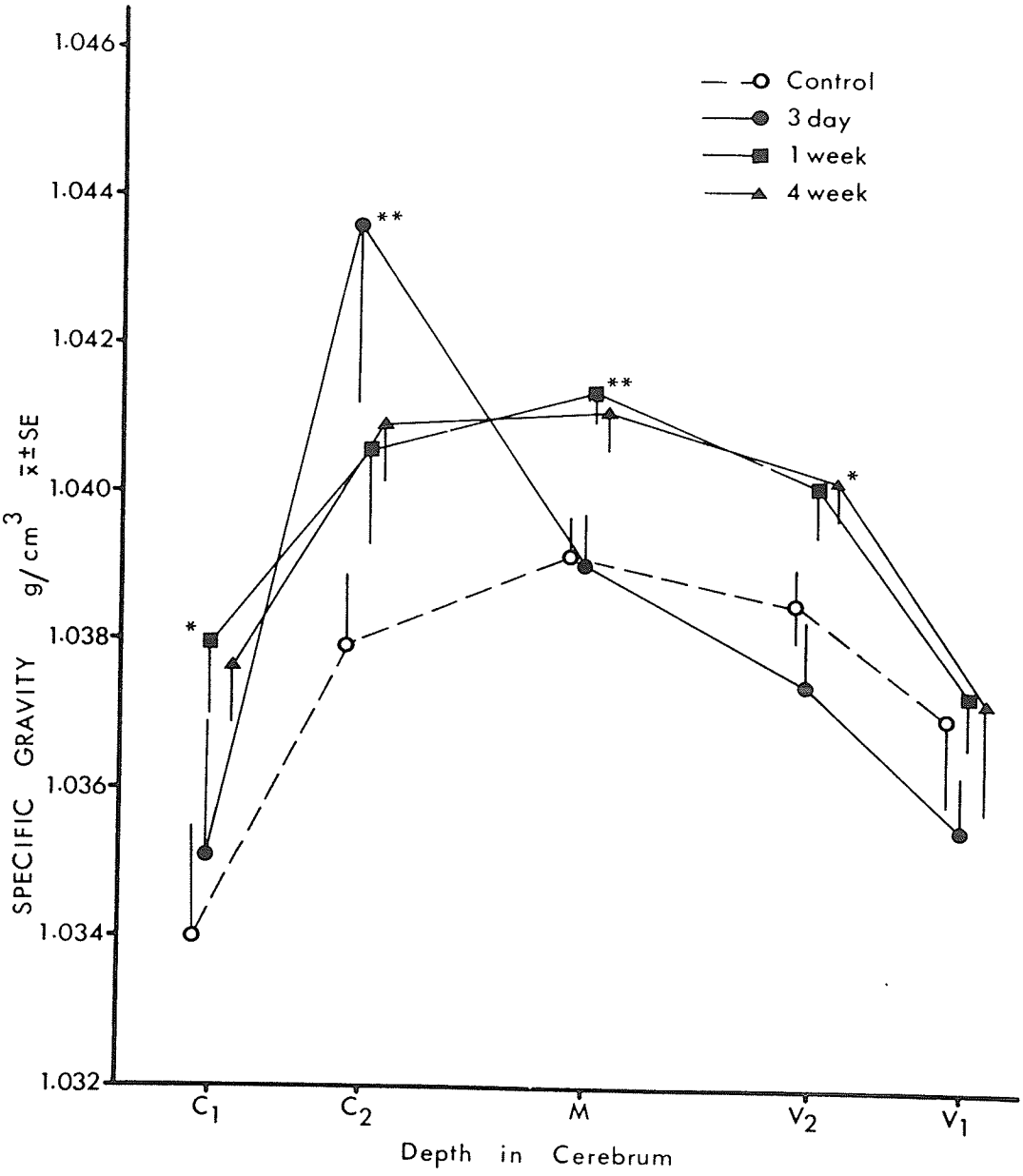
1.046
1.044
1.042
1.040
1.038
1.036
1.034
1.032
SPECIFIC GRAVITY g/cm3 x̄±SE
Control
3 day
1 week
4 week
**
**
*
*
C1
C2
M
V2
V1
Depth in Cerebrum

presumed to reflect the low density of lipids, which are a major component of myelin. Apart from this finding, there were no statistically significant differences between the specific gravity of control and hydrocephalic cerebral tissue at any location sampled.

Mean water content was calculated as described by Nelson et al. (1971) using the values obtained from the wet and dry specific gravity determinations. In control rabbits, the mean water content of gray matter (C1 + C2) was calculated to be 78.6±0.8% whereas that of white matter (V1 + V2) was 72.7±3.0%. Following induction of hydrocephalus, water content of gray matter decreased to 78.1±0.6% at 3 days, 77.8±0.5% at 1 week, and 77.3±0.5% at 4 weeks. The water content of white matter decreased to 71.5±1.3% at 3 days, 71.1±1.2% at 1 week, and 70.9±1.2% at 4 weeks post-injection.

4.4 Morphology of periventricular tissue

4.4.1 Ependymal lining and subependymal region in control rabbits

The lining of the lateral ventricle in untreated and saline injected sham-operated control rabbits consisted of a single continuous layer of ciliated ependymal cells (Figure 10 A, B, C). These cells had large, ovoid nuclei located in the basal cytoplasm and the supranuclear cytoplasm contained numerous mitochondria and profiles of smooth endoplasmic reticulum along with occasional Golgi complexes. In the

Figure 9. Graph showing the specific gravity of desiccated tissue samples taken from control and hydrocephalic rabbit brains. In control and hydrocephalic rabbits, the specific gravity of gray matter (C1,C2,M) was significantly ($P<0.05$) higher than that of white matter (V1,V2). There were no statistically significant differences, however, between control and hydrocephalic rabbits at any location. (ANOVA and post hoc two tailed t-tests)

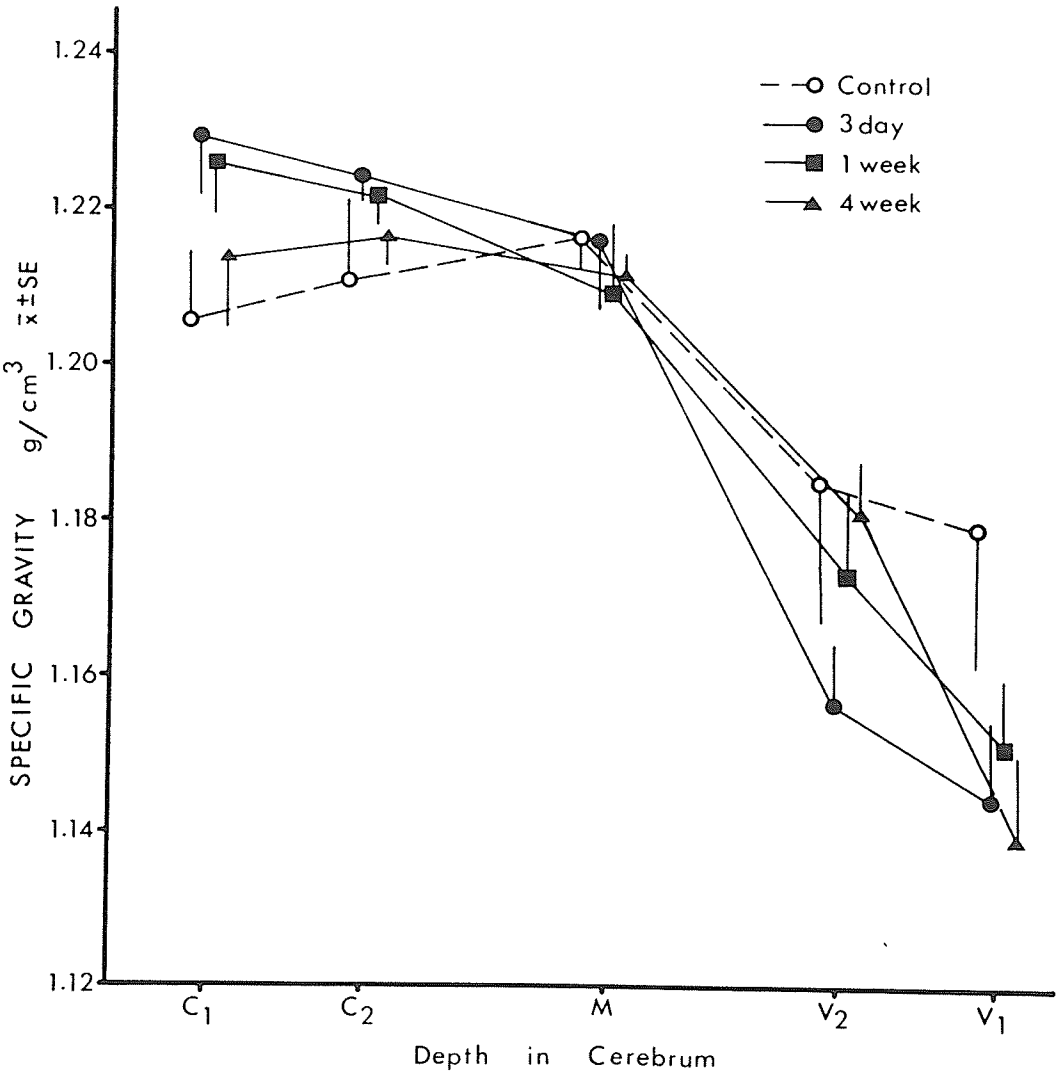
1.24
1.22
1.20
1.18
1.16
1.14
1.12
SPECIFIC GRAVITY g/cm3 x̄±SE
Control
3 day
1 week
4 week
C1
C2
M
V2
V1
Depth in Cerebrum

Figure 10. Transmission electron micrographs showing the ependymal lining of the frontal horn of the lateral ventricle (V) in control rabbits. Over the caudate nucleus (Fig.A), corpus callosum (Fig.B), and septal area (Fig.C) the ependymal cells (E) are arranged in a single layer. They are joined only at the apical lateral borders by zonula adherens junctional complexes (short arrows). Organelles are concentrated within the apical region of the ependymal cytoplasm and the nuclei are situated in the basal region.

A) Ependymal cells (E) over the caudate nucleus are cuboidal and possess numerous cilia (cil) at the ventricular surface. Abutting on the basal surface of the cells is the subependymal region which contains astrocytes and their interwoven processes (long arrow). The extracellular spaces (*) are small.

B) Ependymal cells (E) over the corpus callosum are squamous. Subjacent to the ependyma, is a thin layer of astrocytes (A) and their processes which contain glial filaments (long arrow). Myelinated axons surrounded by large extracellular spaces (*) lie deep to the subependymal region.

C) Ependymal cells (E) over the septal area are columnar. Cilia arise from basal bodies (open arrow) located in the apical cytoplasm of the cells.

All micrographs are the same magnification. Bar scale = 5 um

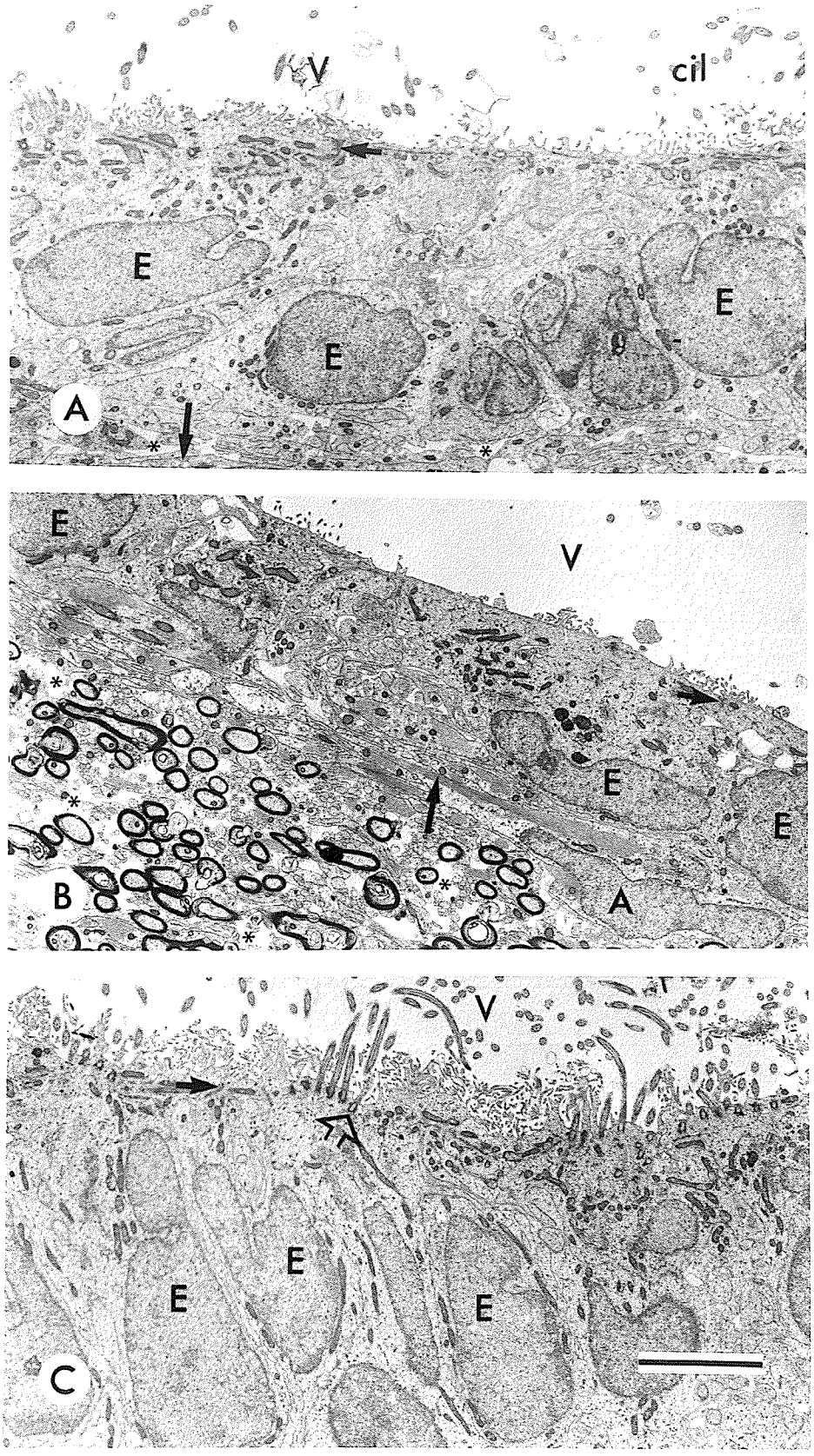
V
cil
E
E
E
A
B
C

cytoplasm adjacent to the luminal surface there was a dense network of microfilaments and a scaffolding of microtubules. Basal bodies, which merged with cilia, were also located in the apical cytoplasm. The lateral borders of adjoining ependymal cells were not extensively interdigitated. Zonulae adherens and occasional gap junctions were located between adjacent cells near their apices. The basal surface of the ependymal cells possessed minimal degrees of cytoplasmic infolding. On the ventricular surface of ependymal cells, cilia arose in clusters of 15-20, often from depressions in the cell surface. Numerous microvilli, partially obscured by the cilia, covered the ependymal surface.

Regional variations in ependymal morphology were encountered. Cilia were most dense on the surface of the caudate nucleus (CN) in the frontal horn of the lateral ventricle and on the dorsal wall of the third ventricle. Cilia were less dense on the ependyma of the corpus callosum (CC), in the cerebral aqueduct, and in the fourth ventricle. Cilia were sparse in the occipital poles of the lateral ventricles where coarctations were common. In the frontal horns of the lateral ventricles, ependymal cells were cuboidal over the CN (Figure 10A), squamous over the CC (Figure 10B), and columnar over the lateral septal area (LSA) (Figure 10C). In spite of differences in shape, all ependymal cells had a similar complement of organelles and junctional complexes.

The extent and composition of the subependymal region also varied considerably in different locations within the

lateral ventricles of control rabbits. Over the CN astrocytes were arranged in layers 2-5 cells thick. In contrast, the subependymal region of the CC and LSA consisted of only 1-2 layers of astrocytes. The astrocytes contained pale staining elongated nuclei, sparse organelles, and an abundance of glial filaments within the electron lucent cytoplasm. Interwoven processes of astrocytes formed most of the subependymal layer (Figures 10 A, B). Residing among the astrocytes were a few microglial cells with inclusion droplets and small undifferentiated cells. Endothelial cells of capillaries and venules that ranged from 7-25 um in diameter were commonly found within the subependymal region. Blood vessels located in the subependymal region were less common over the CC and LSA than over the CN.

The neuropil of the CN and LSA consisted primarily of moderately large (30-50 um) multipolar neurons with large pale staining nuclei and single nucleoli. The neuropil was interspersed with terminal arterioles, capillaries, venules, astrocytes, and microglia. The neuropil of the CC consisted of myelinated axons with occasional oligodendrocytes, astrocytes, and blood vessels. Extracellular spaces were larger in the white matter of the CC than in the gray matter of the CN or LSA (Figures 10A, B).

4.4.2 Changes in ependyma and subependymal region caused by hydrocephalus

Within 3 days of intracisternal injection of silicone oil, the lateral ventricles reached a maximum degree of enlargement. During this period, the separation of clusters of cilia over the CC and LSA indicated that the ependymal lining was stretched as the ventricle enlarged (Figures 11B and 12B). By 1 week, clusters of cilia had commonly retracted into invaginations of the apical cytoplasm of ependymal cells. This phenomenon was also seen to a lesser degree in sham operated rabbits injected with saline solution. Retraction of cilia, therefore, does not appear to be a characteristic of ependymal cells specific to hydrocephalic animals as suggested by Page et al. (1979a). By 4-8 weeks post-induction, most cilia had disappeared completely and the usually abundant microvilli were found mainly at the lateral borders of ependymal cells (Figure 12D). These ependymal surface changes were most pronounced over the CC and LSA. Only a minor degree of separation of clusters of cilia was observed over the CN by 8 weeks (Figure 12C).

On the ependymal surface in all regions of the ventricular system, however, supraependymal macrophages were commonly found from 3 days to 4 weeks after the induction of hydrocephalus. No supraependymal cells contained large vacuoles or inclusions suggestive of active phagocytosis. Processes of presumptive macrophages were observed between

Figure 11. Transmission electron micrographs showing the lining of the frontal horn of the lateral ventricle (V), 8 weeks after the induction of hydrocephalus. The ependymal cells (E) are stretched to varying degrees in different regions of the ventricular lining. The ependymal layer, however, remains continuous and zonula adherens (short arrows) between adjacent cells are preserved.

A) Ependymal cells (E) overlying the caudate nucleus are flattened. Although the nucleus is distorted and the apical cytoplasm thinned, the complement of organelles is unchanged. Numerous astroglial cells (A) are located in the subependymal region. L, capillary lumen.

B) Ependymal cells (E) over the corpus callosum are elongated and severely flattened. Deep to the ependyma are astrocyte processes that are filled with dense accumulations of glial filaments (long arrow). Myelinated axons (open arrow) are intact despite the enlarged extracellular spaces (*).

C) Ependymal cells (E) overlying the septal region are distorted from a columnar to a cuboidal shape. The number of cilia projecting into the ventricle (V) is greatly decreased. Astrocyte (A) processes with dense accumulations of glial filaments (long arrow) are present in the subependymal region.

All micrographs are the same magnification. Bar scale = 5 um

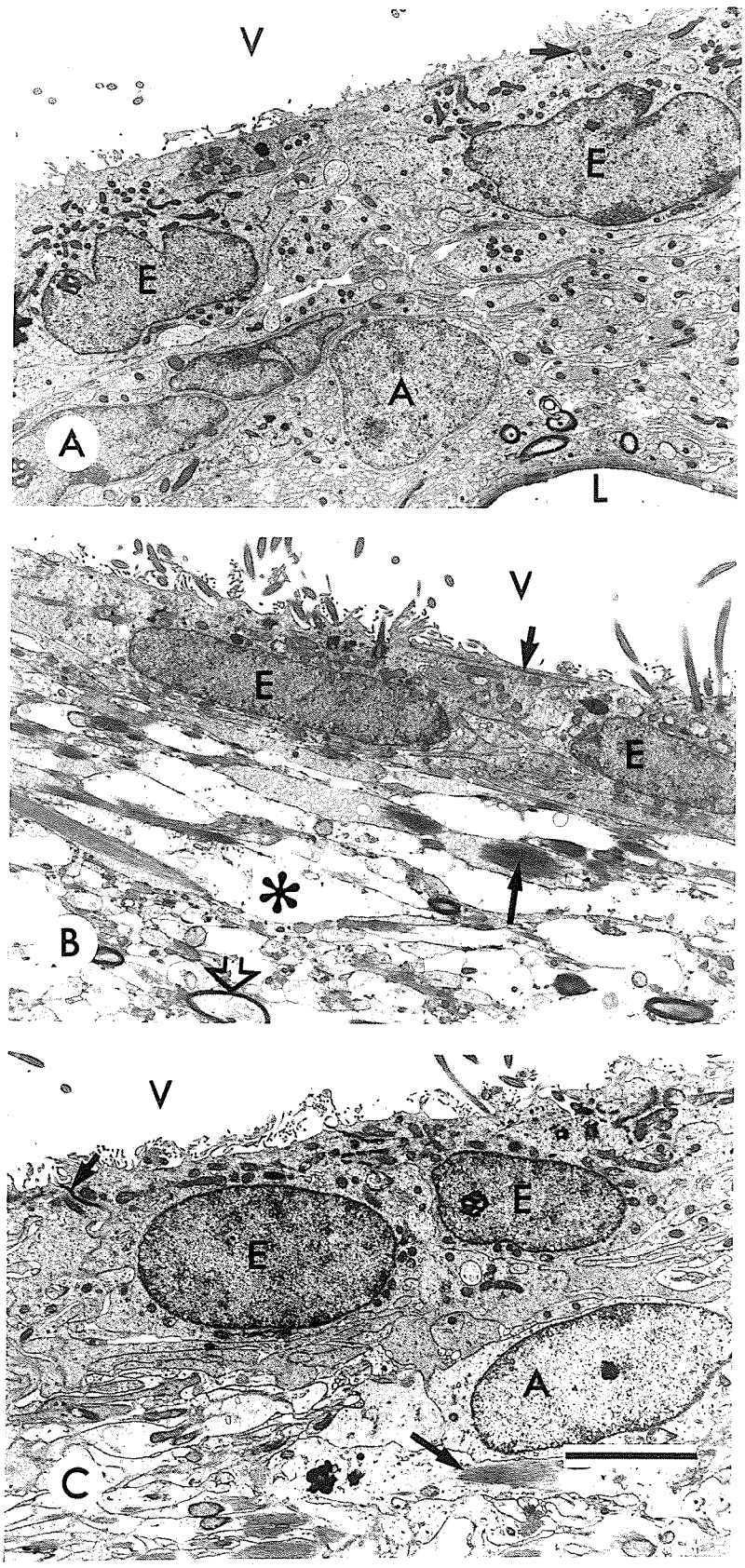
V
E
E
A
A
L
V
E
E
*
B
V
E
E
A
C

Figure 12. Scanning electron micrographs showing hydrocephalus-induced changes of the ependymal surface of the frontal horn of the rabbit lateral ventricle.

A) Normal ependymal cells possess a dense covering of cilia. Numerous microvilli, also present on the ependymal surface, are visible only between clusters of cilia.

B) Ependymal cells overlying the corpus callosum, 3 days after induction of hydrocephalus, are stretched as evidenced by the separation of the clusters of cilia. The microvilli on the ependymal surface are exposed to view. Supra-ependymal axons (small arrow), a normal feature of the surface of the ventricle, are also exposed. Macrophages (M) are commonly observed on the ependymal surface during the early stages of hydrocephalus.

C) Surface of ependymal cells overlying the caudate nucleus, 8 weeks after induction of hydrocephalus. The separation of clusters of cilia is comparable to that over the corpus callosum at 3 days (Fig. 12B) but microvilli commonly are found only at the lateral borders of ependymal cells (open arrow). small arrow, supra-ependymal axons.

D) Ependymal cells over the corpus callosum are almost devoid of cilia in 8 week hydrocephalic rabbits. Only a few short clusters of cilia (solid arrow) remain. In some instances, microvilli remain only along the lateral borders of ependymal cells (open arrow).

All micrographs are same magnification. Bar scale = 10 um

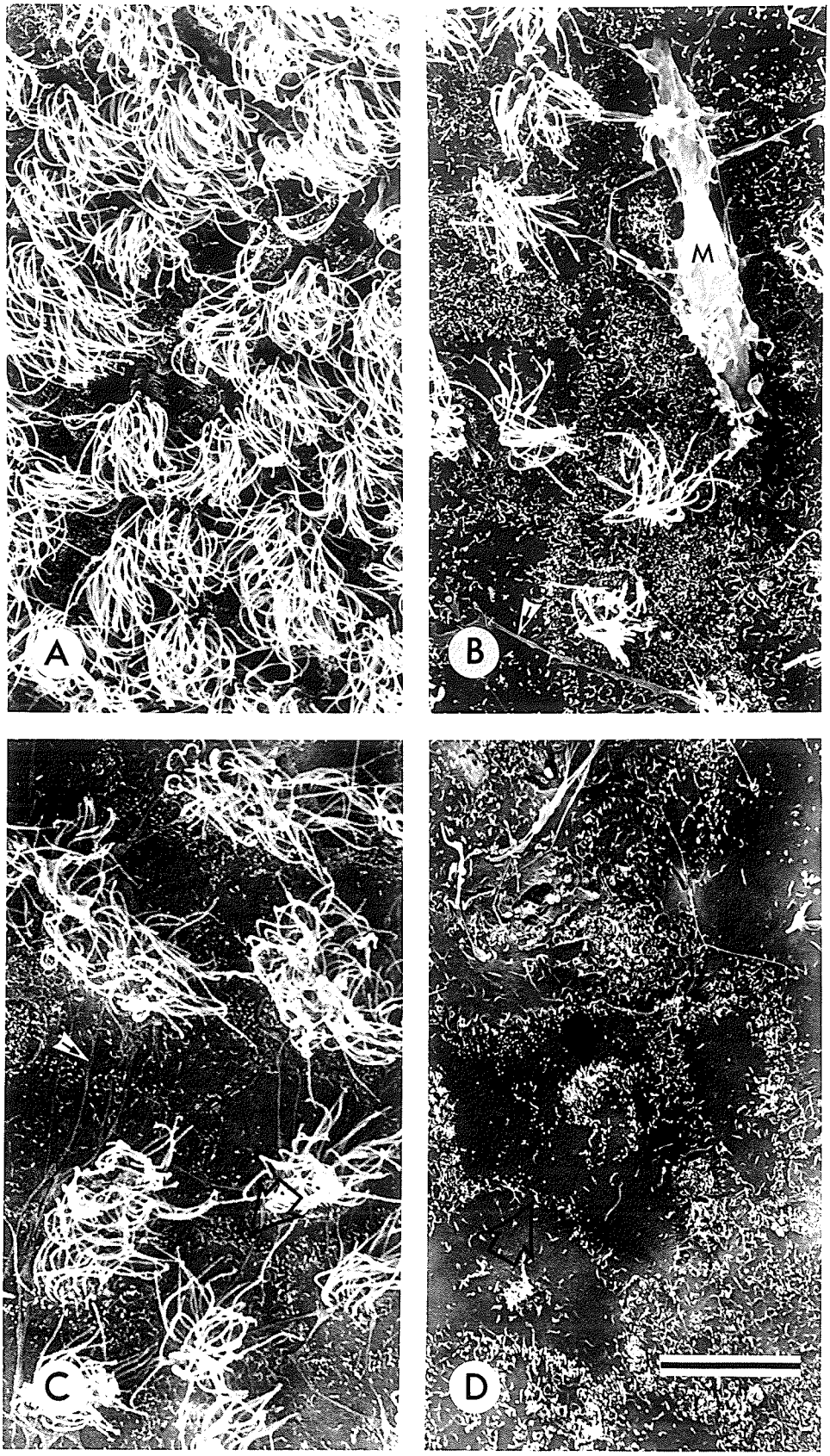
A
B
M
C
D

ependymal cells and projecting into the ventricle at 3 days and 1 week post-induction. No mitotic figures were seen among supraependymal cells. These observations suggest that the intraventricular macrophages migrate from the subependymal regions.

Despite the pronounced alterations to ependymal cell shape and loss of surface features, their intracellular components did not change appreciably due to hydrocephalus. Flattening of ependymal cells forced the organelles of the apical cytoplasm into close proximity with the nucleus (Figures 11 A, B, C). Electron dense inclusions, perhaps the remnants of basal bodies, were occasionally observed within the apical cytoplasm of ependymal cells denuded of cilia. Although the lateral processes between adjacent ependymal cells were highly attenuated, junctional complexes were present and continuity of the ependymal lining was maintained at 4-8 weeks post-induction (Figure 11B).

Ependymal attenuation was most evident at the dorsolateral angle of the frontal horn of the lateral ventricle. The extent of attenuated ependymal cells spread ventromedially along the CC and by 8 weeks involved the whole ventricular lining of the CC (Figure 11B). Over the LSA, columnar ependymal cells were deformed to a cuboidal or squamous shape (Figure 11C). Attenuation of ependymal cells overlying the CN was minimal (Figures 11A and 12C). Comparable changes were not seen in the ependymal lining of the occipital poles of the lateral ventricles nor in the third ventricle.

The number of ependymal cells per 200 um length of ventricular surface ranged from 13 over the CC to 15 over the CN to 21 over the LSA in controls (Figure 13). Quantitative analysis confirmed that the ventricular lining of the CC, CN, and LSA underwent significant ($P<0.001$) stretching. The ependymal lining reached a maximum degree of stretching by 3 days post-injection over the CC and by 1 week over the CN but that over the LSA was progressively stretched for 8 weeks. Eight weeks after the induction of hydrocephalus, the LSA had undergone a 38.8% reduction in the number of ependymal cells per unit length of the surface of the ventricle. In comparison, a 28.7% reduction was found over the CC and a 19.5% reduction was found over the CN. Regression analysis showed that the degree of ventricular dilatation could account for 80% of the change in ependymal cell concentration over the CN ($r=.895$, $P<0.005$) and CC ($r=.89$, $P<0.005$) but only 32% of the change in ependymal cell concentration over the LSA ($r=.57$, $P<0.05$). The duration of hydrocephalus also had a significant effect on the concentration of ependymal cells over the LSA ($r=0.657$, $P<0.025$).

Coexistent with stretching and thinning of the ependymal lining was a significant ($P<0.05$) decrease in the number of astrocytes per unit area within the subependymal region overlying the CC and CN at 3 days and over the LSA at 1 week post-induction (Figure 14). By 1 week, however, there were no longer significantly fewer astrocytes over the CN or

Figure 13. Graph showing the number of ependymal cells per 200 um length of the ventricular lining of the caudate nucleus, corpus callosum, and lateral septal area in the frontal horn. In control rabbits, the number of ependymal cells was significantly greater ($P<0.005$) over the septal area than the other two regions. Following the induction of hydrocephalus there was a decrease in the number of ependymal cells over all three regions by 3 days. Only the lateral septal area showed a further significant decrease from 3 days to 8 weeks. Following the reduction in size of the frontal horn by shunting (broken lines), the number of ependymal cells increased significantly ($P<0.05$) only over the corpus callosum compared to the 1 week hydrocephalus value. *, $P<0.001$ significantly different from sham controls as determined by ANOVA and post hoc t-tests.

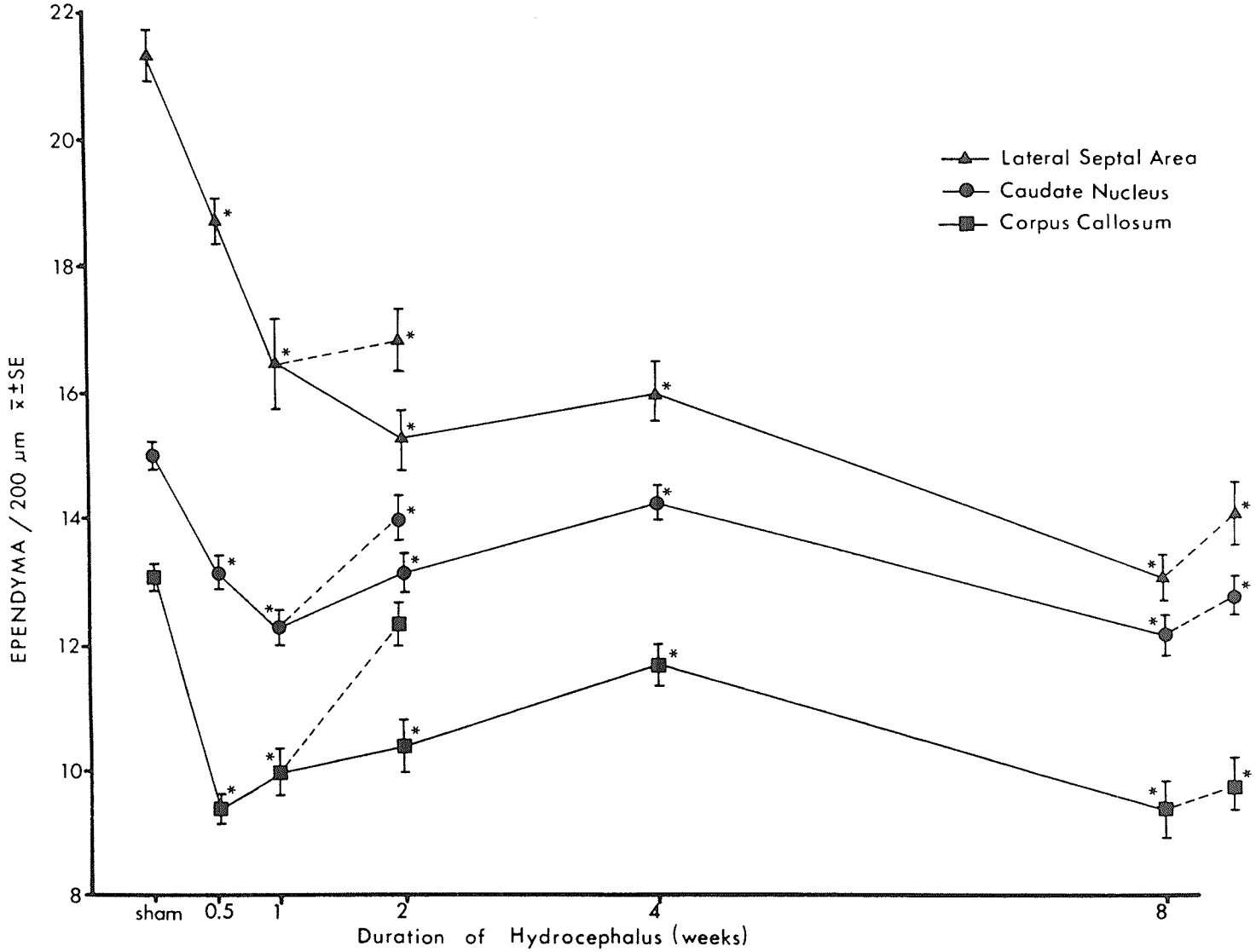
Lateral Septal Area
Caudate Nucleus
Corpus Callosum
EPENDYMA / 200 µm x̄±SE
22
20
18
16
14
12
10
8
sham
0.5
1
2
4
8
Duration of Hydrocephalus (weeks)

Figure 14. Graph showing the number of astrocytes within 30 um of the surface of the ventricle per 200 um length of the ventricular lining over the caudate nucleus, corpus callosum, and lateral septal area of the rabbit. In control rabbits, the number of astrocytes was significantly greater ($P<0.05$) over the caudate nucleus than over the other two regions. Following the induction of hydrocephalus, there was a significant reduction in the number of astrocytes over the caudate nucleus at 3 days and over the lateral septal area at 1 and 8 weeks. Although there was no significant decrease over the corpus callosum at 3 days, the number of astrocytes increased progressively and was significantly greater than controls at 4 and 8 weeks post-induction. *, $P<0.05$; **, $P<0.02$ significantly different from sham controls as determined by ANOVA and post hoc t-tests.

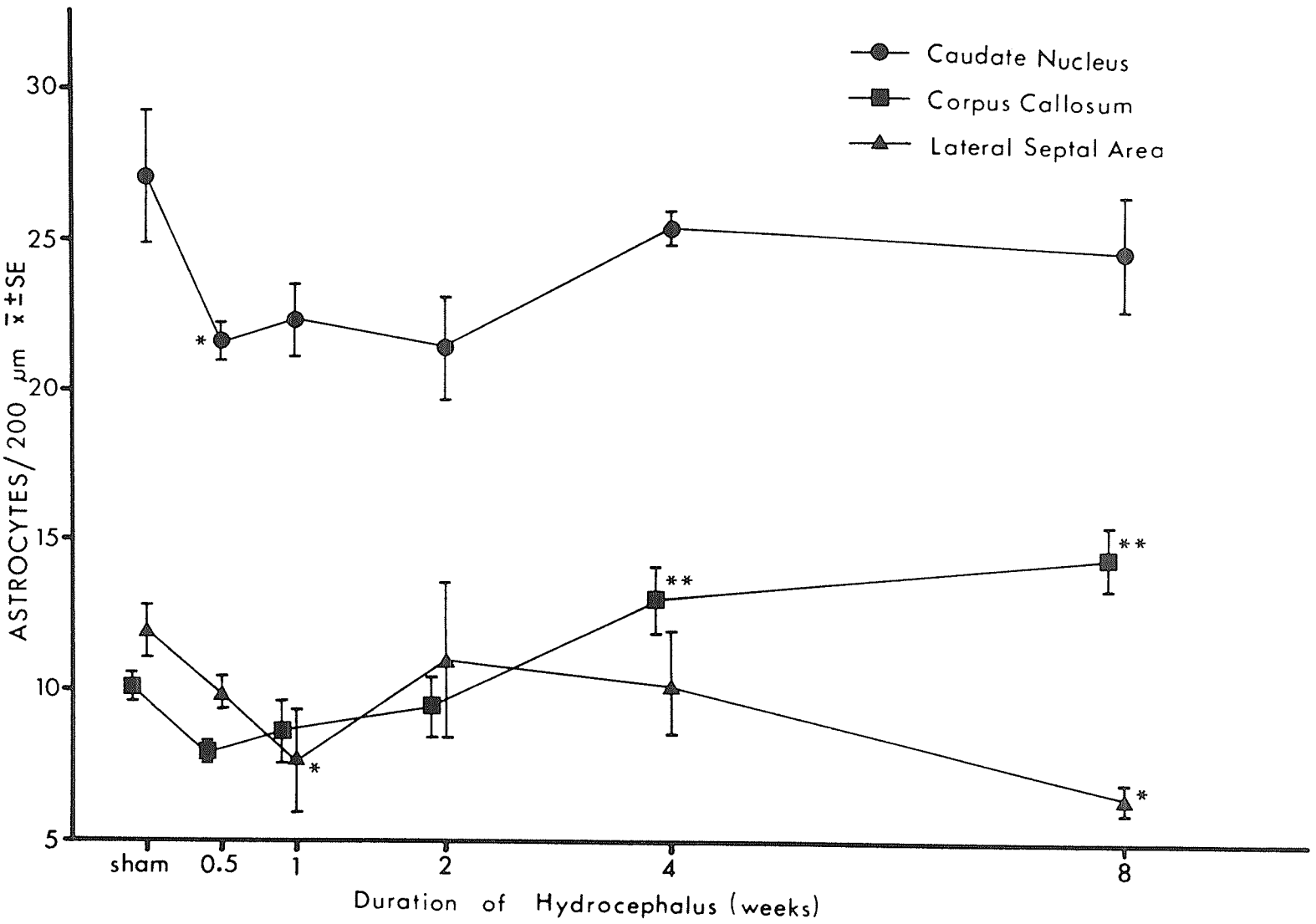
Caudate Nucleus
Corpus Callosum
Lateral Septal Area
ASTROCYTES/200 μm x̄±SE
30
25
20
15
10
5
sham
0.5
1
2
4
8
Duration of Hydrocephalus (weeks)
*
**

CC. By 4 weeks the number of astrocytes over the CC had increased significantly ($P<0.02$) above control values. The number of astrocytes in the subependymal region of the CN, however, did not exceed control values even by 8 weeks. The increased number of astrocytes was accompanied by an increased number of astrocytic processes that contained dense accumulations of glial filaments in the CN (Figure 11A) and CC (Figure 11B). Even over the LSA, where the number of astrocytes did not increase, there were substantially more astrocytic processes in the subependymal region.

Mitotic activity among ependymal and astrocytic cell populations was studied in the region of the frontal horn of the lateral ventricle using colchicine. In controls, the percentage of ependymal cells arrested in metaphase during the 6 hour period was 0.018 and 0.016 over the CC and CN respectively (Table I). Three days following induction of hydrocephalus, mitotic activity increased to a maximum of 0.082% over the CC ($P<0.05$) and returned to control values by 2 weeks. Mitotic figures among ependymal cells over the CN increased at 1 week and reached a maximum of 0.11% ($P<0.01$) at 2 weeks before returning to control values by 4 weeks. Mitotic figures were rarely encountered among ependymal cells over the LSA and the number did not change significantly as a result of hydrocephalus.

Astrocytes in the subependymal region were a more mitotically active population of cells than ependymal cells. In control rabbits, the proportion of mitotic astrocytes

Table I. Number of ependymal cells arrested in metaphase in three regions of the frontal horn of the rabbit lateral ventricle 6 hours after colchicine injection.

Group	No. of Samples	Caudate Nucleus(CN)	Corpus Callosum(CC)	Septal Area (LSA)
Control rabbits				
Sham	8	2 / 12890[a] (0.016%)	2 / 10967 (0.018%)	0 / 3962 (0.0%)
Hydrocephalic rabbits				
3 day	4	1 / 4900 (0.020%)	4 / 4900* (0.082%)	0 / 1906 (0.0%)
1 week	4	3 / 5679 (0.053%)	2 / 5327 (0.038%)	1 / 2875 (0.035%)
2 week	4	4 / 3804** (0.11%)	1 / 4957 (0.020%)	0 / 2325 (0.0%)
4 week	4	1 / 5000 (0.020%)	1 / 5000 (0.020%)	1 / 1850 (0.054%)
8 week	4	1 / 4859 (0.021%)	0 / 4860 (0.0%)	0 / 2347 (0.0%)
One week hydrocephalic rabbits shunted for 1 week				
	3	2 / 2911 (0.069%)	1 / 2796 (0.036%)	NA

a. number of cells in metaphase / total cells counted
( ) percent mitotic cells during a 6 hour period
* P<0.05, ** P<0.01 significantly different from controls as determined by the one tailed z-test
NA not available

during a 6 hour period was 0.57% over the CN, 0.42% over the CC, and 0.13% over the LSA (Table II). The number of mitotic figures increased ($P<0.05$) to peak at 1.58% over the CN and 0.67% over the LSA at 1 week after the induction of hydrocephalus, and 0.65% over the CC by 2 weeks. Increases in mitotic activity among ependymal cells and astrocytes did not correlate with the degree of ventricular dilatation nor with the degree of tissue stretching.

4.4.3 Changes in the neuropil and periventricular cerebrovasculature due to hydrocephalus

Three days following induction of hydrocephalus, enlarged extracellular spaces were observed within the neuropil of the CC to a depth of 100-150 um from the ependymal surface. By 1 week post-induction, the extracellular spaces were considerably reduced in size but even by 8 weeks they were still enlarged as compared to controls. Separation of myelin sheathes was rarely observed, and at no interval after the induction of hydrocephalus was ultrastructural evidence of damage to axons seen.

Enlargement of extracellular spaces comparable to that in the CC was not evident in the CN or LSA following induction of hydrocephalus. Hydrocephalus of 8 weeks duration caused no significant ultrastructural changes in the neurons of the CN or LSA. In the CN-D of control rabbits, 0.4 mm from the ventricular surface, there were 118 ± 9 neurons / mm^2 , in the CN-P at the ventricular surface

Table II. Number of astrocytes arrested in metaphase in three subependymal regions of the frontal horn of the rabbit lateral ventricle 6 hours after injection of colchicine.

Group	No. of Samples	Caudate Nucleus(CN)	Corpus Callosum(CC)	Septal Area (LSA)
Control rabbits				
Sham	8	133 / 23384[a] (0.57%)	36 / 8494 (0.42%)	3 / 2394 (0.13%)
Hydrocephalic rabbits				
3 day	4	38 / 8063 (0.47%)	9 / 4119 (0.22%)	0 / 985 (0.0%)
1 week	4	165 / 10458** (1.58%)	25 / 4712 (0.53%)	9 / 1341* (0.67%)
2 week	4	49 / 6232* (0.79%)	30 / 4624* (0.65%)	7 / 1638* (0.43%)
4 week	4	40 / 8949 (0.45%)	32 / 5699 (0.56%)	1 / 1139 (0.09%)
8 week	4	64 / 9997 (0.64%)	12 / 7987 (0.15%)	0 / 1207 (0.0%)
One week hydrocephalic rabbits shunted for 1 week				
	3	69 / 3823** (1.80%)	23 / 2375** (0.97%)	NA

a. number of cells in metaphase / total cells counted
( ) percent mitotic cells during a 6 hour period
* P<0.05, ** P<0.01 significantly different from controls as determined by the one tailed z-test
NA not available

there were 109±6 neurons and in the LSA there were 69±9 neurons. The number of neurons in the CN and LSA was not significantly different ($P>0.5$) in the 1 and 8 week hydrocephalic rabbits as compared to controls.

In the neuropil surrounding the frontal horns of the lateral ventricles of control rabbits (Figure 3), significant regional differences with regard to the number of blood vessels were observed. Because there were no differences in the numbers of cross sectional, oblique, or longitudinal profiles, these values were pooled to give a total vessel count. The number of patent capillaries (≤10 um diameter) was greatest in the CN-D, 0.43 mm from the ventricle (205±11 / mm^2) followed by the periventricular CN-P (200±12), the periventricular LSA-P (172±9), the periventricular CC-P (152±14), and the deep CC-D (96±7) (Figure 15). The number of capillaries in the CC areas was significantly ($P<0.01$) lower than the number in the CN. The CN-D contained the greatest number of patent vessels in the 10-25 um diameter range (21.4±2.4 /mm^2) followed by the CN-P (19.4±1.9), CC-P (11.1±1.4), CC-D (10.2±1.7), and LSA-P (8.7±1.9). The number of these vessels in the CN was significantly ($P<0.01$) greater than in the CC or LSA. Venules and terminal arterioles, ≥25 um diameter, were most common in regions distant from the ventricular surface. The highest concentration was found in the CN-D (5.8±1.3 / mm^2) followed by CC-D (3.2±0.7), CN-P (2.3±0.7), CC-P (0.8±0.5), and LSA-P (0.7±0.5). There were no significant differences in the number of large blood vessels in any of the five

Figure 15. Graph showing the number of patent blood vessels (<10 um diameter) per mm^2 in the neuropil adjacent to the frontal horn (Figure 3). In control rabbits, the concentration of vessels per unit area was less ($P<0.01$) in the corpus callosum (CC-D and CC-P) than in the caudate nucleus (CN-P and CN-D) or septal area (LSA-P). One week following the induction of hydrocephalus, the number of patent vessels decreased significantly ($P<0.05$) in all regions except the CN-D. There were no significant differences between the 1 and 8 week hydrocephalic rabbits. Shunting of the 1 week hydrocephalic rabbits caused an increase in the number of patent vessels in all regions except the LSA-P. Shunting after 8 weeks of hydrocephalus, however, failed to cause a similar increase. *, $P<0.05$ compared to controls as determined by ANOVA and post hoc two-tailed t-tests.

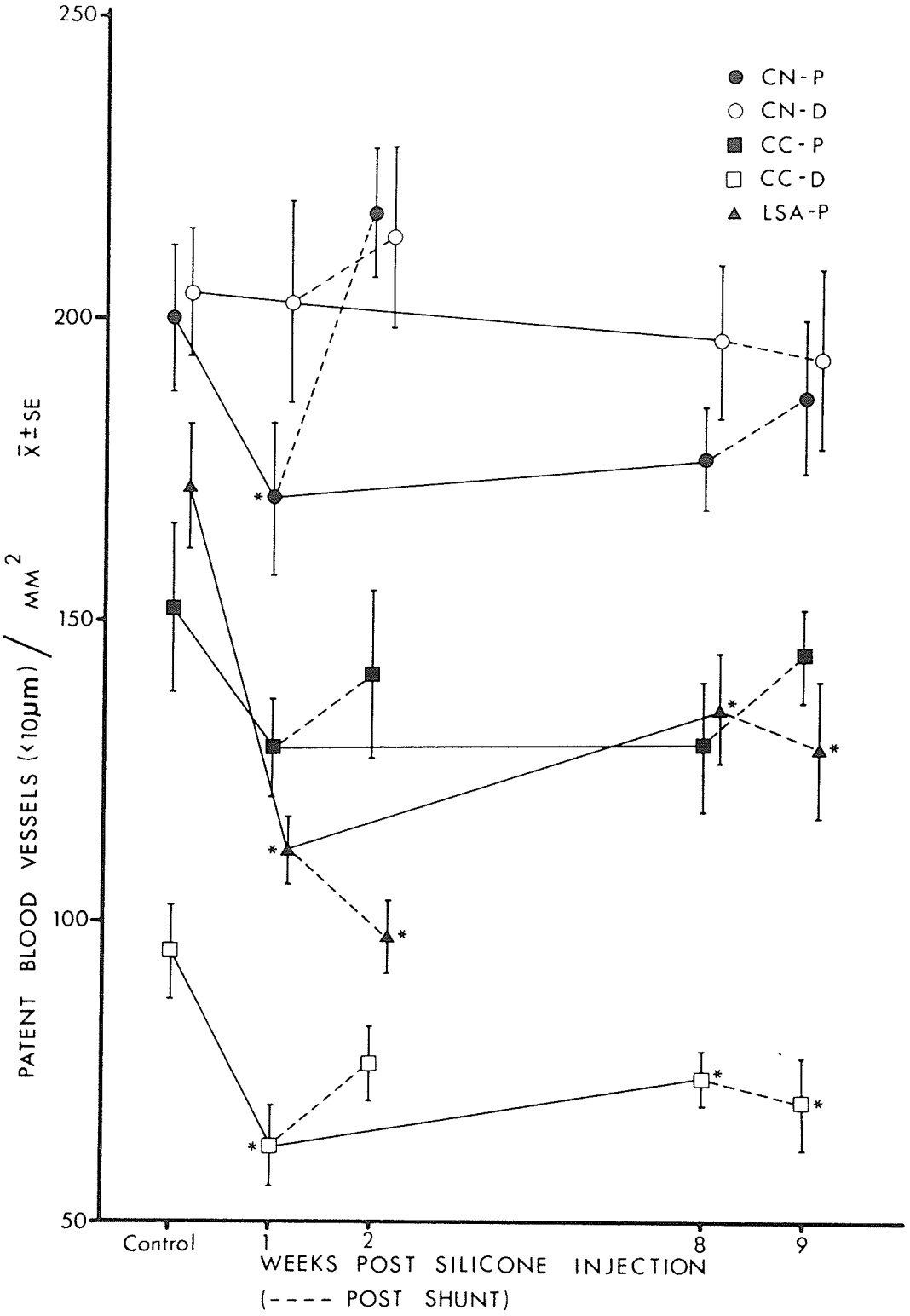
250
200
150
100
50
CN-P
CN-D
CC-P
CC-D
LSA-P
PATENT BLOOD VESSELS (<10μm) / MM2 X̄ ± SE
Control
1
2
8
9
WEEKS POST SILICONE INJECTION
(---- POST SHUNT)

regions examined.

One week following the induction of hydrocephalus a significant ($P<0.05$) decrease in the number of patent capillaries ($\leq$10 um diameter) was observed in all regions except the CN-D (Figure 15). When hydrocephalus progressed for 8 weeks, the number of patent capillaries in the LSA-P increased but remained less than control values. Although changes in the number of 10-25 um vessels were comparable with the changes in the $\leq$10 um vessels, hydrocephalus did not cause significant changes in the numbers of patent vessels 10-25 or $\geq$25 um diameter in any of the locations.

No ultrastructural evidence of endothelial changes resulting from hydrocephalus was detected in the vessels of any region studied.

4.5 Reversal of the pathology in hydrocephalus by shunting

The size of the frontal horns of the lateral ventricles returned to control values within 1 week following shunting of rabbits that had been hydrocephalic for 1 or 8 weeks (Figure 5). However, the appearance of the ventricular surface in the shunted rabbits did not return to normal.

Rabbits shunted 1 week after the induction of hydrocephalus had only slightly fewer cilia on the ventricular surface of the CN, CC, and LSA as compared to controls. Numerous supraependymal macrophages remained scattered on the surface of the ventricle. Except for residual flattening of the ependymal cells, their

ultrastructure was similar to that of controls (Section 4.4.1). The complement of ependymal intracellular organelles was normal and the apical lateral junctional complexes were intact. Compared to 1 week hydrocephalic rabbits, the number of ependymal cells per unit length of ventricular surface had significantly ($P<0.01$) increased over the CN and CC in shunted rabbits (Figure 13). The number of ependymal cells per unit length over the LSA did not increase, however, and remained less than the control value ($P<0.001$). Despite the reversal of ependymal stretching, mitotic activity remained elevated in the ependymal cell populations over the CN ($P<0.052$) and CC (Table I). The number of mitotic figures among astrocytes in the subependymal region reached higher levels over the CN (1.8% per 6 hours, $P<0.01$) and CC (0.97%, $P<0.01$), 1 week following shunting than after 1 week of hydrocephalus (Table II). Gliosis was histologically evident in the subependymal region of the CC and CN of all shunted rabbits. The extracellular spaces in the CC returned to their normal size following shunting.

Shunting of 8 week hydrocephalic rabbits for a comparable 1 week period, however, did not reverse any of the pathologic changes in the periventricular tissue. Ependymal cells with enlarged surface area, few microvilli, and reduced numbers of cilia persisted over the CC and LSA. The ultrastructure of ependymal cells lining the CN, CC, and LSA resembled that of the 8 week hydrocephalic rabbits that had not been shunted (Section 4.4.2). Whereas the number of ependymal cells per unit length of ventricle increased

($P<0.01$) in the shunted 1 week hydrocephalic rabbits, there was no comparable increase after shunting the 8 week hydrocephalic rabbits (Figure 13). Astrogliosis in the subependymal region was prominent in all areas surrounding the frontal horn of the lateral ventricle. A single 8 week hydrocephalic rabbit had small ventricles after 4 weeks of CSF drainage through a cerebral fistula. The ependymal surface had more cilia than after 1 week of shunting but did not resemble the control appearance.

Shunting after 1 week of hydrocephalus caused the number of patent capillaries ($\leq$10 um diameter) to increase in all regions studied except the LSA-P. Shunting after 8 weeks, however, was associated with an equivalent increase in the number of patent vessels only in the CC-P. The number of patent capillaries did not significantly change in the CN-D, CN-P, CC-D, or LSA-P (Figure 15).

4.6 Pathology of the ventricular surface caused by the shunt catheter

4.6.1 Non-functioning shunts implanted into normal rabbits

Implantation of shunt tubing into non-hydrocephalic rabbits was not associated with mortality nor was there evidence of infection at the operative site at any post-operative interval. Unlike controls, the choroid plexus in five of eighteen experimental rabbits extended into the frontal horns and was in contact with the implanted tubing.

At 3 days post-implantation, a fibrinous clot of blood elements lay between the shunt and the ventricular surface. By 1 week the debris had been removed and pathologic changes of the ventricular surface were evident. The ependymal surface adjacent to, but not contacting, the implant had a normal complement of cilia and microvilli (Figure 16A). Ventricular lining in direct contact with the shunt implant was distinguished by an abrupt transition from a densely ciliated surface to one almost devoid of cilia (Figure 16A, 16B). Although microvilli remained prominent on the ependymal surface in regions contacting the shunt for 2 weeks, they too degenerated after 4-8 weeks. In the region near the shunt implant, supraependymal macrophages were commonly observed from 3 days to 4 weeks post-implantation (Figure 16C). Furthermore, the ependymal cells acquired an irregular shape. The extracellular spaces surrounding the ependymal cells were enlarged from 3 days to 4 weeks post-implantation and accommodated numerous folds of the lateral and basal ependymal cytoplasm (Figure 16D).

The surface of the ventricle in direct contact with the implant underwent the most pronounced degenerative changes. Ependymal cells atrophied as evidenced by clefts between the cells (Figure 17A, 17B) leaving enlarged extracellular spaces in direct communication with the CSF (Figure 17B). A featureless ventricular surface developed over the 4 week post-implantation period (Figure 17C). The attenuated ependymal cells in this region often contained dense

Figure 16. Scanning (A,B,C) and transmission electron micrographs (D) showing the lining of the frontal horn of the non-hydrocephalic rabbit in contact with shunt catheter implants for up to 3 weeks.

A) There is an abrupt transition between the densely ciliated normal ependyma (E) and the denuded surface in contact with the shunt. Supra-ependymal cells (M) are scattered on the ependymal surface along the transitional area.

B) Higher magnification of the transitional area shows isolated clusters of ependymal cilia (c), some in the process of degeneration (solid arrow). There is an extensive covering of microvilli (mv) on the ependymal surface.

C) The transitional area is devoid of cilia but populated with numerous supra-ependymal cells (M). These cells, with ovoid cell bodies and multiple short pseudopodia, are presumed to be macrophages.

D) Ependymal cells (E) in the transitional area are irregular in shape with extensive cytoplasmic folds projecting into the enlarged lateral and basal extracellular spaces (*). Zonulae adherens (za) between the lateral processes of ependymal cells remain intact and the integrity of the lining is preserved. V, ventricle; c, cilia.

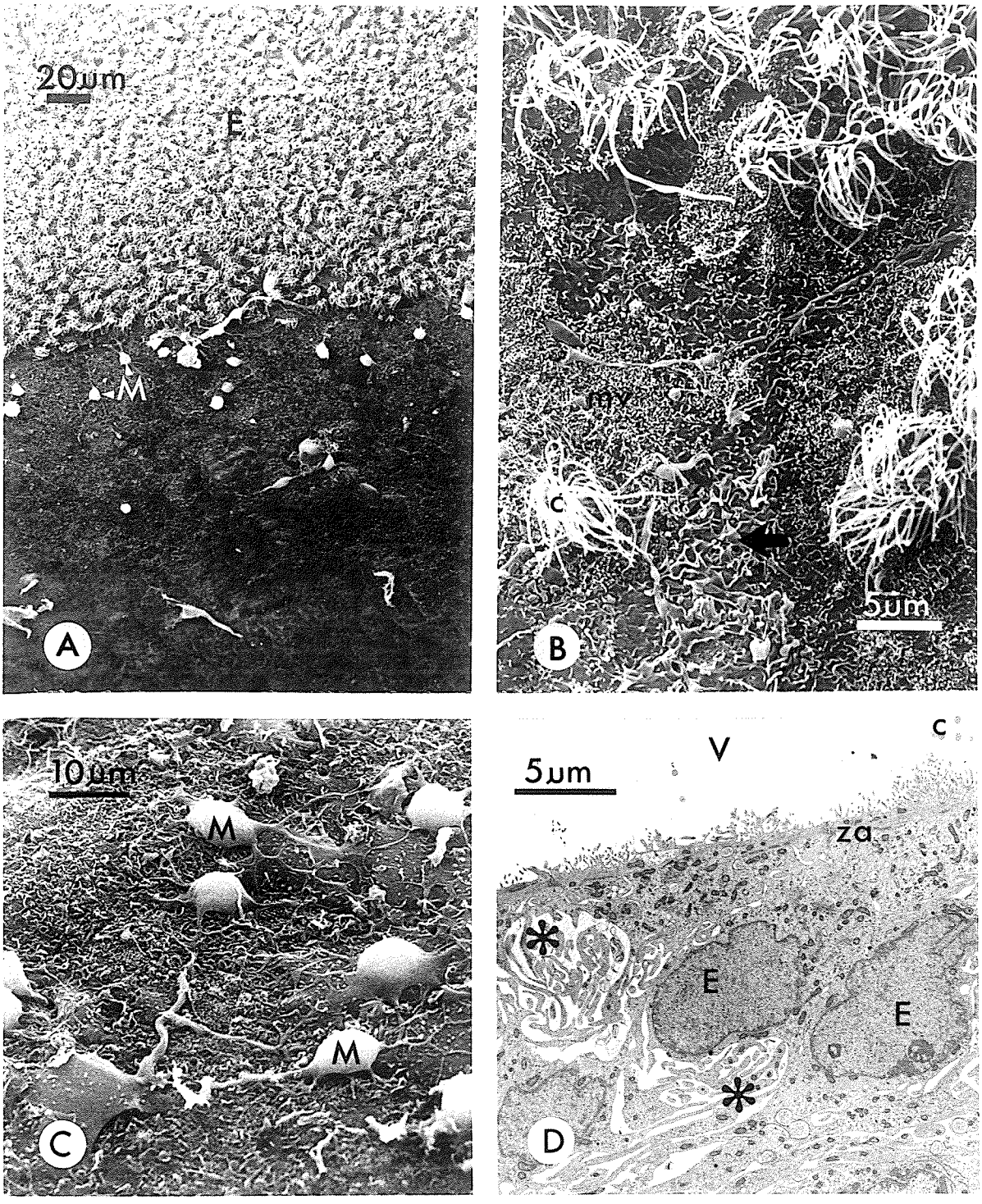
20µm
E
M
A
my
c
5µm
B
10µm
M
M
C
V
c
5µm
za
*
E
E
*
D

Figure 17. Scanning (A,C) and transmission (B,D) electron micrographs (TEM) showing regions of the frontal horn of the rabbit lateral ventricle in direct contact with the shunt tubing.

A) At 3 weeks post-implantation, ependymal cells were covered with microvilli, but cilia were either damaged (c) or entirely absent. More severely damaged ependymal cells (E) were characterized by a featureless surface. Atrophy of ependymal cells produced enlarged intercellular clefts (arrow).

B) TEM of a comparable region showing the atrophied ependymal cells (E). The ventricle (V) and enlarged extracellular spaces (*) communicate freely (arrows). In the subependymal region are atypical electron dense cells that resemble fibroblasts. col, collagen.

C) By 8 weeks post-implantation the ventricular surface is almost featureless. Neither cilia, microvilli, nor the borders of ependymal cells can be discerned.

D) TEM of a comparable region showing an abnormal number of vacuoles (vac) and dense inclusions (inc) within the cytoplasm of the attenuated ependymal cell (E). Numerous astroglial processes with dense accumulations of glial filaments (f) are present deep to the ependyma. V, ventricle; *, enlarged extracellular space.

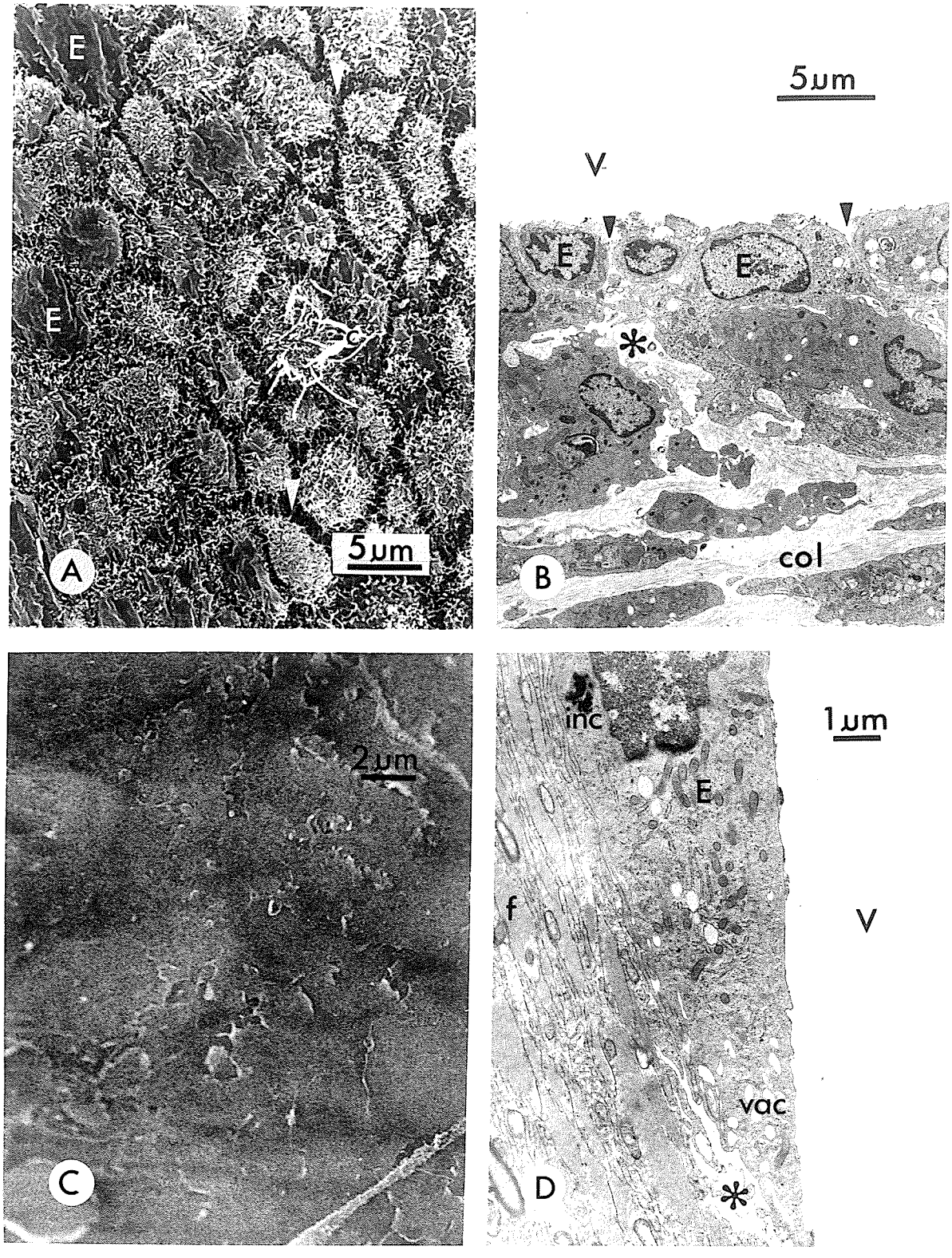
E
E
C
5µm
A
5µm
V
E
E
*
col
B
2µm
C
inc
E
f
V
vac
D
*
1µm

inclusions and many vacuoles (Figure 17D). By 8 weeks post-implantation, progressive degeneration left areas of lining denuded of ependymal cells, exposing underlying astroglial cells and processes to the ventricle. Clusters of normal ependymal cells buried in the subependymal region were occasionally observed at post-operative intervals exceeding 2 weeks. In addition, isolated clusters of fibroblast-like cells interspersed with loosely organized collagen fibers were observed (Figure 17B).

The surface of the ventricle directly adjacent to holes in the shunt catheter implants demonstrated the most dramatic changes. Outgrowths projecting from the ventricular surface into the implant holes were seen at all intervals after 1 week post-implantation. A total of 18 outgrowths were seen in 10 of 22 experimental animals. The outgrowths varied greatly in size and shape but generally enlarged with time. The outgrowths were covered by an ependymal lining that was intact near the base but became progressively more attenuated and damaged toward the apex where a loose meshwork of astroglial cells and processes was often exposed to the CSF (Figure 18B). Initially, the cores of the outgrowths consisted of hypertrophic astrocytes and macrophages surrounded by large extracellular spaces and abundant amorphous material. By 2 weeks post-implantation, hypertrophic astrocytes were more common and by 4 weeks, the outgrowths were densely cellular and had been invaded by capillaries and small venules. No neuronal elements were identified in any of the outgrowths. By 8-16 weeks, the

Figure 18. Scanning electron micrographs of the surface of the frontal horn of the rabbit lateral ventricle adjacent to holes in the shunt catheters.

A) Micrograph of the ventricular surface of a 1 week hydrocephalic rabbit that was shunted for 1 week. The dome-shaped protrusion from the surface is covered by ciliated ependymal cells (E). Surrounding the outgrowth, debris (d) covers the ependymal surface where the shunt tubing contacted the ventricular wall.

B) Micrograph showing a ventricular wall outgrowth in a non-hydrocephalic rabbit that had a shunt catheter implanted for 3 weeks. The outgrowth is partially covered by ciliated ependyma (E) which appears normal near the base. The ependyma is devoid of cilia along the side of the outgrowth and in the surrounding areas where it contacted the shunt catheter (solid arrows). At the apex of the outgrowth (open arrow), ependyma is absent and astrocytic cell processes are exposed to the ventricle. The expansion of astroglial cells partially filled the lumen of the shunt catheter. d, debris

Both micrographs are the same magnification. Bar = 100 um

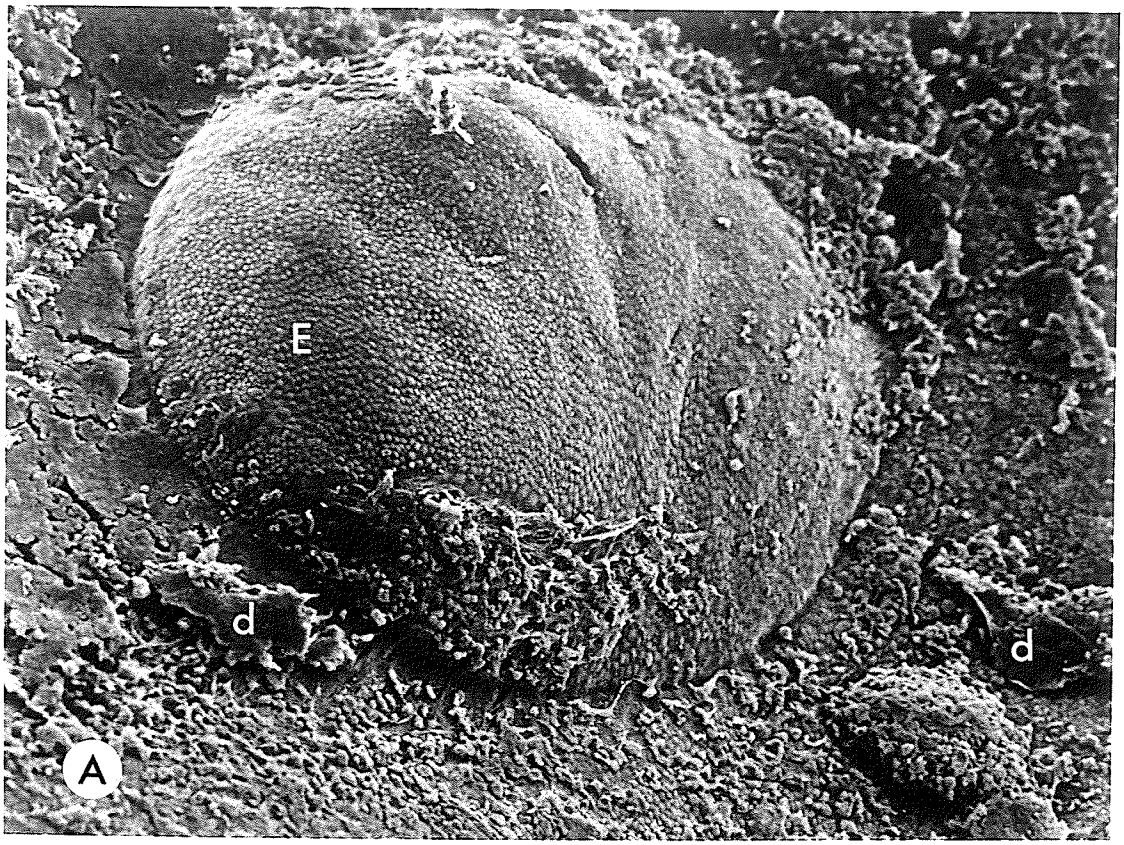
E
d
d
A

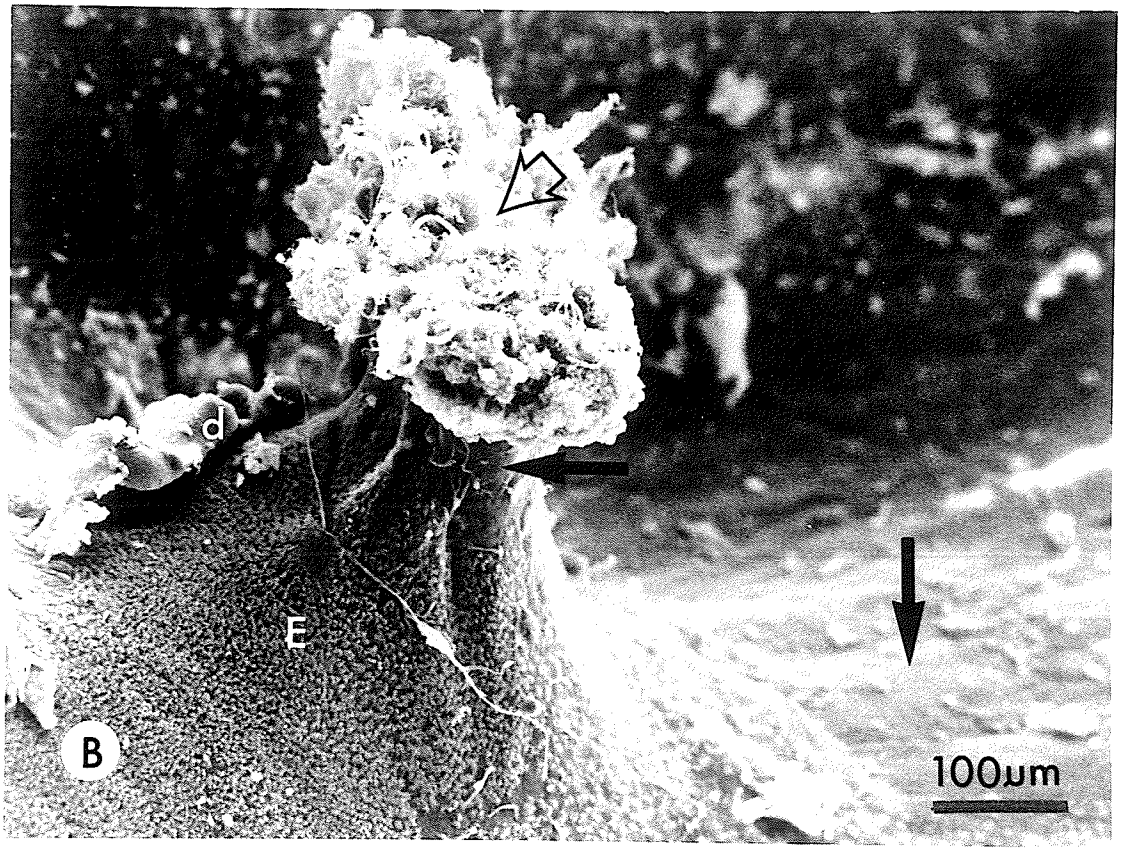
d
E
B
100µm

pedunculated glial outgrowths were well vascularized and often filled the lumen of the implant tubing.

Mitotic ependymal cells were identified near the base of some outgrowths as early as 1 week post-implantation (Figure 19A). In addition, clusters of primitive ependymal cells were frequently seen in the same region at 2 weeks post-implantation (Figure 19B). Near the implanted shunt tubing, mitotic figures among ependymal cells were increased in number above control values at 1 ($P<0.001$) and 2 ($P<0.005$) weeks post-implantation (Table III). Proliferation of astrocytes in the subependymal region adjacent the implants also increased significantly at 3 days ($P<0.001$), reached a peak at 1 week post-implantation ($P<0.001$), and declined thereafter.

4.6.2 Functional shunts in hydrocephalic rabbits

Shunting successfully reduced the size of the ventricles in 8 of 16 (50%) hydrocephalic rabbits. A variety of shunt complications, however, were encountered (Table IV). Two shunted rabbits died, one in the immediate post-operative period due to an intracranial hemorrhage and one on the third post-operative day due to a purulent meningitis. The complete shunt apparatus migrated into the peritoneal cavity of the two rabbits that received a ventriculo-peritoneal shunt. In one of these rabbits, a residual cerebral fistula successfully drained CSF for 4 weeks. There were three proximal shunt obstructions, two due

Figure 19. Transmission electron micrographs showing the ependymal lining of frontal horns of non-hydrocephalic rabbits with implanted shunt catheters.

A) At 1 week post-implantation a mitotic cell, presumed to be ependymal, lies between two attenuated ependymal cells (E) near the base of a ventricular wall outgrowth. The mitotic cell contains abundant dilated smooth endoplasmic reticulum, mitochondria, and condensed chromatin (chr). V, ventricle; col, collagen.

B) At 2 weeks post-implantation, a cluster of primitive ependymal cells lacking the specializations and uniform polarity characteristic of mature ependymal cells is seen in the ventricular wall near the base of a ventricular wall outgrowth. *, enlarged extracellular spaces; V, ventricle.

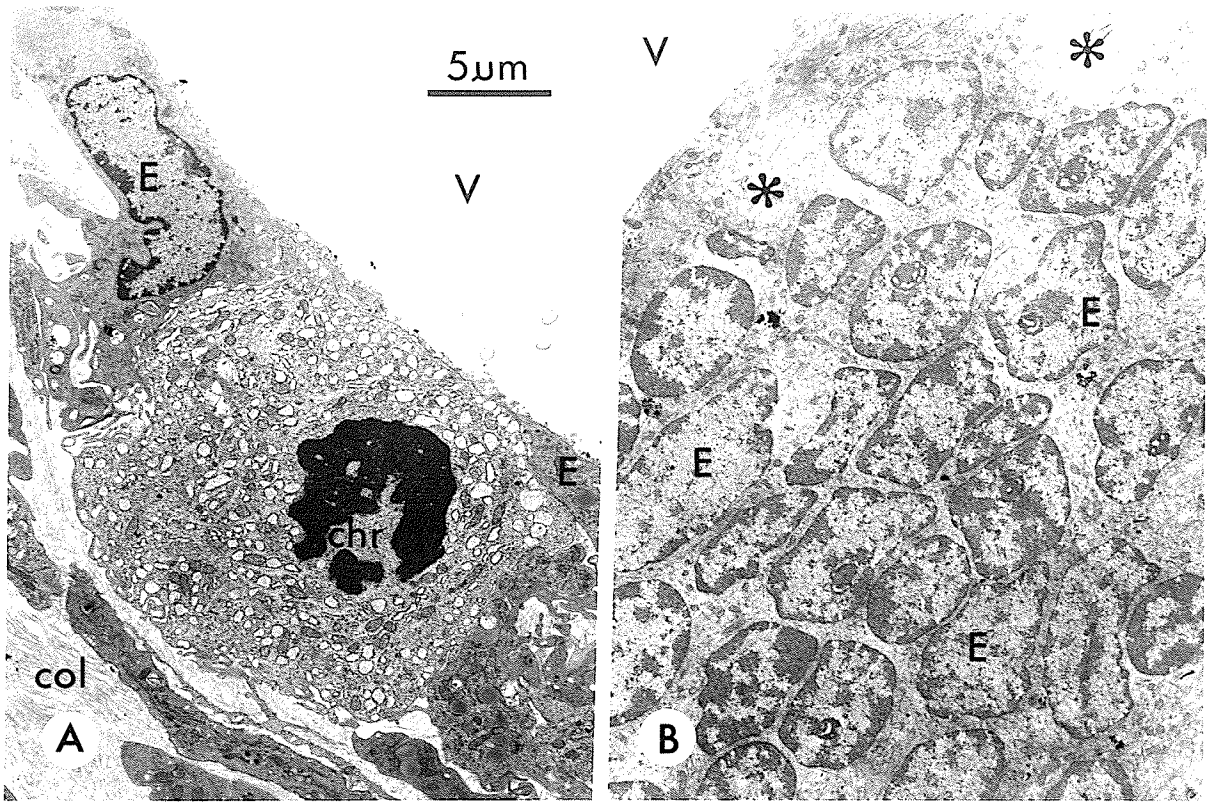
5µm
V
E
E
chr
col
A
V
*
*
E
E
E
B

Table III. Mitotic activity among ependymal cells and astrocytes of the frontal horn of the lateral ventricle of control and shunt-implanted non-hydrocephalic rabbits.

Group	Number of Rabbits	Ependymal Cells	Astroglial Cells
Control rabbits			
Intact	2	6 / 9240[a] (0.065%)	78 / 9555 (0.82%)
Sham-operated	2	12 / 27,016 (0.044%)	245 / 31,594 (0.78%)
Shunt implanted rabbits			
3 Day	1	5 / 3291 (0.15%)	104 / 4257** (2.4%)
1 Week	2	14 / 3480** (0.40%)	80 / 4826** (1.7%)
2 Week	2	7 / 2698* (0.26%)	39 / 6852 (0.57%)
4 Week	2	0 / 1925 (0.0%)	20 / 3055 (0.65%)

a. number of mitotic cells / total cells counted (percent mitotic cells during a 6 hour period)

* $P<0.005$, ** $P<0.001$ significantly different from sham controls as determined by the one tailed z-test

Table IV. Results of shunting hydrocephalic rabbits.

Duration of hydrocephalus (weeks)	Shunt duration (weeks)	Shunt success/ Total shunted	Shunt complications
1	1	4 / 5	1 death - hemorrhage
4	4	0 / 2	1 proximal* silicone oil obstruction, 1 proximal tissue** obstruction
8	1	3 / 5	1 proximal and 1 distal tissue obstruction
8	4	1 / 4	1 death - meningitis, 1 proximal tissue obstruction, 2 shunt migrations***

* Proximal obstructions occur within the lateral ventricle

** Tissue obstructions are due to reactive tissue growth around or into shunt catheter.

*** Complete shunt apparatus pulled out of the brain and migrated along subcutaneous tract into peritoneal cavity

to ventricular tissue ingrowth and one due to retrograde flow of the silicone oil through the ventricular system into the shunt catheter.

The frontal horns of the hydrocephalic rabbits, into which the CSF shunt catheters had been inserted for 1 week, were examined. In all specimens, there was a loss of ependymal surface features. Periventricular gliosis was more severe than that resulting from hydrocephalus alone. At the abrupt transition from the normal ciliated ependymal surface to one lacking cilia were numerous supraependymal macrophages. Erosion of ependymal surface features was comparable to that seen in normal rabbits with non-functioning shunt catheters implanted for 2 weeks (Section 4.6.1, Figure 16).

Four of the fourteen surviving shunted hydrocephalic rabbits exhibited ventricular surface outgrowths similar to those described in non-hydrocephalic rabbits (Figure 18A). Shunt failure in two of these four rabbits was due to growth of periventricular tissue into the shunt catheter. A third shunt obstruction was secondary to a ventricular wall outgrowth in conjunction with choroid plexus invasion. The ventricular wall outgrowth of the fourth rabbit did not completely obstruct the shunt. The outgrowths from the walls of the ventricle were incompletely covered by ependymal cells and had cores of loosely organized glial cells. Although the rate of growth could not be quantified, the size of the outgrowths in hydrocephalic rabbits was not larger than those in normal rabbits with shunt catheters

implanted for comparable durations.

4.7 Reaction of the lining of the fourth ventricle to silicone oil

The floor of the normal fourth ventricle was lined by ciliated ependymal cells which were cuboidal except in the median sulcus where they were columnar and stratified. Their ultrastructure was not examined, but by light microscopic examination they appeared comparable to ependymal cells in the frontal horn of the lateral ventricle (Section 4.4.1). Silicone oil injected into the cisterna magna to create hydrocephalus invariably refluxed into the fourth ventricle. Ependymal cells in direct contact with silicone oil for 1 week were denuded of cilia, pleomorphic, and had enlarged surrounding extracellular spaces. Despite the morphologic changes, there was no associated change in the mitotic activity of the cells; 0 / 5557 ependymal cells in the saline injected control rabbits and 1 / 5445 ependymal cells in the silicone oil injected rabbits were observed to be arrested in metaphase ($P>0.1$). Flattened macrophages were common on the surface of the ventricle. The neuropil deep to the intact ependyma was unaltered by the silicone oil.

5. DISCUSSION

The present study provides new information regarding the pathophysiology of experimental hydrocephalus by correlating ventricular size and chronically recorded intracranial pressure with cytopathology and cerebral water content. Qualitative and quantitative histologic and electron microscopic studies have revealed brain pathology due to hydrocephalus not previously reported.

5.1 Intracranial pressure in hydrocephalic rabbits

In previous studies, ICP has been recorded continuously only during the acute stages of hydrocephalus (Edvinsson and West, 1971a; Matsumoto et al., 1986; Obenchain and Stern, 1973; Portnoy et al., 1985). ICP measured in the epidural space, as in the present study, has been shown to be comparable to CSF pressure recorded in the cisterna magna (Ivan and Choo, 1982) and the subarachnoid space over the convexity of the hemisphere (Coroneas et al., 1972; McGraw, 1974). Epidural sensors are especially suitable for chronic recording because of the low infection rate, minimal invasiveness, and absence of artifactual signals secondary to movement of the subject (Gaab and Heissler, 1984).

During injection of silicone oil into the cisterna magna of the rabbit, ICP was briefly elevated to high levels. The silicone oil flows from the cisterna magna into the fourth ventricle and around the brainstem, thus reducing CSF flow from the cerebral aqueduct and fourth ventricle

respectively (James and Strecker, 1973). Prior drainage of CSF minimized the effect that the acutely injected volume of silicone oil would have on ICP. Immediately following the injection of oil, ICP decreased but remained significantly elevated above control levels for 36 hours thereafter. The complete obstruction of CSF flow caused by injections of hardening silicone rubber lead to continuously high ICP and death (Obenchain and Stern, 1973). It is concluded, therefore, that the volume and viscosity of silicone oil used in this study allowed a restricted flow of CSF.

The return of ICP to control values after 36 hours is consistent with a previous observation that ICP returns to normal within 4 days following kaolin induction of hydrocephalus in rabbits (Edvinsson and West, 1971a). Although the baseline ICP approached control values in the presently studied rabbits, pressure variability with transient elevations were observed in hydrocephalic rabbits for the duration of the experimental period. This phenomenon, not previously reported in an experimental animal model, closely resembles observations of intermittent pressure elevations in human subjects with chronic communicating hydrocephalus (Chawla et al., 1974; DiRocco et al., 1975; Gucer et al., 1980; Symon and Dorsch, 1975). The pressure elevations have been attributed to decreased compliance in the CSF compartment which reduces its ability to buffer perturbations in volume (Gucer et al., 1980). The increased resistance to CSF outflow that causes decreased compliance in hydrocephalic humans (Borgensen, 1984) is

simulated by the silicone oil obstruction to CSF flow in the rabbit model (Del Bigio and Bruni, 1987).

5.2 Ventricular dilatation in hydrocephalus

The frontal horns of the rabbit lateral ventricles increased to a maximum size within 3 days following induction of hydrocephalus and did not change appreciably thereafter. Ventriculomegaly in monkeys has been reported to occur within 12 hours of silicone oil injection (Diggs et al., 1986). Such a rapid dilatation is consistent with the acute mechanical obstruction to CSF flow believed to be caused by silicone oil. In contrast, the inflammatory response induced by kaolin is progressive and the degree of obstruction may increase with time. As in kaolin-induced hydrocephalus (Edvinsson and West, 1971b), however, the ventricles actively dilated only during the period of elevated ICP.

The present results revealed regional differences in the extent of ventricular enlargement. The frontal horns of the lateral ventricles were more dilated than either the occipital regions or temporal horns of the lateral ventricles or the third ventricle. Significant dilatation primarily in the frontal horns is comparable to observations in adult human hydrocephalic brains (Russell, 1949). Regions of the ventricular system with initially large diameters are hypothesized to be more susceptible to increased CSF pressure because a greater stress is created across the

cerebral parenchyma in these regions (Hakim et al., 1976). In control rabbits, the frontal horns were widely patent whereas the occipital poles of the ventricles were slit-like with coarctations as previously reported (Fleischhauer, 1972). Accordingly, the larger frontal horns would be expected to dilate earlier and to a greater degree. A corollary of this hypothesis suggests that once ventricular dilatation has occurred, less pressure is required to maintain the enlarged size of the ventricle. This may explain why ventriculomegaly persists in the silicone oil induced hydrocephalic rabbit even after the ICP returns to control values.

5.3 Cerebral water content

Ventricular dilatation must occur at the expense of one or more components of the brain parenchyma. Water content and solid tissue components of the brain are considered to be the major determinants of brain specific gravity (Bothe et al., 1984; Ferzst et al., 1980; Nelson et al., 1971; Picozzi et al., 1985). The specific gravity measurements of rabbit cerebrum showed that moderate hydrocephalus caused a decrease in brain water content except adjacent to the surface of the ventricle. There was no coexistent change in the solid tissue components of the cerebrum. Loss of water began 3 days after the induction of hydrocephalus and continued throughout the 4 week experimental period (Del Bigio and Bruni, 1987).

Although the specific gravity of fresh cerebral tissue

determined in this study is generally consistent with previously reported values, there are differences which may be attributable to methodology or interspecies variation. The data obtained from control rabbits in the present study indicates that superficial cortical gray matter has a lower specific gravity than white matter whereas gray matter from deeper cortical layers has a higher specific gravity than white matter. Previous reports that fresh white matter has either a higher (Ferzst et al., 1980; Marmarou et al., 1978) or a lower (Bothe et al., 1984; Shigeno et al., 1982; Tengvar et al., 1982) specific gravity than fresh gray matter can be explained on the basis of the specific gravity gradient through the gray matter.

In the present study, the average specific gravity of desiccated gray matter was 1.21 g/cm^3 and that of white matter was 1.18. The specific gravity of anhydrous cerebral tissues has previously been calculated but not directly measured. Specific gravity of dried mouse cortex was calculated to be 1.30-1.32 (Nelson et al., 1971) whereas a value of 1.26 was reported for cat gray matter (Marmarou et al., 1978). Desiccated white matter from cat brains has been calculated to have a specific gravity of 1.146 (Marmarou et al., 1978) and ranges from 1.155 at the ventricular surface to 1.139, 3 mm from the surface (Takei et al., 1987). Differences between calculated values in the literature and the values obtained in this study cannot be reconciled with the limited information available.

Statistically significant differences were not found between desiccated tissues obtained from control and hydrocephalic rabbits at any post-injection interval. This suggests that there were no changes in the composition of the anhydrous cerebral tissues of the hydrocephalic rabbits. Similarly, Rubin et al. (1976a) found no change in the dry weights of kaolin-induced hydrocephalic cat brains. If the periventricular demyelination observed histologically in comparable experimental models of hydrocephalus was widespread (Weller and Wisniewski, 1969), the loss of low density myelin lipids (Higashi et al., 1986) would be expected to increase the specific gravity of periventricular white matter. No such change was demonstrated in acutely or chronically hydrocephalic rabbits in the present study. Because the constituents of solid cerebral tissue were unchanged, the specific gravity changes in fresh brain are attributable to decreased water content. Loss of brain water has also been observed in hydrocephalic cats (Kuchiwaki et al., 1979) but not in kaolin-induced hydrocephalic rabbits (Higashi et al., 1986).

A decrease in the size of the extracellular spaces in the cortex of hydrocephalic mice has been demonstrated (McLone et al., 1973). Extracellular space compression could explain the loss of water from the brains of the hydrocephalic rabbits in this study. That would be consistent with the hypothesis of Hakim etal. (1976) that describes the brain as a "submicroscopic sponge of viscoelastic material whose time dependent 'give' is

provided by venous capillaries [and] the extracellular spaces".

Despite the significant specific gravity increase elsewhere in the cerebrum, there was a decrease in the specific gravity of white matter immediately adjacent to the surface of the ventricle, 3 days following the induction of hydrocephalus. This finding, which is suggestive of an increase in the periventricular water content, is consistent with the observation of enlarged extracellular spaces to a depth of 100 um from the ventricle. Previous findings in hydrocephalic rabbits (Higashi et al., 1986), cats (Hochwald et al, 1975), and dogs (Fishman and Greer, 1963; Inaba et al., 1984) also support the concept of periventricular accumulations of fluid (Lux et al., 1970).

5.4 Cytopathology of silicone oil induced hydrocephalus

The observation of regional variations in the morphology of the ependyma and subependymal region is consistent with previous descriptions of the periventricular tissues in normal rabbits (Page et al., 1979b) and rats (Mitro and Palkovits, 1981). Attenuation of the ependyma, gliosis in the subependymal region, and edema in the periventricular white matter have also been previously described in hydrocephalic animals (Clark and Milhorat, 1970; James et al., 1977; Page and Leure-duPree, 1983; Rubin et al., 1975; Weller and Wisniewski, 1969).

Ventriculomegaly is believed to have occurred as a

result of two phenomena. Firstly, changes in the configuration of the ventricle caused by separation of the opposing ventricular walls occurred without stretching of the ventricular surface. This contributed to enlargement of the occipital poles of the lateral ventricles and the third ventricle. Secondly, the frontal horns enlarged as a consequence of stretching of the periventricular tissues in addition to a change in configuration of the ventricle. The ependymal lining and astrocytes in the subependymal region offer little resistance to stretching forces (Fleischhauer, 1972). Continuity of the ependymal lining was only maintained by ependymal cell stretching (Page et al., 1979a). Discontinuity of the ependymal lining, occurs only with rapid onset or extreme degrees of ventricular dilatation (Collins, 1979).

The number of ependymal cells per unit length of the lining of the ventricle decreased differentially over the caudate nucleus, corpus callosum, and septal area. This observation suggests that the periventricular tissues of the frontal horns of the lateral ventricles were stretched to different degrees as a result of hydrocephalus. Significant stretching of ependymal cells over the caudate and lateral septal nuclei is inconsistent with reports that hydrocephalus causes ependymal alterations only over white matter (Page, 1975; Page et al., 1979a; Torvik, 1981). The present demonstration of irreversible changes in the ependyma and vasculature of the septal area supports previous reports that the septal region is severely damaged

by hydrocephalus (Clark and Milhorat, 1970; De, 1950). Dorsoventral stretching of the septal area is likely the same mechanism that contributes to fenestration of the septum pellucidum in humans with hydrocephalus (Russell, 1949).

As a result of elevated intraventricular CSF pressure, the cerebral ventricles dilate and become more spherical as the surrounding tissues are deformed centrifugally (Hakim et al., 1976). In spite of minimal tensile strength, an arch is known to be more resistant to compressive forces than flat structures of similar composition (White et al., 1976). The caudate nucleus, hippocampus, and other structures presenting an arch-like convex face to the ventricle therefore resist the centrifugal forces resulting from elevated intraventricular pressure. Flat or concave structures such as the septal area and corpus callosum respectively, offer less resistance to the deforming forces of the increased CSF pressure. Consistent with the structural theory is the present observation that, by 8 weeks after induction of hydrocephalus, the ependymal lining of the caudate was stretched by 20% as compared to 29% over the corpus callosum and 39% over the septal area. Thus, stretching of periventricular tissue appears to depend more on its physical configuration than on its cellular characteristics.

5.4.1 Cellular regeneration in hydrocephalus

Prior to this study, hydrocephalus induced ependymal cell regeneration had not been convincingly demonstrated. In the present study, hydrocephalus induced mitotic activity among ependymal cells lining the corpus callosum at 3 days and caudate nucleus at 2 weeks. Weller et al. (1978) did not find any increase in the total number of ependymal cells lining the frontal horns of neonatal rats following induction of hydrocephalus by kaolin. The discrepancy between studies is likely due to species, age, and methodological differences. Because the absolute increase in the rate of ependymal mitotic division was not large, inadequate sample size could easily account for previous failures to conclusively detect changes.

Up to a sixfold increase in mitotic activity was observed among ependymal cells 2 weeks after the onset of ventricular dilatation, yet there was no significant change in the number of ependymal cells per unit length of ventricular lining after maximal ventricular dilatation was reached at 3 days. The peak rate of mitosis was only 0.11 % per 6 hours, a limited response that could provide little compensation for the stretched lining. Stretching of ependymal cells, therefore, was primarily responsible for the maintenance of lining integrity.

In contrast, the increased mitotic activity observed among astrocytes in the subependymal region of the caudate nucleus, corpus callosum, and septal area of hydrocephalic

animals was not unexpected. The level of mitotic activity was ten times greater than that observed among ependymal cells. Russell (1949) reported that internal hydrocephalus commonly is associated with subependymal gliosis. Rubin et al. (1976) concluded from nucleic acid analysis that the gliosis in hydrocephalic cat brains was due to hypertrophy of pre-existing astrocytes and not to an increased number of cells. The present results, however, indicate that hyperplasia and hypertrophy of astrocytes occurred.

As the walls of the ventricle were stretched during the 3 days following induction of hydrocephalus, the number of astrocytes decreased in the subependymal region of the caudate nucleus, corpus callosum, and septal area. By 4 weeks post-induction the number of astrocytes over the corpus callosum had increased above control values, and over the caudate nucleus the number approached control values by 8 weeks. While the mitotic activity indicated the maximum response over the caudate nucleus, the astrocyte cell counts indicated maximal activity over the corpus callosum. Possible explanations for this apparent contradiction exist. Firstly, because the subependymal region of the caudate often extended beyond the sampling area, the increase in the number of astrocytes may have been underestimated. Secondly, mitotic activity among astrocytes peaked at a later time over the corpus callosum and this response may have been more prolonged. The low rates of mitotic activity among septal area astrocytes combined with continuous stretching may explain why the number of subependymal astrocytes did

not increase in the septal region.

What is the stimulus for increased mitotic activity in the periventricular cell populations? Silicone oil had no direct effect on the mitotic activity of ependyma lining the fourth ventricle and therefore is likely not a significant mitogenic factor (Wisniewski, 1961). Increased mitotic activity among ependyma and astrocytes occurred after drainage of CSF by shunting. Presumably any ICP elevations were prevented by shunting therefore elevated ICP alone is not the mitogenic stimulus associated with hydrocephalus.

During the 2 weeks following induction of hydrocephalus and 1 week following reduction of ventricular size by shunting, the ependymal and astroglial cell populations increased their rates of mitotic activity. Surgical trauma to the cerebrum is said to cause the release of chemical mitogens in the ipsilateral hemisphere (Willis et al., 1976), and astrocytes are known to proliferate within a few days around stab wounds in the cerebrum (Cavanagh, 1970). Cultured epithelial cells have been shown to synthesize more DNA in preparation for mitotic cell division when the surface on which they are growing is stretched enough to distort but not destroy the cells (Brunette, 1984). Perhaps mechanical distortion of the periventricular tissues, either stretching due to ventricular dilatation or relaxation following shunting, is sufficient to release mitogens that can cause increased mitotic activity among ependyma and astrocytes. The prolonged response, in comparison to stab

wounds, suggests that the mitogenic stimulus of brain deformation is prolonged over a period of days.

The periventricular tissue overlying the caudate nucleus underwent the least deformation as a result of hydrocephalus, yet ependymal cells and astrocytes in this region exhibited the greatest relative increases in mitotic activity. This observation is consistent with the recognized inherent differences in the mitotic responsiveness of ependyma in different regions of the central nervous system lining (Bruni et al., 1985). Furthermore, the persistence of germinal matrix remnants in the subependymal region over the caudate nucleus into adulthood (Fleischhauer, 1972) may explain why this region exhibited the highest rates of subependymal mitotic activity in the present experiment.

5.4.2 Periventricular vasculature in hydrocephalus

Control rabbits had a significantly greater number of patent capillaries in the caudate nucleus and lateral septal area than in the corpus callosum. The 2:1 ratio of capillaries in gray versus white matter is consistent with observations in cat and rat brains (Campbell, 1939; Cragie, 1920). Density of the capillary network has been shown to correlate with the number of neurons and glia (Sarkisov, 1966) and with regional oxidative metabolism (Friede, 1966; Gross et al., 1987). The observation of a greater number of arterioles and venules in the caudate nucleus than in the corpus callosum is consistent with previous findings in dogs (van den Bergh and vander Eecken, 1968). The periventricular

region of the corpus callosum was observed to be more densely vascular than the deep corpus callosum because of the rich vascularization of the subependymal region in all parts of the lining of the lateral ventricle including over the corpus callosum (Fleischhauer, 1972).

The number of patent capillaries was reduced in the periventricular regions of the caudate nucleus, corpus callosum, and septal area and in the deep corpus callosum of hydrocephalic rabbits. Only in the deep caudate nucleus, 0.5 mm from the ventricular surface, were no changes observed. Because the hydrocephalic brain is compressed and likely contains more vessels in a given volume of tissue, the true decrease in the number of capillaries is likely greater than the decrease determined here.

Potential factors contributing to the decrease in the number of patent capillaries in the neuropil surrounding the hydrocephalic ventricle are summarized in Figure 20. They are as follows:

1) The increased volume of the cerebral ventricles is rapidly compensated for by expulsion of blood and extracellular water from the cerebral parenchyma. Most of the blood volume reduction, however, is due to pressure compression of the large venous capacitance vessels, not the capillaries (Hakim et al., 1976).

2) The intermittent pressure elevations and increased pulse pressure (Dardenne et al., 1969; Matsumoto et al., 1986) may create transient tissue pressure gradients that

Figure 20. Diagram showing mechanisms that may contribute to the decrease in the number of patent capillaries within the periventricular neuropil of the cerebrum in hydrocephalic rabbits. Within the periventricular tissues, stretching of capillaries (small arrows) that accompanies ventricular dilatation and direct compression by the elevated pressures within the ventricle (large arrow) both contribute to the collapse of capillaries. Larger arteries (stippled) that pass through cerebral parenchyma may be compressed (large arrows) by the distorting forces acting upon the hydrocephalic brain. A hypothesized baroreceptor mechanism (?) that causes arteriolar constriction may also reduce capillary blood flow. SAS, subarachnoid space.

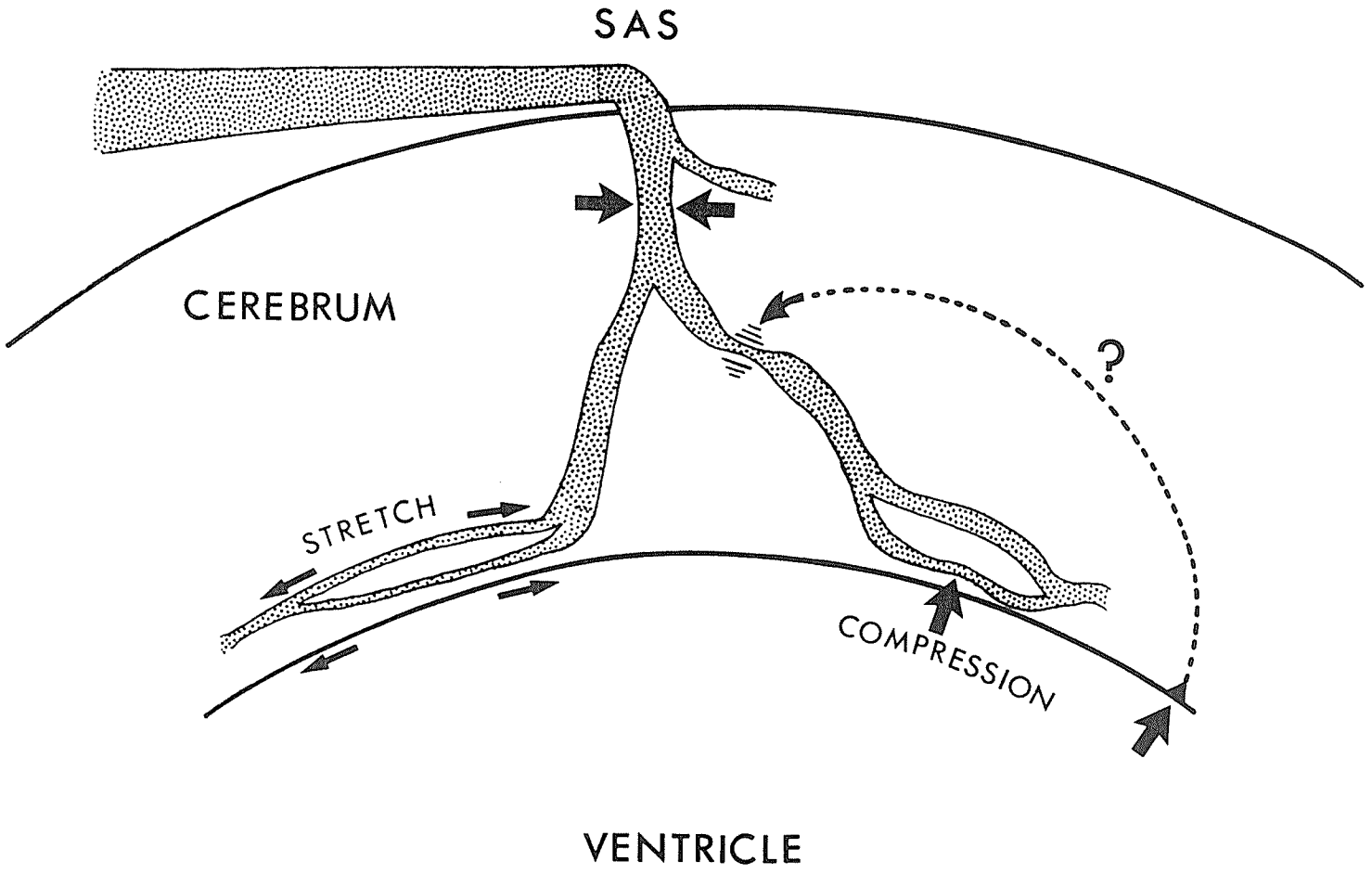
SAS
CEREBRUM
?
STRETCH
COMPRESSION
VENTRICLE

are maximal near the site of an expanding lesion, i.e. the ventricle (Brock et al., 1975; Shulman et al., 1975). However, in the equilibrium state, brain tissue pressure is equal to the ventricular fluid pressure and therefore the ICP (Iannotti et al., 1984). Thus the ICP in rabbits with silicone oil induced hydrocephalus is likely not sufficiently elevated to directly collapse the capillaries which have an intraluminal pressure of approximately 30 mm Hg (Ganong, 1979; Moskalenko et al., 1980).

3) The present results have shown, however, that distortion of the periventricular tissue includes stretching and compression. Both changes in physical configuration may serve to collapse capillaries located within the neuropil that surrounds the dilated ventricle.

4) Physical distortion of the brain by hydrocephalus has been shown to distort larger feeding arteries in the diencephalon and mesencephalon (Plets and van den Bergh, 1973). This in turn might cause collapse of distal vessels.

5) A neurovascular mechanism for capillary collapse is remotely possible. Removal of sympathetic input from the superior cervical ganglia to the cerebrovasculature of hydrocephalic rabbits has been shown to result in elevated intracranial pressure (Edvinsson et al., 1974). There may exist a mechanism by which raised intracranial pressure causes reflex sympathetic arteriolar constriction (Edvinsson et al., 1983; Moskalenko et al., 1980) and subsequent collapse of distal capillaries (Ganong, 1979). This reflex response, however, is unlikely to supersede the demand for

blood by the ischemic hydrocephalic brain (Higashi et al., 1986) and systemic blood pressure is known to increase in response to elevated intracranial pressure, presumably to improve blood flow to the brain (Johnston et al., 1972).

In summary, the reduced number of patent capillaries in the vicinity of the hydrocephalic ventricle is related to multiple factors. The relative contributions of each factor cannot be determined with the available information.

In spite of the vascular changes, evidence of axonal and neuronal degeneration was not observed in the hydrocephalic rabbits. Previous studies of cerebral histopathology following hydrocephalus have also failed to detect morphologic changes in the neural elements (Rowlatt, 1978; Rubin et al., 1976a, 1976c; Weller et al., 1971). This does not exclude the possibility that reduced blood flow due to vascular compression in the hydrocephalic brain may compromise its function (Jagust et al., 1985) without destroying neurons. Damage to neurons and axons undoubtedly occurs in more severe forms of hydrocephalus (McAllister et al., 1985).

5.5 Reversal of pathologic changes in hydrocephalic brains by shunting

Drainage of CSF from the lateral ventricles by shunting caused the ventricles to return to normal size within 1 week regardless of the duration of hydrocephalus. Despite the reduction in ventricular size, the morphology of the

periventricular tissue did not return to normal. Stretching of the ependymal cells was reversed over the caudate nucleus and corpus callosum but not over the septal area of rabbits that had been hydrocephalic for 1 week. There was no reversal of ependymal cell stretching in any region of the frontal horn if shunting was performed 8 weeks after hydrocephalus was induced.

Following shunting of the 1 week hydrocephalic rabbits, an increased number of patent capillaries were seen throughout the caudate nucleus and corpus callosum but not the septal area. The increase in the number of patent capillaries in the 1 week hydrocephalic rabbits suggests that the vessels were collapsed but intact and the reduction of the size of the ventricles allowed blood to reperfuse the capillaries. Shunting rabbits that were hydrocephalic for 8 weeks caused only a small increase in the number of patent capillaries at the ventricular surfaces of the caudate nucleus and corpus callosum. Prolonged distortion of the periventricular tissues may have caused the chronically collapsed vessels to disappear.

Both the ependyma and the periventricular capillaries failed to resume their normal configuration following shunting of rabbits that had been hydrocephalic for 8 weeks. This may be due to the formation of new astrocytes and astrocytic processes with reactive increases in the amount of glial filament material. Accumulation of astrocytes and their processes subjacent to the stretched ependyma and around the collapsed capillaries may fix those structures in

a distorted condition (Figure 21). In this study, reversal of the histopathology due to hydrocephalus was only studied after 1 week of shunting but additional remodeling is likely after prolonged periods of shunting.

In addition to the gliosis caused by hydrocephalus, the rabbits in the present study exhibited a significant increase in mitotic activity among astrocytes in the subependymal region after shunting. This observation suggests that periventricular tissue may be further "stiffened" after the cerebral ventricles have returned to normal size as has been suggested by Foltz (1984).

5.6 Periventricular pathology caused by shunt catheters

A variety of complications of shunting similar to those found in human hydrocephalic patients (Sayers, 1976) were encountered in the rabbit. Of particular interest were the proximal shunt obstructions caused by reactive changes in the periventricular tissue of the lateral ventricle due to the presence of the shunt tubing (Del Bigio and Bruni, 1986). Progressive erosion and attenuation of the ependyma followed by complete degeneration and sloughing of ependymal cells occurred in the most severely affected areas. Mechanical pressure generated by contact of the catheters with the ependymal lining is likely responsible for the changes. At the site of holes in the shunt tubing, evaginations of the ventricular wall resulted from reshaping of periventricular tissue by the mechanical pressure exerted

Figure 21. Schematic summarizing the sequence of pathological changes caused by hydrocephalic dilatation of the cerebral ventricles. In the normal rabbit, ependymal cells (E) lining the ventricle possess cilia (c) and microvilli (mv) on their surfaces. Astrocytes (A) containing glial filaments (f) are found in the subependymal neuropil surrounding capillaries (C).

In acutely hydrocephalic rabbits, the ependymal cells are attenuated. Astrocytes are also stretched and some capillaries are collapsed but their ultrastructure remains unchanged. Reduction of the size of the ventricles by shunting at this stage allows the distorted structures to resume their normal shape.

In chronically hydrocephalic rabbits, the ependyma is further attenuated and the surface specializations are lost. Capillaries in the neuropil are irreversibly collapsed. Proliferation of astrocytes continues and reactive changes have led to increased numbers of astrocyte processes that contain dense accumulations of glial filaments. This astroglial "scarring" reduces the resilience of the tissues and serves to anchor adjacent structures. Shunting at this stage is ineffective in restoring the normal morphology of the periventricular neuropil.

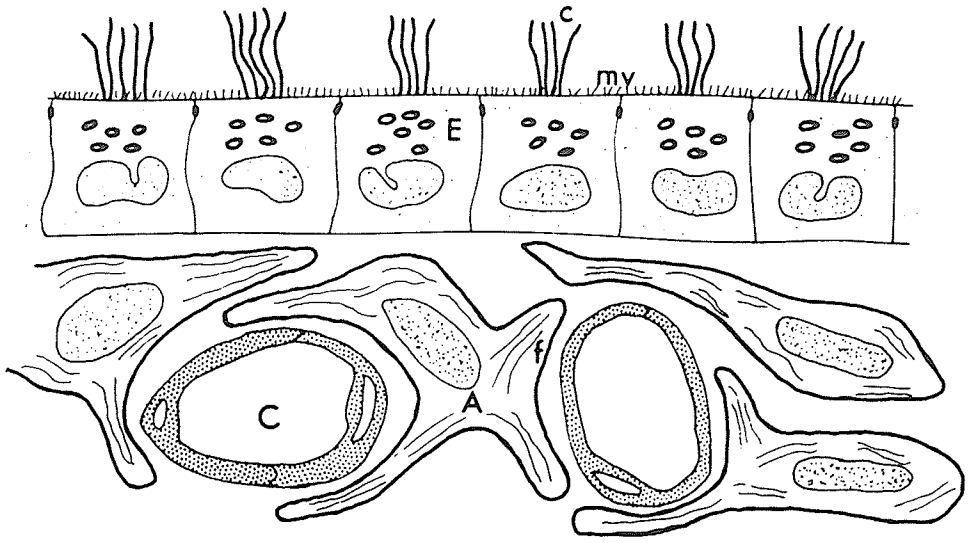

NORMAL

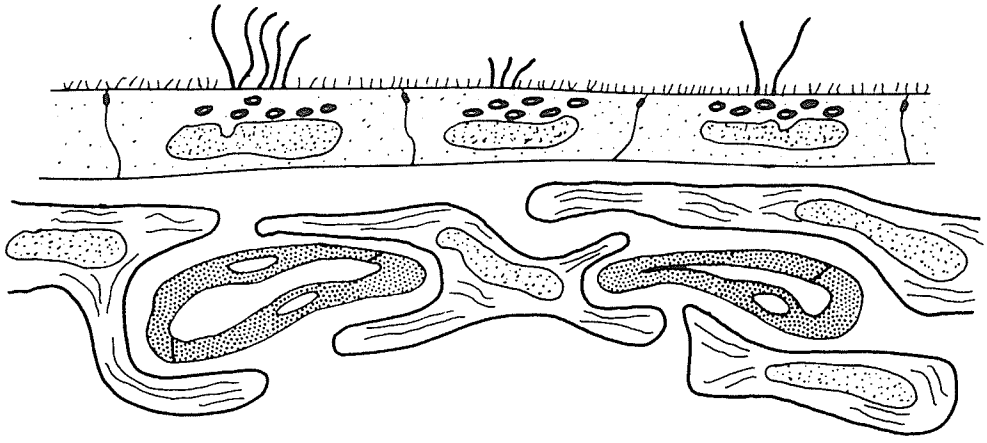

ACUTE HYDROCEPHALUS

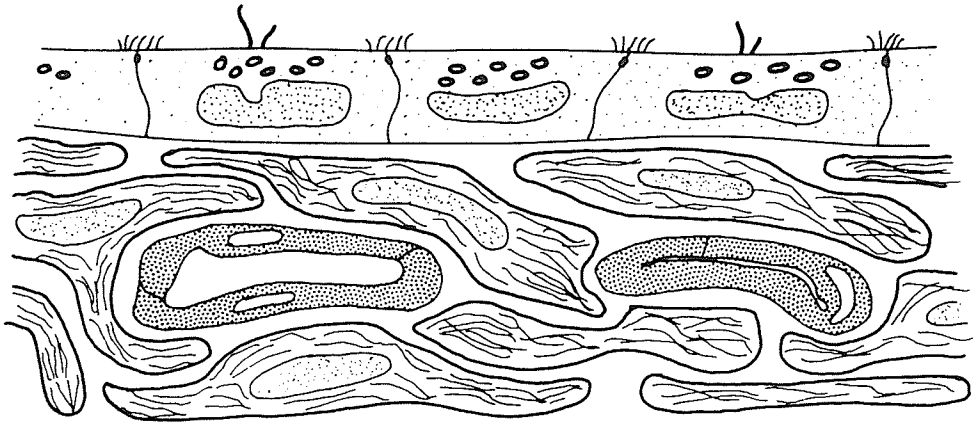

CHRONIC HYDROCEPHALUS

by the shunt. Astrogliosis further contributed to growth of the tissue into the shunt catheter. Similar pathology associated with shunt tubing has been demonstrated in the rat fourth ventricle (Bruni and Del Bigio, 1986).

Increased mitotic activity among ependymal cells was observed in response to the presence of shunt tubing. Peak activity occurred at 1 and 2 weeks following insertion of the catheters and was especially pronounced near the holes of the catheters. Similarly, increased proliferation of astrocytes was observed at 3 days and 1 week post-implantation. The stimulus for the mitotic activity would appear to be direct irritation by the implant as evidenced by the highly localized nature of the response (Del Bigio and Bruni, 1986). These findings are consistent with the theory that there is a reactive response of the ventricular tissue to the ventricular catheter (Giuffre, 1976). The formation of collagen represents a complication of the surgery (Krikorian et al., 1981; Sekhar et al., 1982), not a specific tissue response.

In addition to the mechanical effect of shunt tubing, a chemical irritant or mitogenic effect of the silicone rubber cannot be ruled out. Although silicone is regarded to be relatively inert (Habal, 1984), it has been recognized that silicone implants cause gliosis in the brain (Ammar, 1984). Furthermore, the barium or silver impregnated in the silicone rubber may contribute to the tissue reaction (Irving et al., 1971; Sugar and Bailey, 1974). Regardless of the etiology, the periventricular reaction and outgrowths

may be a factor in the pathogenesis of shunt malfunction.

6. SUMMARY AND CONCLUSIONS

The cerebral changes that occurred in silicone oil induced hydrocephalic rabbits are summarized in Figure 22. Obstruction of CSF flow by the silicone oil caused the intracranial pressure to increase. Increased CSF pressure exerted a centrifugal force on the cerebral parenchyma and, according to accepted physical principles, caused the ventricles to dilate differentially. Within the constant volume of the cranial compartment, ventricular enlargement was compensated by expulsion of extracellular water from the surrounding white and gray matter. Near the ventricular surface studied, however, there was an accumulation of extracellular fluid in the white matter due to CSF movement across the ependymal lining of the ventricle. The lining of the ventricular system was stretched to different degrees at different locations within the ventricle. Ependymal cells flattened and stretched in order to maintain the integrity of the lining.

Thirty-six hours after the induction of hydrocephalus, the ICP returned to control levels and by the day 3 the lateral ventricles reached their maximum size. During those 3 days the ependymal cells were maximally stretched in most regions. Elevated ICP and distortion of periventricular tissues caused the collapse of capillaries in the vicinity of the ventricle. Vascular compression is likely the cause ischemia in the hydrocephalic brain. From 3 days to 2 weeks following the induction of hydrocephalus there was increased mitotic activity in the ependymal cells and the subependymal

Figure 22. Graph summarizing the parameters measured in this study of silicone oil induced hydrocephalus in rabbits. The horizontal axis represents time after silicone oil injection into the cisterna magna. During the injection and for the following 36 hours, intracranial pressure (ICP) was elevated. Although ICP baseline returned to control, the pressure remained highly variable. During the period of increased ICP, the ventricular system dilated primarily at the expense of brain water. Dilatation of the ventricles caused simultaneous stretching and attenuation of the ventricular lining as evidenced by the decrease in number of ependymal cells. Distortion of the surface of the ventricle initiated an increase in the mitotic activity of ependyma and subependymal astrocytes that lasted for 2 weeks. Following an initial decrease in the number of subependymal astrocytes caused by stretching, there was a progressive increase in the number of astrocytes. Ventricular enlargement was also accompanied by a reduction in the number of patent capillaries in the surrounding neuropil.

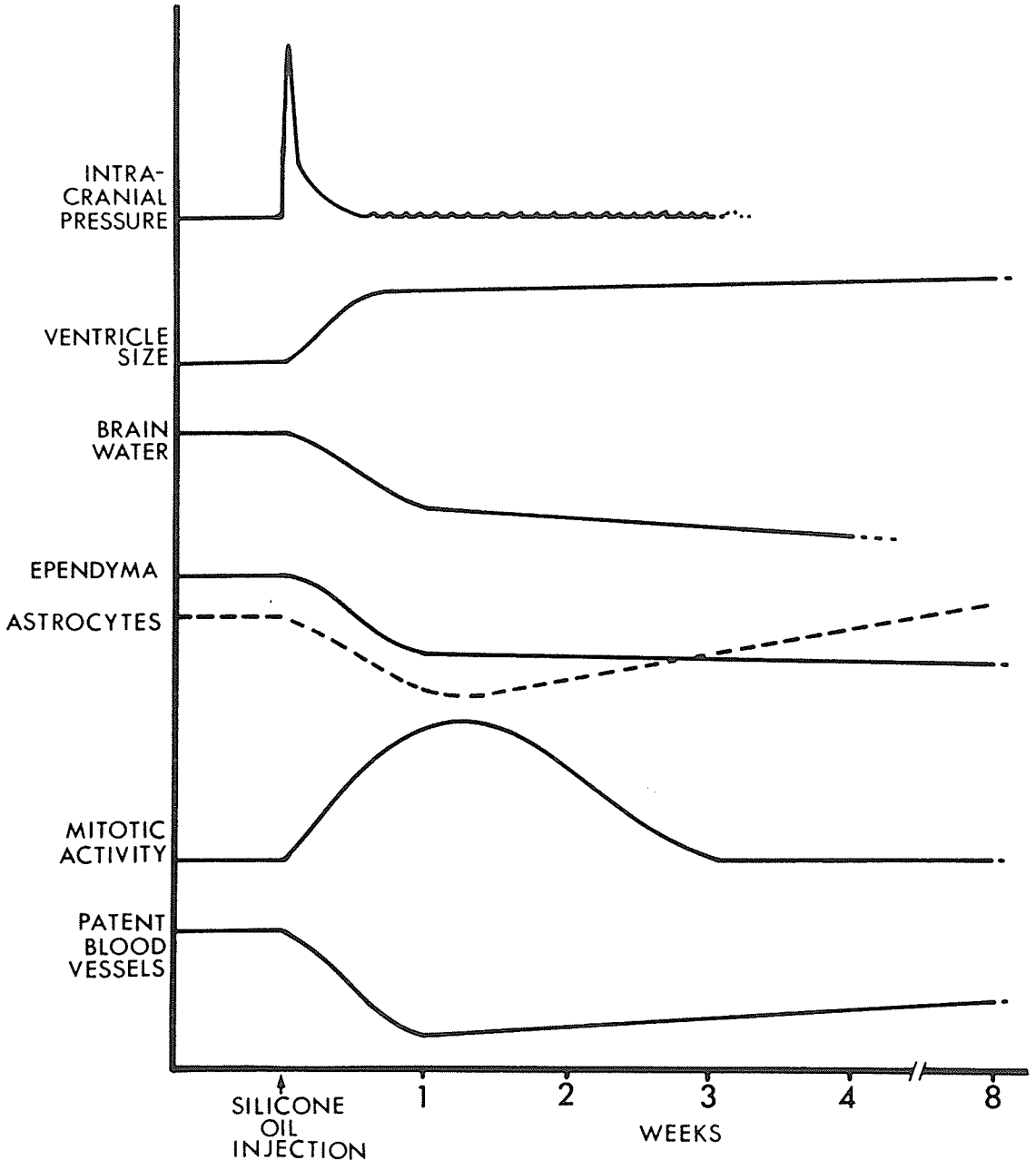
INTRA-
CRANIAL
PRESSURE
VENTRICLE
SIZE
BRAIN
WATER
EPENDYMA
ASTROCYTES
MITOTIC
ACTIVITY
PATENT
BLOOD
VESSELS
SILICONE
OIL
INJECTION
1
2
3
4
8
WEEKS

astrocytes. The addition of new ependymal cells, however, contributed minimally to the continuity of the lining of the ventricle.

The number of astrocytes in the subependymal region increased significantly and they reacted to ventricular dilatation by producing numerous processes filled with abundant glial filaments. As the duration of hydrocephalus increased, loss of water from the gray and white matter continued. The total brain volume changed insignificantly, however, so further loss of water may have allowed reperfusion of some of the previously collapsed capillaries.

Shunting of CSF restored the ventricles to their normal size. Reversal of the ependymal stretching and capillary collapse was possible only if shunting was performed in the early stages of hydrocephalus. Although these findings demonstrate the importance of early treatment of hydrocephalus, reactive changes in the periventricular tissues occur in response to the shunt catheter. Ingrowth of tissue can cause obstruction and failure of the shunt.

7. BIBLIOGRAPHY

Akai,K Uchigasaki,S Tanaka,U Komatsu,A Normal pressure hydrocephalus- neuropathological study. Acta Pathol Jap 37: 97-110, 1987.

Alexander,E,Jr The ideal shunt for hydrocephalus. Clin Neurosurg 28:297-322, 1981.

Ammar,A Tissue compatibility of different intracranial implant materials: in-vivo and in-vitro studies. Acta Neurochir 72: 45-59, 1984.

Andersson,H Acid monoamine metabolites in experimental hydrocephalus. Dev Med Child Neurol Suppl 15: 58-61, 1968.

Andersson,H Roos,BE Acidic monoamine metabolites in cerebrospinal fluid of children with hydrocephalus. Acta Neurol Scand 41 Suppl 13: 149-151, 1965.

Andersson,H Roos,BE The effect of probenecid on the elimination from CSF of intraventricularly injected 5-hydroxyindoleacetic acid in normal and hydrocephalic dogs. J Pharm Pharmacol 20: 879-881, 1968.

Aoyagi,M Evaluation of periventricular hypodensity in adult hydrocephalus with CT cisternography and xenon-enhanced CT. Bull Tokyo Med Dent Univ 31: 99-110, 1984.

Asada,M Tamaki,N Kanazawa,Y Matsumoto,S Matsuo,M Kimura,S Fujii,S Kaneda,Y Computer analysis of periventricular lucency on the CT scan. Neuroradiology 16: 207-211, 1978.

Bannister,CM Chapman,SA Ventricular ependyma of normal and hydrocephalic subjects: a scanning electron microscopic study. Dev Med Child Neurol 22:725-735, 1980.

Bannister,CM Mundy,JE Some scanning electron microscopic observations of the ependymal surface of hydrocephalic Hy 3 mice and a human infant. Acta Neurochir 46: 159-168, 1979.

Bay,C Kerzin,L Hall,BD Recurrence risk in hydrocephalus. Birth Defects Orig Art Ser 15 (5C): 95-105, 1979.

Bering,EA,Jr Sato,A Hydrocephalus: changes in formation and absorption of cerebrospinal fluid within the cerebral ventricels. J Neurosurg 20: 1050-1063, 1963.

Bigner,SH Elmore,PD Dee,AL Johnston,WW The cytopathology of reactions to ventricular shunts. Acta Cytol 29: 391-396, 1985.

Blakemore,WF The ultrastructure of the subependymal plate in the rat. J Anat 104: 423-433, 1969.

Borgensen,SE Conductance to outflow of CSF in normal pressure hydrocephalus. Acta Neurochir 71: 1-45, 1984.

Bothe,HW Bodsch,W Hossmann,KA Relationship between specific gravity, water content, and serum protein extravasation in various types of vasogenic brain edema. Acta Neuropathol 64: 37-42, 1984.

Brock,M Furuse,M Weber,R Hasuo,M Dietz,H Brain tissue pressure gradients. In: Intracranial Pressure II. Lundberg,N Ponten,U Brock,M (eds) Springer-Verlag, New York. 215-217, 1975.

Brooks,DJ Beaney,RP Powell,M Leenders,KL Crockard,HA Thomas,DGT Marshall,J Jones,T Studies on cerebral oxygen metabolism, blood flow, and blood volume, in patients with hydrocephalus before and after surgical decompression using positron emission tomography. Brain 109: 613-628, 1986.

Brunette,DM Mechanical stretching increases the number of epithelial cells synthesizing DNA in culture. J Cell Sci 69:35-46, 1984.

Bruni,JE Del Bigio,MR Reaction of periventricular tissue in the rat fourth ventricle to chronically placed shunt tubing implants. Neurosurgery 19:337-345, 1986.

Bruni,JE Del Bigio,MR Clattenburg,RE Ependyma: normal and pathological. A review of the literature. Brain Res Rev 9:1-19, 1985.

Bullock,R Smith,R Favier,J du Trevou,M Blake,G Brain specific gravity and CT scan density measurements after human head injury. J Neurosurg 63: 64-68, 1985.

Bundgaard,M Pathways across the vertebrate blood-brain barrier: morphological viewpoints. Ann N Y Acad Sci 481: 7-19, 1986.

Burr,CW McCarthy,DJ Acute internal hydrocephalus. A clinical and pathological study. J Exp Med 5: 195-204, 1900.

Campbell,ACP Variation in vascularity and oxidase content in different regions of the brain of the cat. Arch Neurol Psychiatr 41: 223-242, 1939.

Cardoso,ER Rowan,JO Galbraith,S Analysis of the cerebrospinal fluid pulse wave in intracranial pressure. J Neurosurg 59: 817-821, 1983.

Cavanagh,JB The proliferation of astrocytes around a needle wound in the rat brain. J Anat 106: 471-487, 1970.

Chauhan,AN Lewis,PD A quantitative study of cell

proliferation in ependyma and choroid plexus in the postnatal rat brain. Neuropathol Appl Neurobiol 5:303-309, 1979.

Chawla,JC Hulme,A Cooper,R Intracranial pressure in patients with dementia and communicating hydrocephalus. J Neurosurg 40: 376-380, 1974.

Clark,RG Milhorat,TH Experimental hydrocephalus: Part 3. Light microscopic findings in acute and subacute obstructive hydrocephalus in the monkey. J Neurosurg 32:400-413, 1970.

Collins,P Experimental obstructive hydrocephalus in the rat: a scanning electron microscopic study. Neuropathol Appl Neurobiol 5:457-468, 1979.

Collins,P Hockley,AD Woollam,DHM Surface ultrastructure of tissues occluding ventricular catheters. J Neurosurg 48: 609-613, 1978.

Connor,ES Foley,L Black,PM Experimental normal-pressure hydrocephalus is accompanied by increased transmural pressure. J Neurosurg 61: 322-327, 1984.

Coroneos,NJ McDowall,DG Gibson,RM Pickerodt,V Keaney,NP A comparison of extradural pressure with cerebrospinal fluid pressure. Eur Neurol 8: 79-82, 1972.

Cragie,EH On the relative vascularity of various parts of the central nervous system of the albino rat. J Comp Neurol 31: 429-464, 1920.

Dandy,WE Blackfan,KD An experimental and clinical study of internal hydrocephalus. JAMA 61: 2216-2217, 1913.

Dardenne,G Dereymaeker,A Lacheron,JM Cerebrospinal fluid pressure and pulsatility. An experimental study of circulatory and respiratory influences in normal and hydrocephalic dogs. Eur Neurol 2: 193-216, 1969.

Dasheiff,RM Ramirez,LF The effects of colchicine in mammalian brain from rodents to rhesus monkeys. Brain Res Rev 10: 47-67, 1985.

De,SN A study of the changes in the brain in experimental internal hydrocephalus. J Pathol Bacteriol 62: 197-208, 1950.

Del Bigio,MR Bruni,JE Reaction of rabbit lateral periventricular tissue to shunt tubing implants. J Neurosurg 64: 932-940, 1986.

Del Bigio,MR Bruni,JE Chronic intracranial pressure monitoring in conscious hydrocephalic rabbits. Pediatr Neurosci (in press), 1987.

Del Bigio,MR Bruni,JE Cerebral water content in silicone oil-induced hydrocephalic rabbits. Pediatr Neurosci (in press), 1987.

DelBigio,MR Bruni,JE Fewer,HD Human neonatal hydrocephalus: an electron microscopic study of the periventricular tissue. J Neurosurg 63: 56-63, 1985.

de Reuck,J The human periventricular arterial blood supply and the anatomy of cerebral infarctions. Eur Neurol 5: 321-334, 1971.

Dickinson,WH Lectures on chronic hydrocephalus. Lancet 10: 513-517, 1870.

Diggs,J Price,AC Burt,AM Flor,WJ McKanna,JA Novak,GR James,AE,Jr Early changes in experimental hydrocephalus. Invest Radiol 21: 118-121, 1986.

DiRocco,C DiTrapani,G Maira,G Bentivoglio,M Macchi,G Rossi,GF Anatomo-clinical correlations in normotensive hydrocephalus. Reports on three cases. J Neurol Sci 33: 437-452, 1977.

DiRocco,C DiTrapani,G Pettorossi,VE Caldarelli,M On the pathology of experimental hydrocephalus induced by artificial increase in endoventricular CSF pulse pressure. Childs Brain 5:81-95, 1979.

DiRocco,C McLone,DG Shimoji,T Raimondi,AJ Continuous intraventricular cerebrospinal fluid pressure recording in hydrocephalic children during wakefullness and sleep. J Neurosurg 42: 683-689, 1975.

Dohrmann,GJ The choroid plexus: a historical review. Brain Res 18: 197-218, 1970.

Dohrmann,GJ The choroid plexus in experimental hydrocephalus. A light and electron microscopic study in normal, hydrocephalic, and shunted hydrocephalic dogs. J Neurosurg 34: 56-69, 1971.

Drapkin,AJ Sahar,A Experimental hydrocephalus: cerebrospinal fluid dynamics and ventricular distensibility during early stages. Childs Brain 4: 278-288, 1978.

Edvinsson,L Lindvall,M Owman,C West,KA Autonomic nervous control of cerebrospinal fluid production and intracranial pressure. In: Neurobiology of Cerebrospinal Fluid 2, JH Wood (ed). Plenum Press, New York, 661-676, 1983.

Edvinsson,L Nielsen,KC Owman,C Rosengren,E West,KA Concomitant fall in brain dopamine and homovanillic acid in hydrocephalic rabbits. Eur Neurol 37: 647-649, 1972.

Edvinsson,L Nielsen,KC Owman,C West,KA Increase in kaolin-induced intracranial hypertension after decentralization of the superior cervical ganglia in rabbits. Eur Neurol 11: 296-303, 1974.

Edvinsson,L West,KA The time course of intracranial hypertension as recorded in conscious rabbits after treatment with different amounts of intracisternally injected kaolin. Acta Neurol Scand 47: 439-450, 1971a.

Edvinsson,L West,KA Relation between intracranial pressure and ventricular size at various stages of experimental hydrocephalus. Acta Neurol Scand 47: 451-457, 1971b.

Edwards,MSB Harrison,MR Halks-Miller,M Nakayama,DK Berger,MS Glick,PL Chinn,DH Kaolin induced congenital hydrocephalus in utero in fetal lambs and rhesus monkeys. J Neurosurg 60:115-122, 1984.

Ehara,K Matsumoto,S Yoshida,N Kuno,T Tanaka,C Ascending norepinephrine pathways impaired in experimental hydrocephalus. Jap J Pharmacol 32: 205-208, 1982.

Emery,JL Effect of continual decompression using Holter valve on weights of cerebral hemispheres in children with hydrocephalus and spina bifida cystica. Arch Dis Child 39: 379-383, 1964.

Emery,JL Intracranial effects of long-standing decompression of the brain in children with hydrocephalus and meningomyelocele. Dev Med Child Neurol 7: 302-309, 1965.

Epstein,F Rubin,RC Hochwald,GM Restoration of the cortical mantle in severe feline hydrocephalus: a new laboratory model. Dev Med Child Neurol 16 Suppl 32: 49-53, 1974.

Feigin,IH White matter myelinolysis after brain edema. Bull Soc Belge Ophtalmol 208: 481-482, 1983.

Fernell,E Hagberg,B Hagberg,G von Wendt,L Epidemiology of infantile hydrocephalus in Sweden. I. Birth prevalence and general data. Acta Paediatr Scand 75: 975-981, 1986.

Ferszt,R Hahm,H Cervos-Navarro,J Measurement of the specific gravity of the brain as a tool in brain edema research. Adv Neurol 28: 15-26, 1980.

Fischer,EG Lorenzo,A Landis,WJ Welch,K Ofori-Kwakye,SK Dorval,B Hodgens,KJ Kerr,CS Vasculature to the germinal matrix of rabbit pups. J Neurosurg 64:650-656, 1986.

Fishman,RA Greer,M Experimental obstructive hydrocephalus. Changes in the cerebrum. Arch Neurol 8: 156-161, 1963.

Fleischhauer,K Ependyma and subependymal layer. In: The Structure and Function of Nervous Tissue V.6, GH Bourne (ed). Academic Press, New York. 1-46, 1972.

Flor,WJ James,EA,Jr Ribas,JL Parker,JL Sickel,WL Ultrastructure of the ependyma in the lateral ventricles of primates with experimental hydrocephalus. Scanning Electron Microsc III: 47-54, 1979.

Foltz,EL Hydrocephalus and CSF pulsatility: clinical and laboratory studies. In: Hydrocephalus, Shapiro,K Marmarou,A Portnoy,H (eds). Raven Press, New York. 337-362, 1984.

Foltz,EL Shurtleff,DB Five-year comparative study of hydrocephalus in children with and without operation (113 cases). J Neurosurg 20: 1064-1079, 1963.

Foncin,JF Redondo,A LeBeau,J Le cortex cerebral des malades attients d'hydrocephalie a pression normale: etude ultrastructurale. Acta Neuropathol 34: 353-357, 1976.

Friede,RL A quantitative study of myelination in hydrocephalus. J Neuropathol Exp Neurol 21:645-648, 1962.

Friede,RL Topographic Brain Chemistry (Academic Press, New York) 1-15, 1966.

Fujiwara,K Nitsch,C Suzuki,R Klatzo,I Factors in the reproducibility of the gravimetric method for evaluation of edematous changes in the brain. Neurol Res 3: 345-361, 1981.

Gaab,MR Heissler,HE ICP monitoring. CRC Crit Rev Biomed Engineer 11: 189-250, 1984.

Gadsdon,DR Variend,S Emery,JL The effect of hydrocephalus upon the myelination of the corpus callosum. Z Kinderchir 25: 311-319, 1978.

Gadsdon,DR Variend,S Emery,JL Myelination of the corpus callosum. II. The effect of relief of hydrocephalus upon the processes of myelination. Z Kinderchir 28: 314-321, 1979.

Ganong,WF Review of Medical Physiology, 9th Edition.Lange Medical Publications, Los Altos CA. 443-456, 1979.

Geschwind,N The mechanism of normal pressure hydrocephalus. J Neurol Sci 7: 481-493, 1968.

Giuffre,R Choroidal and ependymal reactions. J Neurosurg Sci 20: 123-129, 1976.

Glick,PL Harrison,MR Halks-Miller,M Adzick,NS Nakayama,DK Anderson,JH Nyland,TG Villa,R Edwards,MSB Correction of congenital hydrocephalus in utero. II: efficacy of in utero shunting. J Pediatr Surg 19:870-881, 1984.

Go,KG Ebels,EJ van Woerden,H Experiences with recurring ventricular catheter obstructions. Clin Neurol Neurosurg 83: 47-56, 1981.

Go,KG Stokroos,I Blaauw,EH Zuiderveen,F Molenaar,I Changes of the ventricular ependyma and choroid plexus in experimental hydrocephalus as observed by scanning electron microscopy. Acta Neuropathol 34:55-64, 1976.

Gonzalez-Darder,J Barbera,J Cerda-Nicolas,M Segura,D Broseta,J Barcia-Salorio,JL Sequential morphological and functional changes in kaolin-induced hydrocephalus. J Neurosurg 61: 918-924, 1984.

Gopinath,G Bhatia,R Gopinath,PG Ultrastructural observations in experimental hydrocephalus in the rabbit. J Neurol Sci 43: 333-344, 1979.

Granholm,L Induced reversibility of ventricular dilatation in experimental hydrocephalus. Acta Neurol Scand 42:581-588, 1966.

Greitz,TVB Grepe,AOL Kalmer,MSF Lopez,J Pre- and postoperative evaluation of cerebral blood flow in low-pressure hydrocephalus. J Neurosurg 41: 644-651, 1969.

Gross,PM Sposito,NM Pettersen,SE Panton,DG Fenstermacher,JD Topography of capillary density, glucose metabolism, and microvascular function within the rat inferior colliculus. J Cereb Blood Flow Met 7: 154-160, 1987.

Gucer,G Viernstein,L Walker,AE Continuous intracranial pressure recording in adult hydrocephalus. Surg Neurol 13: 323-328, 1980.

Habal,MB The biologic basis for the clinical application of the silicones. A correlate to their biocompatibility. Arch Surg 119: 843-848, 1984.

Hakim,S Observations on the physiopathology of the CSF pulse and prevention of ventricular catheter obstruction in valve shunts. Dev Med Child Neurol Suppl 20: 42-48, 1969.

Hakim,S Adams,RD The special clinical problem of symptomatic hydrocephalus with normal cerebrospinal fluid pressure. Observations on cerebrospinal fluid dynamics. J Neurol Sci 2: 307-327, 1965.

Hakim,S Venegas,JG Burton,JD The physics of the cranial cavity, hydrocephalus and normal pressure hydrocephalus: mechanical interpretation and mathematical model. Surg Neurol 5: 187-210, 1976.

Hammock,MK Milhorat,TH Baron,IS Normal pressure

hydrocephalus in patients with myelomeningocele. Dev Med Child Neurol Suppl 37: 55-68, 1976.

Hassler,O Angioarchitecture in hydrocephalus. An autopsy and experimental study with the aid of microangiography. Acta Neuropathol 4: 65-74, 1964.

Hay,S Incidence of selected congenital malformations in Iowa. Am J Epidemiol 94: 572-584, 1971.

Haynes,SG Gibson,JB Kurland,LT Epidemiology of neural tube defects and Down's syndrome in Rochester, Minnesota 1935-1971. Neurology 24: 691-700, 1974.

Higashi,K Asahisa,H Ueda,N Kobayashi,K Hara,K Noda,Y Cerebral blood flow and metabolism in experimental hydrocephalus. Neurol Res 8: 169-176, 1986.

Hill,A Volpe,JJ Decrease in pulsatile flow in the anterior cerebral arteries in infantile hydrocephalus. Pediatrics 69: 4-7, 1982.

Hirai,O Handa,H Ishikawa,M Kim,SH Epidural pulse waveform as an indicator of intracranial pressure dynamics. Surg Neurol 21: 67-74, 1984.

Hirano,A Zimmerman,HM Levine,S The fine structure of cerebral fluid accumulation: reactions of ependyma to implantation of Cryptococcal polysaccharide. J Pathol Bacteriol 91:149-155, 1966.

Hiratsuka,H Tabata,H Tsuruoka,S Aoyagi,M Okada,K Inaba,Y Evaluation of periventricular hypodensity in experimental hydrocephalus by metrizamide CT ventriculography. J Neurosurg 56: 235-240, 1982.

Hirayama,A Histopathological study of congenital and acquired experimental hydrocephalus. Brain Dev 2: 171-189, 1980.

Hochwald,GM Animal models of hydrocephalus: recent developments. Proc Soc Exp Biol Med 178: 1-11, 1985.

Hochwald,GM Boal,RD Marlin,AE Kumar,AJ Changes in regional blood flow and water content of brain and spinal cord in acute and chronic experimental hydrocephalus. Dev Med Child Neurol 17 Suppl 35: 42-50, 1975.

Hochwald,GM Lux,WE Sahar,A Ransohoff,J Experimental hydrocephalus: changes in cerebrospinal fluid dynamics as a function of time. Arch Neurol 26: 120-129, 1972.

Hochwald,GM Nakamura,S Camins,MB The rat in experimental hydrocephalus. Z Kinderchir 34:403-410, 1981.

Hochwald,GM Sahar,A Sadik,AR Ransohoff,J Cerebrospinal fluid production and histological observations in animals with experimental obstructive hydrocephalus. Exp Neurol 25:190-199, 1969.

Hoffman,HJ Hendrick,EB Humphreys,RP Management of hydrocephalus. Monogr Neural Sci 8: 21-25, 1982.

Hoffman,HJ Smith,MSM The use of shunting devices for cerebrospinal fluid in Canada. Can J Neurol Sci 13: 81-87, 1986.

Hopkins,LN Bakay,L Kinkel,WR Grand,W Demonstration of transventricular CSF absorption by computerized tomography. Acta Neurochir 39: 151-157, 1977.

Hughes,CP Siegel,BA Coxe,WS Gado,MH Grubb,RL Coleman,RE Berg,L Adult idiopathic communicating hydrocephalus with and without shunting. J Neurol Neurosurg Psychiatr 41: 961-971, 1978.

Iannotti,F Hoff,JT Schielke,GP Brain tissue pressure: physiological observations in anesthetized cats. J Neurosurg 60: 1219-1225, 1984.

Imamoto,K Macrophagic ameboid cells in the brain ventricles of the neonatal rat. Arch Histol Jap 47:271-277, 1984.

Inaba,Y Hirasuka,H Tsuyuma,M Tabata,H Tsuruoka,S Evaluation of periventricular hypodensity in clinical and experimental hydrocephalus by metrizamide computed tomography. In: Brain Edema KG Go, A Baethmann (eds) (Plenum Press, New York) 299-310, 1984.

Irving,IM Castilla,P Hall,EG Rickham,PP Tissue reaction to pure and impregnated silastic. J Pediatr Surg 6: 724-729, 1971.

Ito,M [Significance of shunting operation for compensated hydrocephalus. Experimental study of the ependymal layer with HRP and electron microscopy.](in Japanese) Neurol Med-Chir 16:227-236, 1976.

Ivan,LP Choo,SH A comparative study of epidural and cisternal pressure in dogs. J Neurosurg 57: 511-514 ,(982)

Jagust,WJ Friedland,RP Budinger,TF Positron emission tomography with [F-18] fluorodeoxyglucose differentiates normal pressure hydrocephalus from Alzheimer type dementia. J Neurol Neurosurg Psychiatr 48: 1091-1096, 1985.

James,AE,Jr Burns,B Flor,WJ Strecker,EP Merz,T Bush,M Price,DL Pathophysiology of chronic communicating hydrocephalus in dogs(Canis familiaris), experimental studies. J Neurol Sci 24: 151-178, 1975.

James,AE,Jr Flor,WJ Bush,M Merz,T Rish,BL An experimental model for chronic communicating hydrocephalus. J Neurosurg 41:32-37, 1974.

James,AE,Jr Flor,WJ Novak,GR Ribas,JL Parker,JL Sickel,WL The ultrastructural basis of periventricular edema: preliminary studies. Radiology 135:747-750, 1980.

James,AE,Jr Flor,WJ Novak,GR Strecker,EP Burns,B Epstein,M Experimental hydrocephalus. Exp Eye Res Suppl 435-459, 1977.

James,AE,Jr Strecker,EP Use of silastic to produce communicating hydrocephalus. Invest Radiol 8:105-110, 1973a.

James,AE,Jr Strecker,EP Novak,G Burns,B Correlations of serial cisternograms and cerebrospinal fluid pressure measurements in experimental communicating hydrocephalus. Neurology 23: 1226-1233, 1973b.

Johnston,IH Rowan,O Harper,AM Jennett,WB Raised intracranial pressure and cerebral blood flow: cisterna magna infusion in primates. J Neurol Neurosurg Psychiatr 35: 285-296, 1972.

Kaplan,MS Proliferation of subependymal cells in the adult primate CNS: differential uptake of DNA labeled precursors. J Hirnforsch 24: 23-33, 1983.

Katayama,Y Teuther,S Nakamura,T Becker,DP Hates,RL Continuous recording of intracranial pressure in the awake, drug-free cat. Brain Res Bull 12: 581-583, 1984.

Katzman,R Normal pressure hydrocephalus. Contemp Neurol Ser 5: 69-92, 1977.

Kaufman,HH Dujovny,M Huchton,JD Kossovsky,N Miller,M Carmel,PC "Natural" canine model of infantile hydrocephalus. Neurosurgery 6:142-148, 1980.

Kawano,T Tsujimura,M Mori,K Eujita,Y [Changes in ventricular dopamine and homovanillic acid concentrations in hydrocephalic patients.] (in Japanese) Neurol Med-Chir 20: 373-378, 1980.

Korr,H Proliferation of different cell types in the brain. Adv Anat Embryol Cell Biol 61: 1-69, 1980.

Krikorian,JG Guth,L Donati,EJ Origin of the connective tissue scar in the transected rat spinal cord. Exp Neurol 72: 698-707, 1981.

Kuchiwaki,H Hasuo,M Furuse,M Effect on increases in intracranial pressure in acute experimental communicating hydrocephalus. Brain Nerve 31: 577-582, 1979.

Kurtzke,JF An overview of congenital malformations of the nervous system. In: Clinical Neuroepidemiology, FC Rose (ed) Pitman Medical, London. 264-283, 1980.

Kushner,M Younkin,D Weinberger,J Hutig,H Goldberg,H Reivich,M Cerebral hemodynamics in the diagnosis of normal pressure hydrocephalus. Neurology 34: 96-99, 1984.

LeBlond,CP Walker,BE Renewal of cell populations. Physiol Rev 36: 255-276, 1956.

Levin,VA Milhorat,TH Fenstermacher,JD Hammock,MK Rall,DP Physiological studies on the development of obstructive hydrocephalus in the monkey. Neurology 21: 238-246, 1971.

Lindauer,MA Griffith,JQ,Jr Cerebrospinal pressure, hydrocephalus and blood pressure in the cat following intracisternal injection of colloidal kaolin. Proc Soc Exp Biol Med 39: 547-549, 1938.

Lindvall,M Owman,C Sympathetic nervous control of cerebrospinal fluid production in experimental obstructive hydrocephalus. Exp Neurol 84:606-615, 1984.

Ling,EA Scanning electron microscopic study of epiplexus cells in the lateral ventricles of the monkey (Macaca fascicularis). J Anat 137:645-652, 1983.

Liszczak,TM Black,PMcLTzouras,A Foley,L Zervas,NT Morphological changes of the basilar artery, ventricles, and choroid plexus after experimental SAH. J Neurosurg 61:486-493, 1984.

Lundberg,N Continuous recording and control of ventricular fluid pressure in neurosurgical practice. Acta Psychiatr Neurol Scand Suppl 149:1-193, 1960.

Lux,WE Hochwald,GM Sahar,A Ransohoff,J Periventricular water content. Effect of pressure in experimental chronic hydrocephalus. Arch Neurol 23: 475-479, 1970.

Lying-Tunell,U Lindblad,BS Malmlund,HO Persson,B Cerebral blood flow and metabolic rate of oxygen, glucose, lactate, pyruvate, ketone bodies and amino acids. II. Presenile dementia and normal pressure hydrocephalus. Acta Neurol Scand 63: 337-350, 1981.

Malkinson,TJ Veale,WL Cooper,KE Measurement of intracranial pressure in the unanesthetized rabbit. Brain Res Bull 3: 635-638, 1978.

Mandell,EC Zimmermann,E Continuous measurement of cerebrospinal fluid pressure in unrestrained rats. Physiol Behav 24: 399-402, 1980.

Marmarou,A Poll,W Shulman,K Bhagavan,H A simple gravimetric technique for measurement of cerebral edema. J Neurosurg 49: 530-537, 1978.

Massarotti,M Roccella,P 5 hydroxyindoleacetic acid and homovanillic acid levels in the cerebrospinal fluid of patients with normal pressure hydrocephalus (NPH). IRCS Med Sci Metab Nutr 3: 361-362, 1975.

Matsumoto,S Hirayama,A Yamasaki,S Shirataki,K Fujiwara,K Comparative study of various models of experimental hydrocephalus. Childs Brain 1:236-242, 1975.

Matsumoto,T Nagai,H Kasuga,Y Kamiya,K Changes in intracranial pressure (ICP) pulse wave following hydrocephalus. Acta Neurochir 82: 50-56, 1986.

McAllister,JP,II Maugans,TA Shah,MV Truex,RC,Jr Neuronal effects of experimentally induced hydrocephalus in newborn rats. J Neurosurg 63:776-783, 1985.

McComb,JG Recent research into the nature of cerebrospinal fluid formation and absorption. J Neurosurg 59: 369-383, 1983.

McComb,JG Hyman,S Weiss,MH Cerebrospinal fluid drainage following acute obstruction of the fourth ventricle in the rabbit. Concepts Pediatr Neurosurg 4: 90-101, 1983.

McCullough,DC A critical evaluation of continuous intracranial pressure monitoring in pediatric hydrocephalus. Childs Brain 6: 225-241, 1980.

McGraw,CP Epidural intracranial pressure monitoring. In: Intracranial Pressure II, N Lundberg, U Ponten, M Brock (eds) (Springer-Verlag, Berlin) 394-396, 1974.

McLone,DG Bondareff,W Raimondi,AJ Hydrocephalus-3, a murine mutant: II. Changes in the brain extracellular space. Surg Neurol 1:233-242, 1973.

McLone,DG Raimondi,AJ The hydrocephalic-3 house mouse. In: Hydrocephalus, K Shapiro, A Marmarou, H Portnoy (eds). (Raven Press, New York) 251-269, 1984.

Mendenhall,W Introduction to Probability and Statistics 5th Edition. Duxbury Press, North Scituate, MA. 259, 1979.

Meyer,JS Kitagawa,Y Tanahashi,N Tachibana,H Kandula,P Cech,DA Rose,JE Grossman,RG Pathogenesis of normal-pressure hydrocephalus- preliminary observations. Surg Neurol 23: 121-133, 1985.

Michejda,M Patronas,N Di Chiro,G Hodgen,GD Fetal hydrocephalus. II. Amelioration of fetal porencephaly by in

utero therapy in nonhuman primates. JAMA 251: 2548-2552, 1984.

Milhorat,TH Hydrocephalus and the Cerebrospinal Fluid. (Williams and Wilkins, Baltimore) 1972.

Milhorat,TH Clark,RG Hammock,MK McGrath,PP Structural, ultrastructural, and permeability changes in the ependyma and surrounding brain favoring equilibration in progressive hydrocephalus. Arch Neurol 22:397-407, 1970.

Millen,JW Woollam,DHM The Anatomy of the Cerebrospinal Fluid. Oxford University Press, London. 1-151, 1962.

Millhouse,OE Light and electron microscopic studies of the ventricular wall. Z Zellforsch 127:175-188, 1972.

Mitro,A Palkovits,M Morphology of the rat brain ventricles, ependyma, and periventricular structures. Biblio Anat 21:1-110, 1981.

Miwa,S Inagaki,C Fujiwara,M Takaori,S The activities of noradrenergic and dopaminergic neuron systems in experimental hydrocephalus. J Neurosurg 57: 67-73, 1982.

Miyagami,M Nakamura,S Murakami,T Koga,N Moriyasu,M Electron microscopic study of ventricular wall and choroid plexus in experimentally- induced hydrocephalic dogs. Neurol Med-Chir 16: 15-21, 1976.

Mori,K Handa,H Murata,T Nakano,Y Periventricular lucency in computed tomography of hydrocephalus and cerebral atrophy. Monogr Neural Sci 8: 148-152, 1982.

Moskalenko,YE Weinstein,GB Demchenko,IT Kislyakov,YY Krivchenko,AI Biophysical Aspects of Cerebral Circulation. Pergamon Press, Oxford. 164 pp., 1980.

Mukherjee,A Gopinath,G Bhatia,R Roy,S Some observations on the ventricular system of kaolin induced hydrocephalic rabbits. Indian J Med Res 75:136-141, 1982.

Murata,T Handa,H Mori,K Nakano,Y The significance of periventricular lucency on computed tomography: experimental study with canine hydrocephalus. Neuroradiology 20: 221-227 (1981).

Myrianthopoulos,NC Our load of central nervous system malformations. Birth Defects Orig Art Ser 15 (3): 1-18, 1979.

Nakagawa,Y Cervos-Navarro,J Artigas,J A possible paracellular route for resolution of hydrocephalic edema. Acta Neuropathol 64: 122-128, 1984.

Nakagawa,Y Cervos-Navarro,J Artigas,J Tracer study on a paracellular route in experimental hydrocephalus. Acta Neuropathol 65: 247-254, 1985.

Nakamura,S Hochwald,GM Effects of arterial pCO_2 and cerebrospinal fluid volume flow rate changes on choroid plexus and cerebral blood flow in normal and experimental hydrocephalic cats. J Cereb Blood Flow Met 3: 369-375, 1983.

Nakayama,DK Harrison,MR Berger,MS Chinn,DH Halks-Miller,M Edwards,MS Correction of congenital hydrocephalus in utero I. The model: intracisternal kaolin produces hydrocephalus in fetal lambs and rhesus monkeys. J Pediatr Surg 18: 331-338, 1983.

Nelson,SR Mantz,ML Maxwell,JA Use of specific gravity in the measurement of cerebral edema. J Appl Physiol 30: 268-271, 1971.

Nyberg-Hansen,R Torvik,A Bhatia,R On the pathology of experimental hydrocephalus. Brain Res 95:343-350, 1975.

Obenchain,TG Stern,WE Continuous pressure monitoring in experimental obstructive hydrocephalus. I. The dynamics of acute ventricular obstruction. Arch Neurol 29: 287-294, 1973.

Oberbauer,RW The significance of morphological details for developmental outcome in infantile hydrocephalus. Childs Nerv Syst 1: 329-336, 1985.

Occhipinti,E Fontana,M Giuffre,R Palma,L Biological shunt complications. Adv Neurosurg 8: 267-272, 1980.

Ogata,J Hochwald,GM Cravioto,H Ransohoff,J Light and electron microscopic studies of experimental hydrocephalus. Ependymal and subependymal areas. Acta Neuropathol 21:213-223, 1972.

Oka,N Nakada,JI Endo,S Takaku,A Shinohara,H Morisawa,S [Angioarchitecture in experimental hydrocephalus](in Japanese) Neurol Med Chir 25: 701-706, 1985.

Okuyama,T Hashi,K Sasaki,S Sudo,K Kurokawa,Y Changes in cerebral microvasculature in congenital hydrocephalus of the inbred rat LEW/Jms: light and electron microscopic examination. Surg Neurol 27: 338-342, 1987.

Orton,ST A pathological study of a case of internal hydrocephalus. Am J Insanity 65: 229-278, 1908.

Owman,C Rosengren,E West,KA Influence of various intracranial pressure levels on the concentration of certain arylethylamines in rabbit brain. Experientia 27: 1036-1037, 1971.

Page,LK Cerebrospinal fluid and extracellular fluid: their relationship to pressure and duration of canine hydrocephalus. Childs Nerv Sys 1: 12-17, 1985.

Page,RB Scanning electron microscopy of the ventricular system in normal and hydrocephalic rabbits: preliminary report and atlas. J Neurosurg 42:646-664, 1975.

Page,RB Leure-duPree,AE Ependymal alterations in hydrocephalus. In: Neurobiology of Cerebrospinal Fluid 2. JH Wood (ed) Plenum Press, New York. 789-820, 1983.

Page,RB Rosenstein,JM Dovey,BJ Leure-duPree,AE Ependymal changes in experimental hydrocephalus. Anat Rec 194:83-104, 1979a.

Page,RB Rosenstein,JM Leure-duPree,AE The morphology of the extrachoroidal ependyma overlaying gray and white matter in the rabbit lateral ventricle. Anat Rec 194:67-81, 1979b.

Peacock,WJ Currer,TH Hydrocephalus in childhood: a study of 440 cases. S Afr Med J 66: 323-324, 1984.

Penfield,W Notes on cerebral pressure atrophy. Res Publ Assoc Nerv Ment Dis 8: 246-362, 1929.

Penn,RD Bacus,JW The brain as a sponge: a computed tomographic look at Hakim's hypothesis. Neurosurgery 14: 670-675, 1984.

Picozzi,P Todd,NV Crockard,AH The role of cerebral blood volume changes in brain specific-gravity measurements. J Neurosurg 62: 704-710, 1985.

Plets,C Mechanisms of ventricular dilatation in experimental hydrocephalus. Acta Neurochir Suppl 28: 509-513, 1979.

Plets,C van den Bergh,R L'influence de l'hydrocephalie experimentale sur la vascularisation cerebrale. Acta Neurol Belg 73: 50-55, 1973.

Portnoy,HD Branch,C Chopp,M The CSF pulse wave in hydrocephalus. Childs Nerv Syst 1: 248-254, 1985.

Price,DL James,AE,Jr Sperber,E Strecker,EP Communicating hydrocephalus: cisternographic and neuropathologic studies. Arch Neurol 33:15-20, 1976.

Privat,A Leblond,CP The subependymal layer and neighboring region in the brain of the young rat. J Comp Neurol 146: 277-301, 1972.

Pudenz,RH The surgical treatment of hydrocephalus- an historical review. Surg Neurol 15:15-26, 1981.

Reinhardt,V Nau,HE Histological investigations and clinical considerations on shunt dysfunctions. Adv Neurosurg 8:267-272, 1980.

Richards,HK Pickard,JD Punt,J Local cerebral glucose utilization in experimental chronic hydrocephalus in the rat. Z Kinderchir 40 Suppl 1: 9, 1985.

Rogers,KJ Dubowitz,V 5 hydroxyindoles in hydrocephalus. A comparative study of cerebrospinal fluid and blood levels. Dev Med Child Neurol 12: 461-466, 1970.

Rosenberg,GA Saland,L Kyner,WT Pathophysiology of periventricular tissue changes with raised CSF pressure in cats. J Neurosurg 59: 606-611, 1983.

Rowlatt,U The microscopic effects of ventricular dilatation without increase in head size. J Neurosurg 48: 957-961, 1978.

Rubin,RC Hochwald,GM Reconstitution of the cerebral mantle following hydrocephalus. In: Neurobiology of Cerebrospinal Fluid 2 JH Wood (ed) Plenum Press, New York. 821-833, 1983.

Rubin,RC Hochwald,GM Tiell,M Epstein,F Ghatak,N Wisniewski,H Hydrocephalus: III. Reconstitution of the cerebral cortical mantle following ventricular shunting. Surg Neurol 5: 179-183, 1976a.

Rubin,RC Hochwald,GM Tiell,M Liwnicz,BH Hydrocephalus: II. Cell number and size, and myelin content of the pre-shunted cerebral cortical mantle. Surg Neurol 5:115-118, 1976b.

Rubin,RC Hochwald,GM Tiell,M Liwnicz,BH Epstein,F Reconstitution of the cerebral cortical mantle in shunt-corrected hydrocephalus. Dev Med Child Neurol Suppl 35:151-156, 1975.

Rubin,RC Hochwald,GM Tiell,M Mizutani,H Ghatak,N Hydrocephalus: I. Histological and ultrastructural changes in the pre-shunted cortical mantle. Surg Neurol 5: 109-114, 1976c.

Russell,DS Observations on the pathology of hydrocephalus. Med Res Coun Spec Rep Ser 265: 1-138, 1949.

Sahar,A Experimental hydrocephalus in young animals. Childs Brain 5:14-23, 1979.

Sahar,A Hochwald,GM Kay,WJ Ransohoff,J Spontaneous canine hydrocephalus: cerebrospinal fluid dynamics. J Neurol Neurosurg Psychiatr 34: 308-315, 1971.

Sahar,A Hochwald,GM Ransohoff,J Alternate pathway for

cerebrospinal fluid absorption in animals with experimental obstructive hydrocephalus. Exp Neurol 25: 200-206, 1969.

Sahar,A Hochwald,GM Sadik,AR Ransohoff,J Cerebrospinal fluid absorption: in animals with experimental obstructive hydrocephalus. Arch Neurol 21:638-644, 1969.

Sari,A Okuda,Y Takeshita,H The effect of ketamine on cerebrospinal fluid pressure. Anaesth Analges Curr Res 51: 560-565, 1972.

Sarkisov,SA The Structure and Functions of the Brain. (Indiana University Press, Bloomington) 80-96, 1966.

Sato,O Ohya,M Nojiri,K Tsugane,R Microcirculatory changes in experimental hydrocephalus: morphological and physiological studies. In: Hydrocephalus, Shapiro,K Marmarou,A Portnoy,H (eds). Raven Press, New York. 215-230, 1984.

Sayers,MP Shunt complications. Clin Neurosurg 23: 393-400, 1976.

Schurr,PH McLaurin,RL Ingraham,FD Experimental studies on the circulation of the cerebrospinal fluid and methods of producing communicating hydrocephalus in the dog. J Neurosurg 10: 515-525, 1953.

Sekhar,LN Moossy,J Guthkelch,AN Malfunctioning ventriculoperitoneal shunts. Clinical and pathological features. J Neurosurg 56:411-416, 1982.

Shackelford,GD Neurosonography of hydrocephalus in infants. Neuroradiology 28: 452-461, 1986.

Shapiro,K Takei,F Fried,A Kohn,I Experimental feline hydrocephalus. The role of biomechanical changes in ventricular enlargement in cats. J Neurosurg 63: 82-87, 1985.

Shaywitz,BA Brain inulin space in hydrocephalic and hyponatremic kittens using ventriculocisternal perfusion. Exp Neurol 34: 16-24, 1972.

Shenkin,HA Greenberg,JO Grossman,CB Ventricular size after shunting for idiopathic normal pressure hydrocephalus. J Neurol Neurosurg Psychiatr 38: 833-837, 1975.

Shigeno,T Brock,M Shigeno,S Fritschka,E Cervos-Navarro,J The determination of brain water content: microgravimetry versus drying-weighing method. J Neurosurg 57: 99-107, 1982.

Shulman,K Marmarou,A Pressure-volume considerations in infantile hydrocephalus. Dev Med Child Neurol Suppl 25: 90-95, 1971.

Shulman,K Marmarou,A Weitz,S Gradients of brain interstitial fluid pressure in experimental brain infusion and compression. In: Intracranial Pressure II. Lundberg,N Ponten,U Brock,M (eds). Springer-Verlag, New York. 221-223, 1975.

Sibayan,RQ Begeman,PC King,AI Gurdjian,ES Thomas,LM Experimental hydrocephalus: ventricular cerebrospinal fluid pressure and waveform studies. Arch Neurol 23:165-172, 1970.

Sprung,C Grumme,T CT images of periventricular lucency (PVL) in various forms of hydrocephalus. Adv Neurosurg 8: 172-182, 1980.

Steel,RGD Torrie,JH Principles and Procedures of Statistics. With special reference to the biological sciences. McGraw-Hill Book Co., Inc., Ney York. 112-114, 1960.

Strecker,EP James,AE,Jr Konigsmark,B Merz,T Autoradiographic observations in experimental communicating hydrocephalus. Neurology 24: 192-197, 1974.

Strecker,EP Novak,GR Kauffmann,G Hemmer,R James,AE,Jr Cerebrospinal fluid pressure alterations in experimental communicating hydrocephalus. Response of cerebrospinal fluid pressure to increase in arterial carbon dioxide tension. Eur Neurol 25:141-147, 1986.

Sturrock,RR A developmental study of epiplexus cells and supraependymal cells and their possible relationship to microglia. Neuropathol Appl Neurobiol 4:307-322, 1978.

Sturrock,RR Age related changes in cellularity, mitotic activity and pyknotic cell number in the mouse subependymal layer. J Anat 141:19-26, 1985.

Sugar,O Bailey,OT Subcutaneous reaction to silicone in ventriculoperitoneal shunts. Long-term results. J Neurosurg 41: 367-371, 1974.

Sutton,LN Wood,H Brooks,BR Barrer,SJ Kline,M Cohen,SR Cerebrospinal fluid myelin basic protein in hydrocephalus. J Neurosurg 59: 467-470, 1983.

Symon,L Dorsch,NWC Use of long term intracranial pressure measurement to assess hydrocephalic patients prior to shunt surgery. J Neurosurg 42: 258-273, 1975.

Takei,F Shapiro,K Kohn,I Influence of the rate of ventricular enlargement on the white matter water content in progressive feline hydrocephalus. J Neurosurg 66: 577-583, 1987.

Tamaki,N Kusunoki,T Wakabayashi,T Matsumoto,S Cerebral hemodynamics in normal-pressure hydrocephalus. Evaluation by

^{133}Xe inhalation method and dynamic CT study. J Neurosurg 61: 510-514, 1984.

Tengvar,C Forssen,M Hultstrom,D Olsson,Y Pertoft,H Pettersson,A Measurement of edema in the nervous system. Use of Percoll density gradients for determination of specific gravity in cerebral cortex and white matter under normal conditions and in experimental cytotoxic brain edema. Acta Neuropathol 57: 143-150, 1982.

Shurtleff,DB Stuntz,JT Hayden,PW Experience with 1201 cerebrospinal fluid shunt procedures. Pediatr Neurosci 12: 49-57, 1986.

Tennyson,VM Pappas,GD An electron microscopic study of ependymal cells of the fetal, early postnatal and adult rabbit. Z Zellforsch 56:595-618, 1962.

Thomas,WS Experimental hydrocephalus. J Exp Med 19: 106-119, 1914.

Torack,RM Historical aspects of normal and abnormal brain fluids. II. Hydrocephalus. Arch Neurol 39: 276-279, 1982.

Torvik,A Bhatia,R Nyberg-Hansen,R The pathology of experimental hydrocephalus. Neuropathol Appl Neurobiol 2: 41-52, 1976.

Torvik,A Stenwig,AE The pathology of experimental obstructive hydrocephalus. Electron microscopic observations. Acta Neuropathol 38: 21-26, 1977.

Torvik,A Stenwig,AE Finseth,I The pathology of experimental obstructive hydrocephalus. A scanning electron microscopic study. Acta Neuropathol 54:143-147, 1981.

van den Bergh,R vander Eecken,H Anatomy and embryology of cerebral circulation. Prog Brain Res 30: 1-25, 1968.

Vorstrup,S Christensen,J Gjerris,F Sorensen,PS Thomsen,AM Paulson,OB Cerebral blood flow in patients with normal-pressure hydrocephalus before and after shunting. J Neurosurg 66: 379-387, 1987.

Wagner,EM Traystman,RJ Hydrostatic determinants of cerebral perfusion. Crit Care Med 14: 484-490, 1986.

Wallman,LJ Shunting for hydrocephalus: an oral history. Neurosurgery 11: 308-313, 1982.

Welch,K The principles of physiology of the cerebrospinal fluid in relation to hydrocephalus including normal pressure hydrocephalus. Adv Neurol 13:247-332, 1975.

Welch,K Selected topics relating to hydrocephalus. Exp Eye

Res Suppl 345-375, 1977.

Weller,RO Mitchell,J Cerebrospinal fluid edema and its sequelae in hydrocephalus. Adv Neurol 28: 111-123, 1980.

Weller,RO Mitchell,J Griffin,RL Gardner,MJ The effects of hydrocephalus upon the developing brain. Histological and quantitative studies of the ependyma and subependyma in hydrocephalic rats. J Neurol Sci 36: 383-402, 1978.

Weller,RO Shulman,K Infantile hydrocephalus: clinical, histological, and ultrastructural study of brain damage. J Neurosurg 36:255-265, 1972.

Weller,RO Williams,BN Cerebral biopsy and assessment of brain damage in hydrocephalus. Arch Dis Child 50: 763-768, 1975.

Weller,RO Wisniewski,H Histological and ultrastructural changes in experimental hydrocephalus in adult rabbits. Brain 92: 819-828, 1969a.

Weller,RO Wisniewski,H Ishii,N Shulman,K Terry,RD Brain tissue damage in hydrocephalus. Dev Med Child Neurol Suppl 20:1-7, 1969b.

Weller,RO Wisniewski,H Shulman,K Terry,RD Experimental hydrocephalus in young dogs: histological and ultrastructural study of brain tissue damage. J Neuropathol Exp Neurol 30: 613-626, 1971.

Willis,P Berry,M Riches,AC Effects of trauma on cell production in the subependymal layer of the rat neocortex. Neuropathol Appl Neurobiol 2: 377-388, 1976.

White,RN Gergely,P Sexsmith,RG Structural Engineering. Combined Edition. Wiley, New York. 91-95, 1976.

Wislocki,GB Putnam,TJ Absorption from the ventricles in experimentally produced internal hydrocephalus. Am J Anat 29: 313-320, 1921.

Wisniewski,H Research on experimental filling of the ventricular system of dogs. Acta Neuropathol 1: 238-244, 1961.

Wisniewski,H Weller,RO Terry,RD Experimental hydrocephalus produced by the subarachnoid infusion of silicone oil. J Neurosurg 31:10-14, 1969.

Wolf,AV Brown,MG Prentiss,PG Concentrative properties of aqueous solutions: conversion tables. In: CRC Handbook of Chemistry and Physics, RC Weast and MJ Astle (eds) (CRC Press, Inc., Boca Raton, FL) D227-D276, 1983.

Wozniak,M McLone,DG Raimondi,AJ Micro- and macrovascular changes as the direct cause of parenchymal destruction in congenital murine hydrocephalus. J Neurosurg 43: 535-545, 1975.

Yakovlev,PI Paraplegias of hydrocephalus. (A clinical note and interpretation). Am J Mental Defic 51: 561-576, 1947.

Yates,CM Minns,RA Monoamine metabolites and ventricular fluid pressure in children. Childs Brain 8: 138-144, 1981.

Zumstein,B Landolt,AM Untersuchung des an Ventrikelkathetern hydrozephaler Patienten haftenden Gewebes im Licht- und Electronenmikroskop. Acta Neurochir 30: 287-298, 1974.